Universitat de Girona

DOCTORAL THESIS

Electro-bioremediation of nitrate-contaminated groundwater:

from laboratory to *on-site* pilot plant

Alba Ceballos-Escalera Lopez

2024

DOCTORAL THESIS

Electro-bioremediation of nitrate-contaminated groundwater:

from laboratory to *on-site* pilot plant

Alba Ceballos-Escalera Lopez

2024

Doctoral programme in **Water Science and Technology**

Supervised by: Dr. Sebastià Puig Broch, Dra. Maria Dolors Balaguer Condom and Dr. Narcís Pous Rodríguez

Tutor: Dr. Sebastià Puig Broch

Doctoral thesis submitted to the University of Girona for the degree of Doctor

Universitat de Girona

Dr. Sebastià Puig Broch, Dra. Maria Dolors Balaguer Condom and Dr. Narcís Pous Rodríguez of the Laboratory of Chemical and Environmental Engineering (LEQUiA) of the University of Girona:

WE DECLARE:

That the thesis entitled "***Electro-bioremediation of nitrate-contaminated groundwater**: from laboratory to on-site pilot plant*", submitted by **Alba Ceballos-Escalera López** for a doctorate degree, has been completed under our supervision and meets the requirements to opt for an International Doctorate mention.

For all intents and purposes, this document is hereby signed by us.

Sebastià Puig Broch - DNI 40348024K (TCAT)
Digitally signed by Sebastià Puig Broch - DNI 40348024K (TCAT)
Date: 2023.11.16 14:29:19 +01'00'

Maria Dolors Balaguer Condom - DNI 40518357Q (TCAT)
Firmado digitalmente por Maria Dolors Balaguer Condom - DNI 40518357Q (TCAT)
Fecha: 2023.11.16 13:40:35 +01'00'

Narcis Pous i Rodriguez - DNI 77922471N (TCAT)
Digitally signed by Narcis Pous i Rodriguez - DNI 77922471N (TCAT)
Date: 2023.11.16 15:54:49 +01'00'

Signature,

Girona, 19 Gener 2025

Agraïments

Aquest viatge de més de 4 anys va començar durant una classe de bioremediació, on vaig reunir el coratge per enviar tímidament un correu al meu antic supervisor del TFG, preguntant si hi havia una oportunitat per realitzar un doctorat. En aquell moment, les implicacions d'emprendre un doctorat i el seu significat eren tot un misteri per a mi. No obstant això, sorprenentment, en Sebastià em va dir que hi havia un lloc per a mi. En aquest punt, el meu camí va començar amb el seu suport constant, de la Marilós i del Narcís, cadascun en el seu respectiu àmbit. Gràcies a en Sebastià per donar-me l'oportunitat, el suport i preocupar-se abans per com estic que dels resultats. A la Marilós per donar-me l'oportunitat de donar docència i per debatre els problemes del reactor des d'un punt de vista més d'enginyeria. I, sobretot, a en Narcís, pel seu recolzament constant i per aquells silencis que diuen molt.

M'he considerat afortunada (per sort i esforç constant) de poder gaudir d'aquest aprenentatge sense grans obstacles al laboratori. Fora d'aquest àmbit, s'hi amaguen històries "interessants," com ara perdre un vol a la Xina, i a més, un mes abans de l'arribada de la Covid-19. Al laboratori, vull expressar el meu agraïment, sobretot al suport dels meus companys amb els quals ens recolzàvem mútuament. Des del principi, la Giulia va ser la primera amb la qual vaig començar a treballar al laboratori. Durant tot el doctorat, sobretot vull expressar el meu agraïment per haver conegut la Meri (que sabia el que em passava abans de saber-ho jo mateixa), la Laura, la Sílvia, l'Emma i també les noves incorporacions, tot i que ja sabeu que vaig a poc a poc. Gràcies per aguantar-me a mi i les pèrdues d'aigua dels meus reactors. I de nou, gràcies a en Narcís!

Després de treballar al laboratori envoltada de gent, vaig fer el pas de treballar a la planta pilot de Navata, on la soledat i algunes dificultats em van acompanyar durant un any. Just quan estava totalment aclimatada a la vida a la planta pilot, vaig haver de deixar-la. La meva aventura va continuar a Leipzig, on vaig haver de canviar el xip, ja que els reactors de 2 metres de la planta pilot ara eren mini grànuls de 3 mil·límetres. Thank you Falk and Benni for the guidance during these 3 months and for all the support during the whole Ph.D.

Finalment, vull expressar el meu agraïment a les persones que sempre han estat al meu costat fora del laboratori. Sé que pot semblar un tòpic, però gràcies als meus pares, al meu germà i als meus avis, que durant el confinament no podien entendre per què passava mesos escrivint

un únic article. El meu pare va arribar a preguntar-me si era un article de 100 pàgines! També vull agrair a les meves amigues per aguantar-me malgrat la distància que ens separa. Estic profundament agraïda de poder haver conegut als meus companys de casa i, sobretot, a la meva parella, que ha estat al meu costat durant aquesta última etapa del doctorat. Mario, la teva infinita paciència amb mi és imaginable.

En resum, han estat 4 anys plens de reptes científics, d'alts i baixos, però sobretot, plens de bones persones.

Per finalitzar, dedico a mi mateix aquesta tesi amb gratitud per tota la feina feta, l'esforç i la paciència, i per haver recuperat la confiança en mi mateix cada vegada que semblava que això no acabaria mai. Recorda, Alba del futur, que si hem pogut amb això, no ens pararà res!

Acknowledgements

This work was funded through the European Union's Horizon 2020 project ELECTRA [no. 826244, 2019]. A.C-E. received a PhD grant from the University of Girona (IF_UDG2020) and a mobility grant (IFMOB2021). LEQUIA has been recognised as a "consolidated research group" (Ref 2021 SGR01352) by the Catalan Agency of Research and Universities.

List of contents

List of peer-reviewed publications presented as chapters of Ph.D. thesis

This Ph.D. thesis has been written as published peer reviewed articles compendium based on the specific regulations of the Ph.D. program of the University of Girona.

Peer-reviewed publications submitted as chapters of this thesis:

Ceballos-Escalera, A., Pous, N., Chiluiza-Ramos, P., Korth, B., Harnisch, F., Bañeras, L., Balaguer, M.D., Puig, S., 2021. Electro-bioremediation of nitrate and arsenite polluted groundwater. Water Research. 190, 116748. https://doi.org/10.1016/j.watres.2020.116748

Impact factor: 13.4 (2021, 1st quartile)

Ceballos-Escalera, A., Pous, N., Balaguer, M.D., Puig, S., 2022. Electrochemical water softening as pretreatment for nitrate electro bioremediation. Science of the Total Environment. 806, 150433. https://doi.org/10.1016/J.SCITOTENV.2021.150433

Impact factor: 9.8 (2022, 1st quartile)

Ceballos-Escalera, A., Pous, N., Korth, B., Harnisch, F., Balaguer, M.D., Puig, S. Ex-situ electrochemical characterisation of fixed-bed denitrification biocathodes: a promising strategy to improve bioelectrochemical denitrification. Chemosphere. (Accepted on 10 November 2023) https://doi.org/10.1016/j.chemosphere.2023.140699

Impact factor: 8.8* (2022, 1st quartile)

The chapters of this thesis are ready for submission or have already been submitted as journal articles:

Ceballos-Escalera, A., Pous, N., Balaguer, M.D., Puig, S., Nitrate electro-bioremediation and water disinfection for rural areas.

Ceballos-Escalera, A., Pous, N., Bañeras, L., Balaguer, M.D., Puig, S., Advancing towards electro-bioremediation scaling-up: on-site pilot plant for successful nitrate-contaminated groundwater treatment

List of abbreviations

As(III)	Arsenite
As(V)	Arsenate
BES	Bioelectrochemical systems
CA	Chronoamperometry
$CaCO_3$	Calcium carbonate
CAPEX	Capital expenditure
CE	Counter electrode
CE_{an}	Anodic coulombic efficiency
CE_{cat}	Cathodic coulombic efficiency
CEM	Cation exchange membrane
CV	Cyclic voltammetry
DET	Direct electron transfer
EAMs	Electroactive microorganisms
EET	Extracellular electron transfer
E^f	Formal redox potential
E_{ox}	Oxidative peak potential
E_{red}	Reductive peak potential
F	Faraday constant
H_2	Hydrogen gas
HRT	Hydraulic retention time
HRT_{cat}	Cathodic hydraulic retention time
j	Current density
j_g	Gravimetric current density
K_M^{app}	Apparent nitrate affinity constant
MDC	Microbial desalination cell
MEC	Microbial electrolysis cell
MET	Microbial electrochemistry technology
MET / IET	Mediated/indirect electron transfer
MFC	Microbial fuel cell
N	Nitrogen
N_2	Dinitrogen gas
N_2O	Nitrous oxide
NAC	Net liquid volumes of the anode compartment
Nar	Nitrate reductase
NCC	Net liquid volumes of the cathode compartment
Nir	Nitrite reductase
NO	Nitric oxide
NO_2^-	Nitrite
NO_3^-	Nitrate
Nor	Nitric oxide reductase
Nos	Nitrous oxide reductase
OPEX	Operating expenditures
P	Power
q	Charge
R^2	Coefficient of determination
rAs(III)	Arsenite oxidation rate
$rCaCO_3$	Carbonate removal/precipitation rate
Ref	Reference electrode

rN_2O	Nitrous oxide reduction rate
rNO_2^-	Nitrite reduction rate
rNO_3^-	Nitrate reduction rate
r_{xy}	Pearson correlation coefficient
TEA	Terminal electron acceptor
Ti-MMO	Titanium coated with mixed metal oxide
TRL	Technology readiness level
TOTEX	Total expenditures
v_{max}^{app}	Apparent maximum nitrate uptake rate
WE	Working electrode

List of Tables

List of Figures

Summary

The issue of water stress, notably water pollution, is becoming increasingly alarming. This issue is particularly critical in rural areas where nitrate pollution is increasing, mainly due to modern agricultural and intensive livestock production practices. In addition, limited access to water management services in these regions exacerbates the problem. In such challenging situations, there is an urgent need to move from traditional centralised treatment to more environmentally friendly decentralised solutions. This Ph.D. thesis focuses on the development, optimisation and validation of electro-bioremediation as a promising treatment for nitrate-contaminated groundwater.

This research extends the scope of electro-bioremediation studies from laboratory-scale experiments (TRL 3-4) to an *on-site* pilot plant (TRL 5), addressing the challenges associated with scaling-up bioelectrochemical systems and *on-site* treatment. Efforts at the laboratory-scale were focused on enhancing the treatment's effectiveness and efficiency. These included enhancing the nitrate reduction rate, improving water quality by addressing not only nitrate and nitrite levels but also final disinfection and other co-contaminants such as arsenic, and ensuring cost competitiveness. For this proposal, considerable attention was given to the challenges presented by the reactor configuration as well as by the water matrix, from its low electrical conductivity through the potential presence of co-contaminants to the high hardness of the groundwater. First, a laboratory-scale study achieved a nitrate reduction rate of 2.3 kg NO_3^- $m^{-3}d^{-1}$ (HRT_{cat} 1.5 h), which combined the complete oxidation of arsenite to arsenate at a maximum rate of 90 g As(III) m^{-3} d^{-1}. In a subsequent study, it was enhanced to 5.0 kg NO_3^- $m^{-3}d^{-1}$ (HRT_{cat} 0.7 h) by implementing pH control at 6.75 ± 0.25, which also addressed water disinfection with a free chlorine concentration of up to 4.4 ± 1.4 mg Cl_2 L^{-1}. Notably, to the best of the author's knowledge, this is the highest nitrate reduction rate reported to date. In parallel, *ex-situ* electrochemical characterisation of granular graphite sampled from a running reactor proved to be a powerful tool for understanding its behaviour, highlighting extracellular electron transfer as the limiting step in the denitrification process of the studied biocathode. It also revealed a direct correlation between biocathode performance and pH as well as temperature, with the highest activity observed at pH 6 and 35°C.

Finally, the knowledge gained at laboratory-scale was then applied to the development and operation of an *on-site* pilot plant at Navata (Spain). Three months of continuous operation provided sufficient data to validate electro-bioremediation in a real-world environment (TRL 5), reaching a maximum nitrate reduction rate of 0.9 kg NO_3^- $m^{-3}d^{-1}$ at an HRT_{cat} of 2.0 h with a competitive OPEX cost of 0.40 € m^{-3}. In summary, this thesis represents a significant step towards harnessing the full potential of electro-

bioremediation to address the pressing challenges of nitrate-contaminated groundwater. It sets the foundation for further development of electro-bioremediation at a pilot-scale and encourages further research in this area.

Resum

El problema de l'escassetat d'aigua, especialment la seva contaminació, està esdevenint cada vegada més preocupant. Aquesta qüestió és particularment crítica a les àrees rurals on la contaminació per nitrats està augmentant, principalment a causa de l'agricultura intensiva i la producció ramadera. A més, l'accés limitat als serveis de gestió de l'aigua en aquestes regions agreuja el problema. En aquestes situacions tan complexes, hi ha una necessitat urgent de passar de tractaments centralitzats tradicionals a solucions descentralitzades més respectuoses amb el medi ambient.

Aquesta tesi doctoral es centra en el desenvolupament, optimització i validació de l'electro-bioremediació com a tractament prometedor per a les aigües subterrànies contaminades per nitrats. Aquesta recerca amplia l'abast dels estudis d'electro-bioremediació des d'experiments a escala de laboratori (TRL 3-4) fins a una planta pilot *on-site* (TRL 5), abordant els reptes associats a l'ampliació dels sistemes bioelectroquímics i al tractament *on-site*. Els esforços realitzats a escala de laboratori es van centrar a millorar l'eficàcia i l'eficiència del tractament. Això va incloure millorar la velocitat de reducció de nitrats, millorar la qualitat de l'aigua aprofundint no només els nivells de nitrats i nitrits sinó també la desinfecció final i altres co-contaminants com l'arsènic, a més de garantir la competitivitat econòmica. Per això, es va prestar atenció als reptes plantejats per la configuració del reactor així com per la matriu de l'aigua, des de la seva baixa conductivitat elèctrica fins a la possible presència de co-contaminants i l'alta duresa de l'aigua subterrània. En primer lloc, un estudi a escala de laboratori va aconseguir una velocitat de reducció de nitrats de 2.3 kg NO_3^- $m^{-3}d^{-1}$ (TRH_{cat} de 1.5 h), el qual combinava l'oxidació completa de l'arsenit a arseniat a una velocitat màxima de 90 g As(III) m^{-3} d^{-1}. En un estudi posterior, es va augmentar a 5.0 kg NO_3^- $m^{-3}d^{-1}$ (TRH_{cat} 0.7 h) mitjançant el control del pH a 6.75 ± 0.25, la qual també va abordar la desinfecció de l'aigua amb una concentració de clor lliure de fins a 4.4 ± 1.4 mg Cl_2 L^{-1}. Notablement, fins al millor coneixement de l'autor, aquesta és la velocitat de reducció de nitrats més elevada reportada fins al moment. Alhora, la caracterització electroquímica ex-situ de gränuls de grafit mostrejats d'un reactor en funcionament va demostrar ser una eina potent per comprendre el seu comportament, posant de manifest la transferència d'electrons extracel·lular com a pas limitant en el procés de desnitrificació del biocàtode estudiat. També va revelar una correlació directa entre el seu rendiment i el pH, així com la temperatura, amb una activitat màxima observada a pH 6 i 35 °C.

Finalment, els coneixements adquirits a escala de laboratori es van aplicar al desenvolupament i operació d'una planta pilot *on-site* a Navata (Espanya). Tres mesos d'operació contínua van proporcionar suficients dades per validar l'electro-bioremediació en un entorn real (TRL5), aconseguint

aconseguint una velocitat màxima de reducció de nitrats de 0.9 kg NO_3^- $m^{-3}d^{-1}$ amb un TRH_{cat} de 2.0 h i un cost operacional competitiu de 0.40 € m^{-3}. En resum, aquesta tesi representa un pas significatiu cap a l'aprofitament de tot el potencial de l'electro-bioremediació per fer front als reptes urgents plantejats per les aigües subterrànies contaminades per nitrats. Estableix les bases per al futur desenvolupament de l'electro-bioremediació a escala pilot i encoratja una major recerca en aquest àmbit.

Resumen

El problema de la escasez de agua, especialmente su contaminación, se está volviendo cada vez más alarmante. Esta cuestión es particularmente crítica en las áreas rurales donde la contaminación por nitratos está aumentando, principalmente debido a la agricultura intensiva y la producción ganadera. Además, el acceso limitado a los servicios de gestión del agua en estas regiones agrava el problema. En tales escenarios desafiantes, la transición de los métodos de tratamiento convencionales centralizados a soluciones descentralizadas más rentables y respetuosas con el medio ambiente se vuelve urgente.

Esta tesis doctoral se centra en el desarrollo, optimización y validación de la electro-biorremediación como un tratamiento prometedor para las aguas subterráneas contaminadas por nitratos. Esta investigación amplía el alcance de los estudios de electro-biorremediación desde experimentos a escala de laboratorio (TRL 3-4) hasta una planta piloto *on-site* (TRL 5), abordando los desafíos asociados con la ampliación de los sistemas bioelectroquímicos y el tratamiento *on-site*. Los esfuerzos a nivel de laboratorio se centraron en mejorar la eficacia y eficiencia del tratamiento. Esto incluyó mejorar la velocidad de reducción de nitratos, mejorar la calidad del agua abordando no solo los niveles de nitratos y nitritos, sino también la desinfección final y otros co-contaminantes como el arsénico, y garantizar la competitividad económica. Para este propósito, se prestó considerable atención a los desafíos presentados por la configuración del reactor y la matriz del agua, desde su baja conductividad eléctrica hasta la posible presencia de co-contaminantes y la alta dureza del agua subterránea. En primer lugar, un estudio a escala de laboratorio logró una velocidad de reducción de nitratos de 2.3 kg NO_3^- $m^{-3}d^{-1}$ (TRH_{cat} de 1.5 h), que incluyó la completa oxidación del arsenito a arseniato una velocidad máxima de 90 g As(III) m^{-3} d^{-1}. En un estudio posterior, se aumentó a 5.0 kg NO_3^- $m^{-3}d^{-1}$ (TRH_{cat} 0.7 h) mediante el control del pH a 6.75 ± 0.25, el cual también abordó la desinfección del agua con una concentración de cloro libre de hasta 4.4 ± 1.4 mg Cl_2 L^{-1}. Notablemente, hasta donde llega el conocimiento del autor, esta es la velocidad de reducción de nitratos más alta reportada hasta la fecha. Paralelamente, la caracterización electroquímica *ex-situ* de gránulos de grafito muestreados de un reactor operativo demostró ser una herramienta poderosa para comprender el comportamiento de un biocátodo, mostrando la transferencia extracelular de electrones como el paso limitante en el proceso de desnitrificación del biocátodo estudiado. También reveló una correlación directa entre su rendimiento y el pH, así como con la temperatura, observándose una actividad máxima a pH 6 y 35 °C.

Finalmente, los conocimientos adquiridos a nivel de laboratorio se aplicaron al desarrollo y operación de una planta piloto *on-site* en Navata (España). Tres meses de operación continua proporcionaron

suficientes datos para validar la electro-biorremediación en un entorno real (TRL 5), logrando una velocidad máxima de reducción de nitratos de 0.9 kg NO_3^- $m^{-3}d^{-1}$ con un TRH_{cat} de 2.0 h y un costo competitivo de operación de 0.40 € m^{-3}. En resumen, esta tesis representa un paso significativo hacia el aprovechamiento del potencial completo de la electro-biorremediación para abordar los desafíos planteados por las aguas subterráneas contaminadas por nitratos. Establece las bases para el futuro desarrollo de la electro-biorremediación a escala piloto y alienta una mayor investigación en este ámbito.

CHAPTER 1:

Introduction

1.1. Water scarcity and groundwater contamination: challenges to safe drinking water accessibility

Water scarcity is a global concern, driven primarily by a decline in the availability of safe water sources. Alarming indicators highlight the need to intensify efforts in the water sector, such as the mentioned in Figure 1. Nearly two-thirds of the global population experience severe water scarcity for at least one month every year (UNICEF, 2021), which significantly restricts access to safe drinking water and hampers basic hygiene practices, leading to social, economic, and environmental consequences. Population growth and the subsequent increase in water demand are key contributing factors to this issue. Moreover, the contamination of freshwater bodies, with 40% of this resource exhibiting inadequate quality, exacerbates the problem by diminishing the availability of safe drinking water (UN Water, 2021). Consequently, 10% of the global population resides in countries facing critical water stress, where the water demand exceeds the available amount during specific periods or when quality standards are not fulfilled (FAO and UN Water, 2021). Recognising the urgency of the situation, the United Nations has adopted the 2030 Agenda, encompassing the goal of universal access to safe drinking water (SDG 6, A/RES/70/1). This objective seeks to address the 2 billion people who still lacked proper water management in 2020. Efforts to achieve this goal are particularly necessary in rural areas, where the coverage of safely managed water services is 60% compared to 86% in urban areas (WHO and UNICEF, 2021).

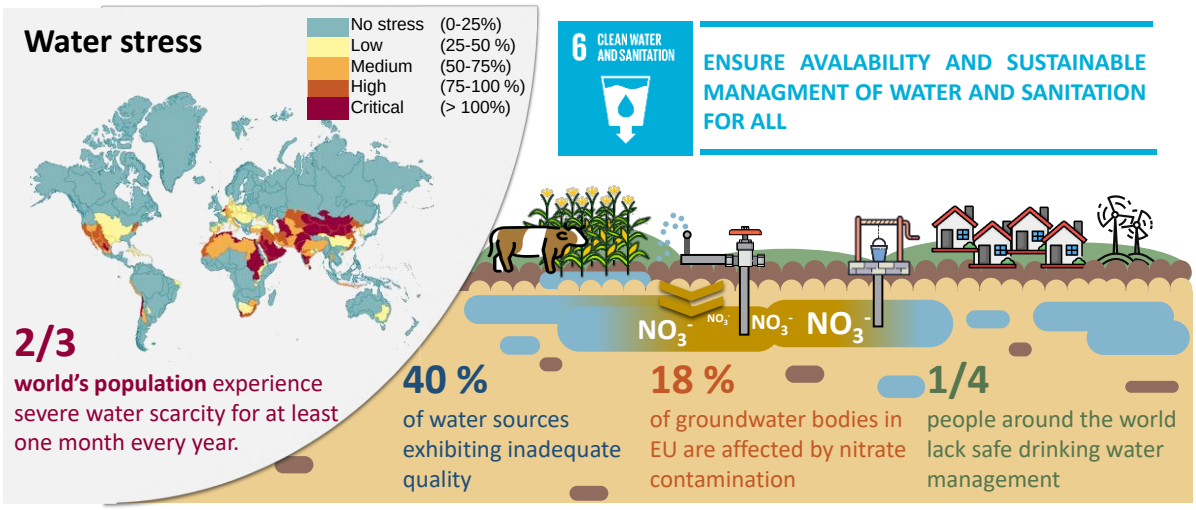

Figure 1: Water scarcity problematic and some indicators (EEA, 2018; FAO and UN Water, 2021; UN Water, 2021; WHO and UNICEF, 2021). The map provides a global representation of the level of water stress spatially disaggregated by major river basin. It is calculated as the ratio between the amount of total freshwater resources withdrawn in the three economic sectors (Agriculture, Service and Industry) and the total renewable freshwater resources after detracting the amount of water needed to support existing environmental services ("FAO AQUAMAPS, Level of water stress (SDG 6.4.2) by major river basin," 2022).

In rural areas, groundwater is particularly susceptible to contamination from modern agricultural and livestock practices. Specifically, the application of fertilisers to enhance agricultural productivity, alongside inadequate disposal of animal manure, contributes to approximately 81% of the nitrogen applied infiltrating into groundwater (European Commission, 2021; Shukla and Saxena, 2020; Suthar et al., 2009). Consequently, exemplifying this trend, 18% of the groundwater bodies in Europe in 2018 were contaminated by nitrate (NO_3^-) (EEA, 2018) (Figure 1). This contamination poses a significant threat to the overall quality and safety of freshwater resources, making them unsuitable for human consumption. Long-term exposure to elevated nitrate concentrations can cause serious health risks, such as methemoglobinemia (blue baby syndrome) or stomach cancer (Picetti et al., 2022). Moreover, nitrate can also be reduced and accumulated as nitrite, and both compounds serve as precursors for the endogenous formation of N-Nitroso compounds, known carcinogens and teratogens (Ward et al., 2018). For this reason, the European Directive 2020/2184 sets a nitrate concentration limit of 50 mg NO_3^- L^{-1} and 0.5 mg NO_2^- L^{-1} to ensure safe drinking water quality.

Although nitrate is one of the most prevalent groundwater contaminants, it is also essential to recognise that numerous other pollutants can significantly influence water quality. These pollutants, whether accumulated by human activity or naturally (e.g., erosion of sediments), can adversely affect human health and the environment (Li et al., 2021). Some examples of contaminants that can be found in water include various nutrients and organic compounds like chlorinated solvents, hydrocarbons, and polycyclic aromatic hydrocarbons. In addition, inorganic compounds such as heavy metals and metalloids (including arsenic) may also be present, as well as other emerging contaminants such as pesticides and pharmaceuticals (Pradhan et al., 2023). Additionally, water can serve as a passive carrier for numerous pathogens, including viruses, bacteria, protozoa, and larvae (Ashbolt, 2004). Overall, the implementation of comprehensive strategies for monitoring, managing, and treating pollutants is vital to ensure the long-term protection and sustainability of groundwater resources, ultimately providing clean and safe drinking water for present and future generations.

1.2. Decentralised nitrate-contaminated water treatment: available conventional technologies

Universal access to safe water relies on two fundamental aspects: the availability of fresh and safe water sources or the implementation of appropriate water treatment methods to address contamination. Currently, large centralised water treatment plants play a significant role in decontaminating water and providing safe drinking water to urban populations. Nevertheless, in certain situations, like in rural areas, centralised water treatment can be prohibitively expensive due to the need for large

infrastructures. As a result, untreated natural water sources are often used in these areas with lower access to safe water services (Peter-Varbanets et al., 2009).

Decentralised water treatment systems are a viable solution to increase access to treated water in areas where centralised systems are not practical due to high costs or low population density. These systems treat water on a smaller scale and can be easily implemented in remote areas where centralised infrastructure is lacking (Rabaey et al., 2020). Specifically, decentralised treatment systems for nitrate removal are essential in rural areas, as they are characterised by intensive agriculture and livestock practices that directly contribute to groundwater contamination. Furthermore, these decentralised systems can also contribute to the technological transition within the water sector by promoting innovative and sustainable water treatment approaches, integrating advanced technologies and methods that enhance efficiency, reduce energy consumption, and minimise environmental impacts. There are various decentralised treatment methods, including conventional and emerging approaches, to address the issue of nitrate contamination in water. These methods aim to effectively remove or reduce the concentration of nitrates in water, ensuring safe drinking water (Table 1).

Table 1: Overview of the main advantages and challenges of the common traditional water treatment methods able to remove nitrates while ensuring safe drinking water quality. Additionally, electro-bioremediation is presented as an alternative treatment.

		Advantages	Challenges	References
Conventional treatments				
Physical methods	**Reverse osmosis (RO)**	High efficiency Widely implemented	High energy demand: RO: 0.9 - 6.1 kWh m^{-3} ED: 1.1 – 1.5 kWh m^{-3} Brines generation Water fraction rejection	(Bosko et al., 2014; Liu et al., 2017; Mohsenipour et al., 2014; Rezvani et al., 2017; Twomey et al., 2010)
	Electrodialysis (ED)			
	Ion Exchange resin		Resin regeneration is needed Brines generation	
Chemical methods	**Activated metals (e.g., zero-valent iron)**	Low energy demand Low-cost Low-maintenance	Low selectivity (i.e. ammonia and nitrite as end-products) Continuous chemical demand Metal sludge production Acidic conditions to increase efficiency (pH < 2-3)	(Xu et al., 2012; Zhu and Getting, 2012)
	Photocatalysts	Low energy demand No-brines generation	Low selectivity (i.e. ammonia and nitrite as end-products) High cost of catalysts	(Yang et al., 2022; Zhao et al., 2020)
Biological denitrification		Low energy demand High selectivity to N_2	Sludge production in heterotrophic denitrification (up to 0.8 g SSV $g^{-1}N$) Continuous chemical demand (e.g., organic matter or H_2)	(Rezvani et al., 2019; Vandekerckhove et al., 2018; Zhao et al., 2022)
Alternative and novelty methods				
Electro-bioremediation		Low energy demand: 0.15 kWh m^{-3} High selectivity to N_2	Not yet applied in real environments Challenges on scalability	(Cecconet et al., 2020; Pous et al., 2017)

1.2.1. Physicochemical removal methods

Several popular and conventional treatment technologies are available for nitrate removal, including reverse osmosis, electrodialysis, and ion exchange. These methods only involve the physical separation of the nitrate through a membrane or adsorption to specific materials. These conventional methods are widely employed in the water sector, as they reduce nitrate pollution and address other contaminants present in groundwater to ensure drinking water quality. Although these conventional treatments for nitrate removal are effective, it is crucial to consider their associated costs, challenges and environmental sustainability (Table 1). These treatments often require significant energy consumption. For instance, reverse osmosis, which requires high pressure to facilitate the separation process, exhibits an energy consumption ranging from 0.9 to 6.1 kWh m^{-3} (Twomey et al., 2010). Furthermore, the regeneration of adsorbents and the disposal of concentrated brines that are generated during the treatment process also pose environmental challenges and incur additional costs (Rezvani et al., 2019).

Alternatively, chemical methods can be employed to remove nitrate from groundwater. The process involves continuous dosing of chemical reducing agents, such as active metals and hydrogen (Fanning, 2000). One approach is nitrate reduction using activated metals like zero-valent iron or magnesium. However, metal powder can be difficult to separate after this treatment. Active metal particles may simplify the separation process but also have their own complexities (Feng et al., 2022). An alternative method involves photocatalysts that utilise semiconductor materials (e.g., titanium oxide) to reduce nitrates using light. This approach replaces chemical agents with catalysts, but these are often expensive (Tugaoen et al., 2017). Both procedures can be used as decentralised treatments to convert nitrate into less harmful nitrogen species. However, the poor selectivity of the mentioned chemical methods may generate undesired products like ammonium and nitrite (Pasinszki and Krebsz, 2020).

1.2.2. Biological removal technologies

Biological technologies provide a cost-effective alternative to chemical catalysts in nitrate removal. These technologies involve the use of microorganisms, which can selectively reduce nitrate into harmless dinitrogen gas (N_2) through the denitrification process (Zhao et al., 2022). Denitrification involves a sequence of four reduction steps, progressing from nitrate to nitrite (NO_2^-), then to nitric oxide (NO) and on to nitrous oxide (N_2O), ultimately to dinitrogen gas (N_2). These steps correspond to redox potentials of +0.32, -0.04, +0.98, and +1.15 V vs. Ag/AgCl at pH 7 (Figure 2D). Overall, 5 moles of electrons are required per mole of nitrate for the conversion to dinitrogen gas. This is a respiratory process to gain energy that is catalysed by four types of nitrogen reductases in sequence, each responsible for the reduction of a specific intermediate: nitrate reductase (Nar), nitrite reductase (Nir),

nitric oxide reductase (Nor) and nitrous oxide reductase (Nos) (Vilar-Sanz et al., 2018; Zhong et al., 2021; Zumft, 1997). These enzymes are either situated in the periplasm or bound to the plasma membrane (Bleam, 2017).

Over 60 genera of Bacteria and Archaea, along with some Eukaryotes, have been identified as autotrophic and heterotrophic denitrifiers (Canfield et al., 2010). Most of these denitrifiers are facultative anaerobes that can use nitrate or denitrification intermediates as electron acceptors in the respiratory process (Knowles, 1982). In heterotrophic denitrification, organic matter serves as both the electron donor and carbon source. On the other hand, autotrophic microorganisms employ hydrogen, reduced sulphur, or other compounds as electron donors coupled with bicarbonate or carbon dioxide as a carbon source. The effectiveness and selectivity of the treatment in both scenarios depend on the presence and availability of an electron donor. The high selectivity of biological reduction in achieving complete denitrification, wherein nitrate is converted to dinitrogen gas (an inert gas), stands as a significant advantage. Otherwise, incomplete denitrification leads to the accumulation of denitrification intermediates such as nitrite, nitrous oxide and ammonium, which pose greater risks. The selectivity may be affected by different parameters. The electron donor is the major factor affecting the nitrate reduction efficiency and selectivity (Zhao et al., 2022). Therefore, achieving the proper ratio between nitrogen and the electron donor is crucial for completing denitrification, ensuring its availability and bioavailability. However, there are other factors that influence the selectivity. High dissolved oxygen levels can hinder denitrification enzymes like Nar or Nir, potentially altering bacterial biofilm composition (Gómez et al., 2002; Wang and Chu, 2016). The enzymatic activities are also significantly influenced by pH, with Nar and Nir exhibiting optimal pH levels at 7.5 and 6.5, respectively (Stevens et al., 1998). In parallel, other parameters, such as temperature, influence microbial activity as well as the hydrolysis of substrates, especially those containing complex organic matter (Wang and Chu, 2016). Finally, the contact time of the microorganism with the nitrate (i.e., the hydraulic retention time, HRT, in continuous feed treatments) significantly influences denitrification and its selectivity. Biological treatments typically operate with an HRT in the range of hours (Liu et al., 2020; Zhai et al., 2017).

Several bioreactor configurations have been developed to enable both heterotrophic and autotrophic denitrification, comprising setups with suspended microorganisms and biofilm-based systems. Suspended sludge systems are relatively simple and commonly employed in wastewater treatment plants. However, biofilm-based systems (e.g., packed and fluidized beds) typically have longer biomass retention times, which contribute to increased effectiveness (Wu et al., 2021). Packed bioreactors typically use porous carrier materials that provide a large attachment-specific surface area for microbial growth. For instance, a study using a degradable polymer as an electron donor and biofilm support

achieved a nitrate reduction rate of 1.5 kg NO_3^- $m^{-3}d^{-1}$ at HRT between 5 to 7 h (Chu and Wang, 2017). Fluidised beds, where the support is fluidised at high recirculation rates, provide an approach to overcome the mass transfer limitations that sometimes exist in packed bed reactors with minimal pressure drop. This method has shown high nitrate reduction rates (e.g., sulphur-based autotrophic denitrification achieved 2.7 kg NO_3^- $m^{-3}d^{-1}$ at HRT of 1 h) (Gu et al., 2024).

These treatments rely on adequate electron donors inherently present in the contaminated water or added externally. Particularly in groundwater, the availability of electron donors is constrained, lacking both organic matter and specific inorganic sources. It is, therefore, necessary to add electron donors (organic matter or inorganic electron donors) to facilitate denitrification through continuous chemical dosing. Heterotrophic denitrification requires the addition of organic matter. If the aim is to potabilise nitrate-polluted groundwater, a readily metabolisable pure source, such as acetate or ethanol, is required. Additionally, the uncontrollable growth of these heterotrophic bacteria results in sludge production as a residue that must be separated and disposed of. Furthermore, providing other reduced compounds like hydrogen may present challenges, primarily due to their low solubility. Finally, the continuous chemical addition can alter the chemical characteristics of the water, presenting challenges for its use as drinking water. Overall, this underlines the need for a new approach to provide a more suitable electron donor.

1.3. Electro-bioremediation: a promising new decentralised treatment for nitrate removal?

Conventional nitrate removal methods present challenges that restrict their implementation as sustainable decentralised water treatment, including their reliance on chemicals, high-energy costs, brine generation and/or low selectivity. As a result, there is a growing need for technologies that address these challenges by being cost-effective and environmentally friendly for decentralised nitrate treatment. In this context, electro-bioremediation has emerged as a potential sustainable water treatment approach based on microbial electrochemical technologies (MET). Indeed, electro-bioremediation of nitrate is an attractive alternative that uses a cathode to provide an unlimited electron donor.

1.3.1. Microbial electrochemical technologies: from electroactive microorganisms to their potential applications

A primary MET, a subfield of bioelectrochemical systems (BESs), merges microbiology, electrochemistry, chemical engineering and electronics (Schröder et al., 2015). Within primary MET, electroactive microorganisms (EAMs) can perform various redox reactions, acting as biocatalysts by

connecting their metabolic activities to an external electric circuit. This reduces the use of chemicals by utilising an electrode as an unlimited source of either electron donors (cathode) or electron acceptors (anode). Typically, the anode and cathode electrodes are made of solid conductive materials connected through an external electric circuit. The oxidation of an electron donor takes place in the anode compartment, whereas the reduction of an electron acceptor occurs in the cathode compartment. In some BES setups, an ion exchange membrane divides the two compartments to create two different environments for better control of the respective reactions.

EAMs are found as either planktonic microorganisms or forming a biofilm over the electrodes (or conductive materials). EAMs exchange electrons with electrodes through extracellular electron transfer (EET), and their mechanisms and efficiency are crucial for the performance of BESs. Two main EETs are described, as shown in Figure 2B: direct electron transfer (DET) or mediated/indirect electron transfer (MET / IET). For DET, EET occurs through direct contact between microorganisms and electrodes using surface proteins such as porin-cytochrome complexes, cell-surface exposed cytochromes, as well as other redox proteins like copper and iron-sulphur proteins (Costa et al., 2018). DET can also work through cellular appendages such as pili or conductive nanowires. Alternatively, MET or IET occurs through the utilisation of electron shuttles that mediate the exchange of electrons between EAMs and the electrode. These molecules can be oxidised and reduced, enabling them to act as electron carriers in multiple redox reactions. Common examples of electron shuttles include quinones, flavins, humic substances, and conductive polymers (Brutinel and Gralnick, 2012; Wang et al., 2022) and also some by-products (e.g., H_2 and formate). Planktonic microorganisms can perform EET via IET by utilising soluble electron shutters or DET by occasional contact with the electrode through punctual collisions. Meanwhile, biofilms are composed of polymeric substances that contribute to both IET (accumulating electron shuttles near the electrode) (Xiao et al., 2017) and DET, ensuring uninterrupted contact between the microorganism and the electrode.

The microbial energy harvest has an important role in those target redox reactions, the EET, and how EAMs link them to their metabolism. In microbial electron transport chains, electrons are transferred from a low-potential electron donor to a higher-potential electron acceptor, generating an ion gradient used for ATP synthesis (Anraku, 1988). The energy gain depends on the redox potential difference (ΔE) between the electron donor and the electron acceptor. EAMs appear to be unable to conserve energy between the electrode potential and the formal redox potential (E^f) of the electron carrier involved in EET (Korth and Harnisch, 2019; Kracke et al., 2015; Rosenbaum et al., 2011). Nevertheless, the electrode potential directly impacts the redox reactions and their kinetics in the system (Korth and

Harnisch, 2019). Although the available information supports this hypothesis for anodic reactions, knowledge about electron uptake from a cathode is limited.

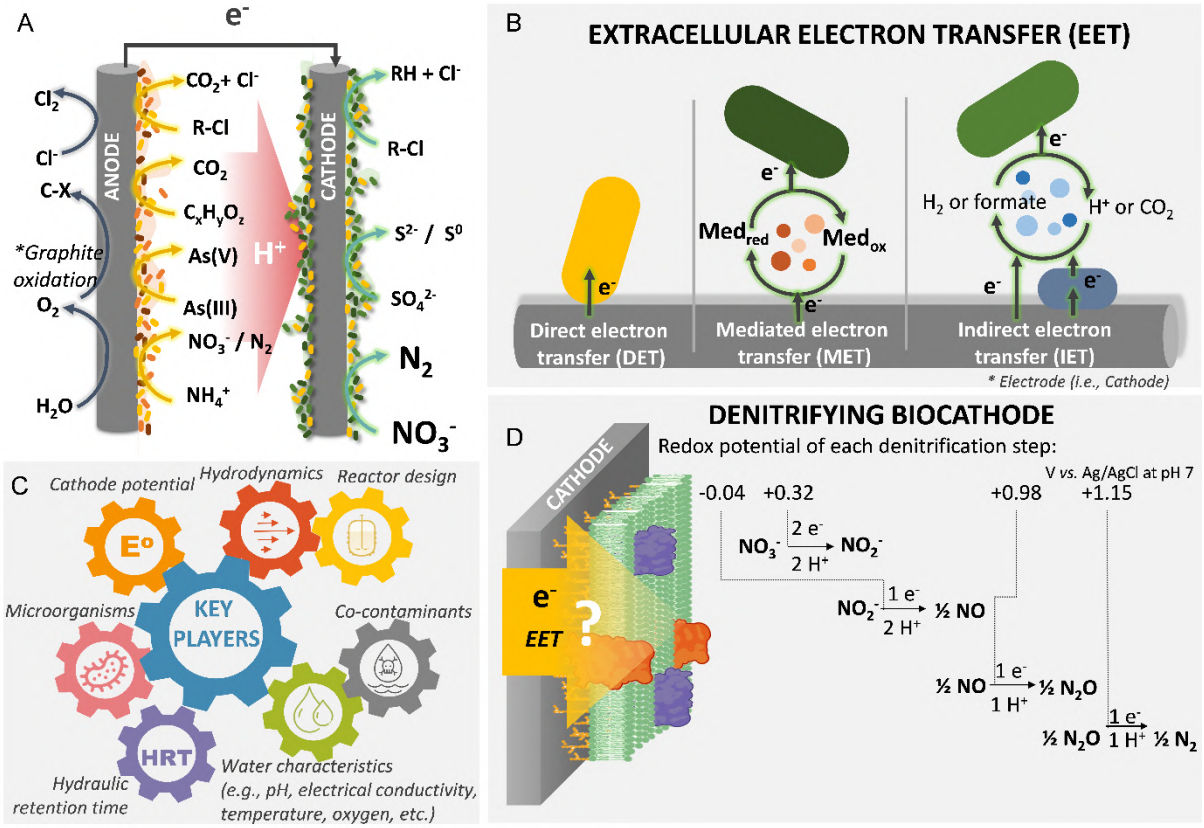

Figure 2: (A) Summary of the electrochemical reactions of some pollutants that may coexist with nitrate. (B) Main mechanism of extracellular electron transfer in a biocathode. (C) Key players in denitrification performance (D) Overview of denitrifying biocathode mechanisms showing the main denitrification reactions.

This unique capability of EAMs to use solid electrodes as unlimited electron acceptors/donors and perform specific redox reactions opens up a wide range of applications in environmental engineering across various fields, including sustainable energy production, environmental remediation, sustainable production, and resource recovery. Early METs were developed to recover energy from wastewater through the oxidation of organic matter in microbial fuel cells (MFCs) (Liu and Logan, 2004; Logan et al., 2006). Subsequently, the technology was further developed for other applications that required minimal energy consumption (microbial electrolysis cells, MECs). Some such as (i) the production of high added-value products such as hydrogen, methane, or volatile fatty acids in MECs (Batlle-Vilanova et al., 2014; Dessì et al., 2021; Villano et al., 2010), (ii) low-cost desalination in microbial desalination cells (MDCs) (Cao et al., 2009), (iii) water or soil remediation through the removal or recovery of inorganic and organic compounds in electro-bioremediation processes (Figure 2A) (Aulenta et al., 2010; Choi et al., 2009; Pous et al., 2018a) and (iv) development of biosensors (Kaur et al., 2013).

1.3.2. Denitrifying biocathode and bioelectrochemical system for nitrate reduction.

Within the broad scope of MET applications, electro-bioremediation has emerged as a promising and sustainable approach to address worldwide concerns regarding nitrate-contaminated groundwater. When nitrate reduction is the target reaction, autotrophic denitrification is performed by EAMs using only the cathode as an electron donor and inorganic carbon as the carbon source (Clauwaert et al., 2007). The cathode, together with the associated EAMs responsible for denitrification, is commonly known as a denitrifying biocathode. Bioelectrochemical denitrification follows the principles of conventional biological denitrification, as mentioned above, but with the cathode serving as the electron donor for the sequential reduction of nitrate to nitrogen gas (Figure 2D).

One option for utilising a denitrifying biocathode is through MFCs, where organic matter is oxidised in the anode and nitrate is reduced in the cathode, generating an electric current (Puig et al., 2012; Virdis et al., 2008; Wang et al., 2016). However, this method could only be suitable for nitrate-contaminated waters presenting high organic matter concentrations or if a secondary residue with a high organic content is available nearby. In the case of groundwater, which is characterised by low organic matter, MECs can be used supported by other oxidations (Figure 2A), such as water oxidation (Cecconet et al., 2018; Pous et al., 2017). These types of systems offer interesting advantages in the field of water treatment, particularly in decentralised approaches. The primary advantage lies in the fact that the sole consumable resource required for the treatment is electricity, which can be provided by renewable sources (Rovira-Alsina et al., 2021). Furthermore, there is no water rejection as the system effectively uses the same water in both the anode and cathode compartments and cleaning periods are unnecessary. This is an important improvement over some conventional treatments, such as membrane separation, which reject some of the treated water and require some cleaning steps. This feature is important for future developments in water treatment in the context of water scarcity.

Electro-bioremediation is a versatile treatment approach that can also effectively address nitrate even with the presence of other co-contaminants in the matrix. For instance, it has been observed that nitrate reduction can coexist with reductive dechlorination of cis-dichloroethylene and sulphate reduction (Lai et al., 2015). Furthermore, electro-bioremediation is able to use anodic reactions to efficiently oxidise a wide range of contaminants, including substances such as metals and metalloids (e.g. arsenite), inorganic nutrients (e.g. ammonium), and chlorinated and aromatic hydrocarbons (e.g. vinyl chloride) (Botti et al., 2023; Lai et al., 2015; Nguyen et al., 2016b). Anodic oxidations can also be employed to address the disinfection of the final water by producing chlorine or other radicals (e.g., hydroxyl radicals) (Bergmann, 2021; Botti et al., 2023; Puggioni et al., 2021).

1.3.3. Key players on the denitrifying biocathode performance

The denitrifying biocathode is a complex system that integrates a microbial community with electrochemical reactions. The colonisation of the cathode typically occurs through selective pressure, utilising mixed inoculums such as those obtained from wastewater plants and sediments (Gadegaonkar et al., 2023). Consequently, a wide variety of microorganisms are identified in denitrifying biocathodes, most of them belonging to the ß-*Proteobacteria* class (Rogińska et al., 2023). In fact, different characteristics of microbial communities impact biocathode performance. Alongside the microbial community, denitrifying biocathode performance (i.e., nitrate reduction efficiency, rate and final product selectivity) is also mainly influenced by the electrochemical conditions, water matrix and operating parameters. Determining the ideal operational parameters and anticipating specific variable impacts can, therefore, be challenging.

The cathode potential should be carefully selected to promote the growth of denitrifying EAMs. The cathode potential plays a crucial role in determining the feasible redox reactions, reducing the occurrence of side reactions. Cathode potentials ranging from -0.32 (Pous et al., 2017) to -0.90 V *vs*. Ag/AgCl (Nguyen et al., 2016c) have been reported to be suitable for denitrifying biocathodes. Under lower potentials, bioelectrochemical hydrogen production may compete with nitrate reduction. Although denitrifiers can also use H_2 as an electron donor (hydrogenotrophic denitrification), this process is expected to present a lower efficiency due to the low solubility of H_2. Finding the right cathode potential is critical to achieving a balance between EAM growth, nitrate reduction and energy efficiency in denitrifying biocathodes. Electrochemical characterisation through voltammetry studies provides insights into the electrochemical behaviour and formal potentials of denitrifying biocathodes. Literature has revealed various formal redox potentials associated with denitrifying biocathodes, which can vary based on the microbial community composition and operational conditions. These differences highlight the complexity of denitrifying biocathodes and their dependence on various factors. For instance, Pous et al. (2014) showed two formal potentials at -0.300 V and -0.700 V *vs*. Ag/AgCl (pH 8) of a biocathode mainly formed by *Thiobacillus* spp. Other studies reported electroactive redox sites at -0.374 V *vs*. Ag/AgCl (pH 7) for a denitrifying biofilm mainly covered by *Geobacter* (Pous et al., 2016), or -0.487 V and -0.406 V *vs*. Ag/AgCl (pH 7) in the case of a microbiome composed of *Pseudomonas nitroreducens* and *Paracoccus versutus* (Korth et al., 2022). In parallel, Gregoire et al. (2014) identified two formal potentials at -0.240 V and -0.450 V *vs*. Ag/AgCl (pH 7) in a biocathode predominant by Betaproteobacteria, including *Rhodocyclales* and *Burkholderiales*. These potentials correspond to either a single or multiple redox cofactors and are associated with the electron transfer from the cathode to the binding and reduction of the nitrate within cells, which is recognised as the limiting step.

The water matrix can also significantly influence the denitrifying biocathode performance. The oxygen that may be present in the water can directly compete with the nitrate as a terminal electron acceptor since the formal potential of oxygen reduction (+0.86 V *vs*. Ag/AgCl at pH 7) is higher than nitrate reduction (+0.78 V *vs*. Ag/AgCl at pH 7). Hence, anoxic conditions are preferred to suppress O_2 competition. However, this competition does not permanently damage the biocathode, as the microbiome consists of facultative anaerobes (Chen et al., 2006; Yang et al., 2018). Regarding temperature, groundwater can naturally emerge between 2 and 20 °C (Tissen et al., 2019), significantly impacting denitrification activity, which is negligible below 5 °C and increases until a maximum of around 25-30 °C (Skiba, 2008). The pH also plays a crucial role in bioelectrochemical systems since the pH affects not only microbial activity but also the thermodynamics of denitrification. As the redox reaction involves H^+, the formal potential is pH-dependent according to the Nernst equation. Determining an optimal pH for bioelectrochemical denitrification is challenging due to the diverse configurations and microorganisms involved. As a result, optimal pH values have been reported over a wide range, from neutral (Clauwaert et al., 2009) to pH 11-12 (Albina et al., 2021). Normally, pH balance in these systems relies on cathodic reactions consuming protons (e.g., nitrate reduction) and anodic reactions generating protons (e.g., water oxidation), which migrate from the anode to the cathode through an ion exchange membrane. Additionally, the low groundwater electrical conductivity, typically below 1 mS cm^{-1}, can further limit proton diffusion from the anode to the cathode. Consequently, bioelectrochemical denitrification is negatively impacted in terms of efficiency and selectivity due to this low conductivity. This limitation results in the dominance of certain overpotentials within the system, including pH gradients and energy losses associated with ion transport resistances (Puig et al., 2012). Another challenge in treating groundwater is the high levels of hardness, which can irreversibly damage the biocathode by forming scale on the cathode surface. Finally, other pollutants, such as sulphate, that may be present in the water may also compete with nitrate reduction (Nguyen et al., 2016a). Therefore, coexisting contaminants should be carefully considered and managed to ensure effective denitrification in water treatment processes.

In addition to the factors mentioned earlier, other crucial operational parameters in the treatment process include the hydrodynamics inside the reactor and the HRT. In continuous flow mode, the HRT determines the time available for microorganisms to denitrify. Studies, such as the one by Pous et al. (2017), have reported a minimum cathodic hydraulic retention time (HRT_{cat}) of 0.46 h in denitrifying bioelectrochemical systems. Specifically, in this study, this short HRT increased substrate availability and improved water distribution, resulting in a maximum nitrate removal rate of 0.85 kg N m^{-3} d^{-1} (3.7 kg NO_3^- m^{-3} d^{-1}). Proper water distribution is crucial for the operation of a reactor to avoid heterogeneity in the nitrate distribution, other essential ions (e.g., protons) as well as biofilm formation and

distribution, as this can lead to inactive "dead zones" (Vilà-Rovira et al., 2015). These considerations gain even more relevance when low-conductivity waters, such as groundwater, are considered.

1.3.4. Challenges for nitrate electro-bioremediation implementation

Electro-bioremediation has shown promising results in the treatment of nitrate-contaminated groundwater at the laboratory-scale with encouraging outcomes (Technology Readiness Level, TRL 3-4) (Clauwaert et al., 2009; Molognoni et al., 2017; Pous et al., 2017, 2013). However, the transition to real implementation and commercialisation relies on the scaling-up bottleneck. Unfortunately, less than 1% of the studies performed using MET have addressed the challenge of scaling-up (Jadhav et al., 2022a). The existing gap between laboratory-scale expectations and pilot-scale studies highlights the need to increase the research effort to gain knowledge in this area.

Simply increasing the volume of the reactors, a common approach used to scale-up biological water treatment reactors, will not effectively address the scalability problem in METs (Jadhav et al., 2022a). Due to the inherent complexity of the system, the employment of modular reactors that can be connected electrically and hydraulically in series or parallel configurations provides a flexible and scalable approach to address this challenge (Baeza et al., 2017; Dekker et al., 2009; Flimban et al., 2019). Several factors must be addressed to transfer the good performances observed at the laboratory-scale to the pilot-scale, such as the distance between electrodes, redox potential distribution, electrode materials and water distribution (Kadier et al., 2020; Rossi and Logan, 2022). The distance between electrodes plays a crucial role in determining the ohmic resistances within the system. In consequence, short distances between electrodes reduce the overall resistance. For instance, short electrode distances facilitate the migration of important ions (e.g., protons) towards the cathode (Kondaveeti et al., 2017; Wu et al., 2022). Besides, electrode materials and their stability, biocompatibility, electrical conductivity and economic cost are critical aspects of reactor design. (Jadhav et al., 2022b). Carbon-based materials are often preferred for METs due to their lower cost and biocompatibility. However, some of these materials, such as granular graphite, have lower electrical conductivity compared to metal-based electrodes (e.g., stainless steel, titanium). This difference can lead to a heterogeneous distribution of the redox potential across the electrode surface (Quejigo et al., 2018). This non-uniform distribution, as well as the water distribution, has a direct impact on the performance of the system, particularly on the pilot-scale.

Additionally, several other parameters must be considered for a successful transition from laboratory-scale to real-world implementation and commercialisation. The evaluation and optimisation of the technology under realistic conditions is one of the key guidelines to achieve this transition. This involves considering specific water characteristics (Dell'Armi et al., 2022) and addressing the less controlled

conditions associated with on-site treatment and long-term operations. Despite the complexity and challenges associated with METs scaling-up, some successful trials provide indications for *on-site* application and future commercialisation (Cusick et al., 2011; Jadhav et al., 2020; Prado de Nicolás et al., 2022). To increase the number of successful attempts at larger scales, it is crucial to further expand the knowledge in this field. Besides, it is important to thoroughly assess the economic viability, social and water authorities' acceptances, and environmental effects of the technology during the pilot-scale validation process. These considerations are essential to ensure the continued feasibility of the treatment and its potential for future implementation.

CHAPTER 2:

Research objectives and outline of this thesis

Electro-bioremediation is a promising decentralised treatment process for addressing concerns related to nitrate-contaminated groundwater. However, the main challenge in implementing electro-bioremediation lies in scaling-up the technology and validating its feasibility in real environments. **This Ph.D. thesis seeks to facilitate the progression of nitrate electro-bioremediation from the laboratory to real-world applications. This transition will provide crucial insights and knowledge gained at the laboratory-scale for its successful application to an *on-site* pilot facility** (Figure 3).

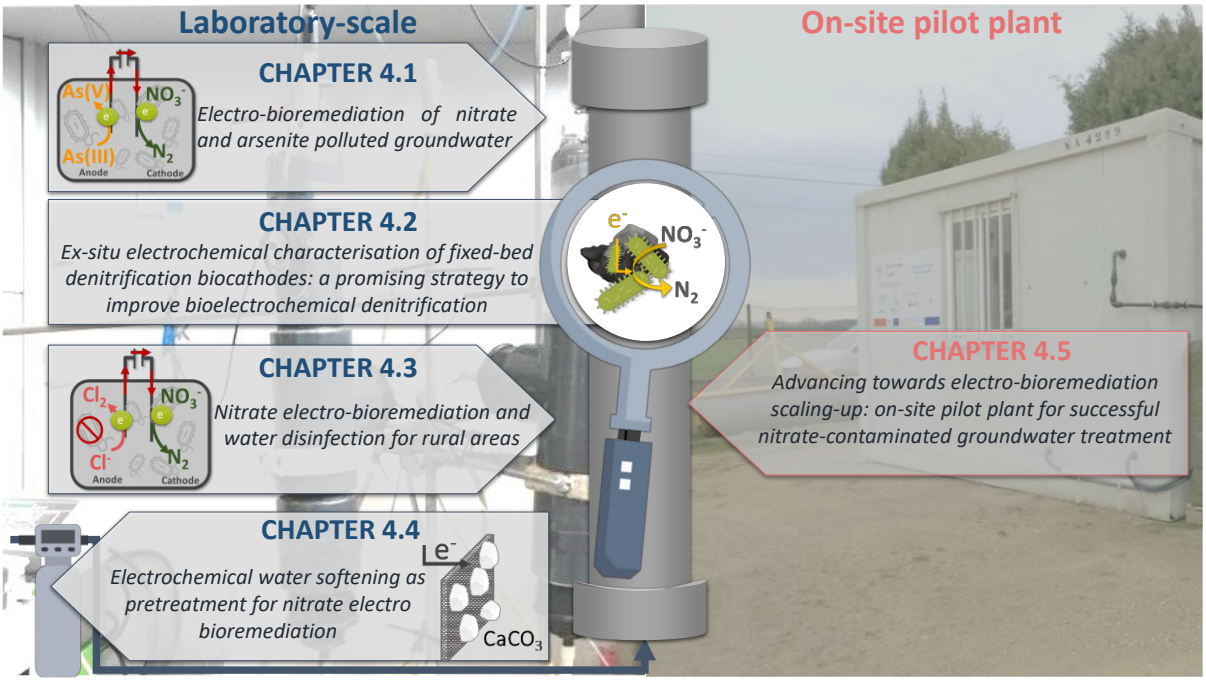

Figure 3: Schematic overview of the presented thesis. The chapters are divided into laboratory-scale studies (*Chapters* 4.1-4.4) and on-site pilot-scale (*Chapter* 4.5).

The main research questions of this thesis were:

(i) **Is nitrate electro-bioremediation a competitive water treatment? How can it become more effective?**

Electro-bioremediation holds significant promise as a sustainable approach to the remediation of nitrate-contaminated groundwater. By combining electrochemical and biological processes, it offers a versatile method for efficiently removing nitrates and various contaminants from groundwater. However, improving the nitrate reduction rate is essential to make this treatment more competitive. This thesis included both laboratory-scale investigations (*Chapters* 4.1 to 4.4) and pilot-scale experiments (*Chapter* 4.5) with the aim of understanding and optimising the treatment rate in more realistic conditions. At the same time, other key aspects, such as economic costs and water quality, have been assessed throughout the thesis. This holistic approach aims to provide relevant results to assess the potential of electro-bioremediation as a decentralised water treatment solution.

(ii) Can electro-bioremediation offer a solution to the concurrent presence of arsenic and nitrate in water?

The coexistence of multiple contaminants is an exacerbated problem in groundwater contamination. In the field of electro-bioremediation, current studies often focus on treating contaminants individually rather than considering the coexistence of different contaminants. This limited focus on individual contaminants may not reflect the complex reality of groundwater contamination. Therefore, it is necessary to develop a treatment that is capable of treating more than one contaminant and to explore the synergistic or antagonistic effects of different contaminants. Specifically, *Chapter* 4.1 of this thesis evaluates the coexistence of arsenite and nitrate in the same water matrix. The aim is to explore the potential of electro-bioremediation for the simultaneous remediation of both contaminants.

(iii) How can *ex-situ* electrochemical characterisation be used to understand and optimise the performance of a denitrifying biocathode?

The electrochemical characterisation of a denitrifying biocathode is a valuable tool for understanding and potentially guiding the operation of denitrifying bioelectrochemical reactors, ultimately improving their performance and effectiveness in nitrate removal. However, the electrochemical fingerprint of each bioelectrochemical reactor is different. Therefore, a simple methodology for analysing each denitrifying biocathode is essential. *Chapter* 4.2 evaluates an *ex-situ* electrochemical characterisation method designed to analyse inoculated granular graphite from the biocathode of a running bioelectrochemical denitrifying reactor. This methodology aims to streamline the electrochemical characterisation process within a relatively short timeframe and with minimal disruption to the operation of the reactor. The ultimate goal is to understand the mechanism and performance of the biocathode under study.

(iv) Can groundwater disinfection and nitrate reduction be effectively addressed within a single electro-bioremediation reactor?

Water disinfection is a crucial requirement for ensuring drinking water quality. However, it often involves additional steps in biological treatments, thereby increasing overall treatment costs. Moreover, in decentralised treatment scenarios, such as remote areas, the transportation of disinfection agents can pose challenges. Therefore, an integrated treatment approach that incorporates disinfection within electro-bioremediation can be an attractive solution. This approach is investigated at a laboratory-scale in *Chapter* 4.3, involving nitrate reduction through the denitrifying biocathode and disinfection through the production of free chlorine in the anodic compartment.

(v) Can electrochemical water softening be considered a sustainable treatment for the reduction of hardness ions prior to the application of the electro-bioremediation process?

High levels of hardness ions in groundwater pose a significant challenge for implementing electro-bioremediation, as scale formation can cause irreversible damage to the system. Conventional treatments for water softening have associated environmental impacts that need to be addressed in order to become a sustainable solution. In this context, electrochemical water softening offers several advantages that warrant further exploration. *Chapter* 4.4. aims to explore the development of an electrochemical softener as a suitable pretreatment for a denitrifying bioelectrochemical reactor.

(vi) Can bioelectrochemical systems be successfully scaled-up? Are there constraints on their performance when they are operated *on-site*?

Scaling-up bioelectrochemical systems is currently a challenge. The existing gap between laboratory-scale expectations and pilot-scale studies highlights the need for increased knowledge and research efforts in this area. When operating in the field, the performance of the system may be affected by the complexity of the real-world environment and treatment expectations. Therefore, modifications to the design and optimisation of the system at pilot-scale are often required to ensure efficient mass transfer, appropriate electrode spacing, effective management of biofilm growth, and to replicate the laboratory results in terms of nitrate removal rates and efficiencies. *Chapter* 4.5 aims to address these challenges by carefully consolidating and applying the knowledge gained in the previous chapters at the laboratory-scale (TRL 3-4, *Chapters* 4.1 to 4.4). *Chapter* 4.5 aspires to validate electro-bioremediation in a real-world environment (TRL 5) by evaluating the treatment of nitrate-contaminated groundwater in a pilot plant.

CHAPTER 3:

Materials and methods

3

3.1 General consideration

The redox potential was consistently reported in reference to the Ag/AgCl sat. KCl electrode (+0.197 V vs. SHE at 25 °C), which serves as the standard reference electrode in all experimental setups. Unless otherwise stated, the operational temperature was maintained at room temperature (25 ± 1 °C). All chemicals used in this work were obtained from Sigma-Aldrich (Germany), Merck Life Science (Spain and Germany) or Sharlab S.L. (Spain).

Over the entire thesis, where the reactors were operated in continuous flow mode, a minimum of 3 replicates at different time points were considered to perform the study. The reported values are presented as the averages of these replicates, along with their corresponding standard deviations. This approach ensures the robustness and reliability of the experimental data by taking into account the variability observed over time.

3.2 Reactors setup and operation

Four different reactor configurations were used during the experiments, ranging from laboratory-scale to pilot-scale. Table 2 summarises the reactors and their main characteristics corresponding to the respective chapters of the thesis.

<table>
<tr><th></th><th>Location and scale</th><th colspan="2">Reactors and operation</th><th>Denitrifying inoculum</th><th>Influent water</th></tr>
<tr><td>Ch 4.1</td><td rowspan="4">Off-site and laboratory-scale</td><td rowspan="4"><u>Reactor</u>:
Tubular denitrifying bioelectrochemical reactor
<u>Operation</u>:
CA: WE at -0.32 V vs. Ag/AgCl</td><td rowspan="2"><u>Reactor</u>: eClamp
<u>Operation</u>:
CA: WE at -0.32 V vs. Ag/AgCl
CV: scan rate of 1 mV s^{-1}</td><td rowspan="3">Effluent from a BES reactor</td><td>Synth. NO_3^- and As(III) contaminated groundwater</td></tr>
<tr><td>Ch 4.2</td><td rowspan="2">Synth. NO_3^- contaminated groundwater</td></tr>
<tr><td>Ch 4.3</td><td rowspan="2"><u>Reactor</u>: Electrochemical water softener
<u>Operation</u>:
CA: WE at -1.20 V vs. Ag/AgCl</td></tr>
<tr><td>Ch 4.4</td><td rowspan="2">Real NO_3^- contaminated groundwater</td></tr>
<tr><td>Ch 4.5</td><td>On-site
Pilot-scale</td><td colspan="2"><u>Reactor</u>: Denitrifying bioelectrochemical pilot plant
<u>Operation</u>: Fixed cell potential from 1.20 to 1.77 V</td><td>Effluent and enriched culture from BES reactor</td></tr>
</table>

Table 2: Summary of the location and scale, main reactor configuration, electrical operation, denitrifying inoculum, and feeding utilised in each chapter of the thesis. Ch: Chapter; WE: Working electrode; CA: Chronoamperometry; CV: Cyclic voltammetry; Synth.: Synthetic.

3.2.1 Tubular denitrifying bioelectrochemical reactor

This Ph.D. thesis evaluated two primary setups for the tubular bioelectrochemical reactor, which presented two different anode materials: (i) granular graphite or (ii) titanium coated with mixed metal

oxide (Ti-MMO). Their main configuration and characteristics are presented in Figure 4. Both tubular BES reactors were assembled using a polyvinyl chloride tubular structure (PVC, diameter of 55 mm and length of 350 mm). The cathode (inner part) and anode (outer part) compartments were separated with a tubular cation-exchange membrane (CEM, CMI-7000, Membranes Int., USA) with an internal diameter of 45 mm (*Chapters* 4.1, 4.2 and 4.4) or 40 mm (*Chapter* 4.3).

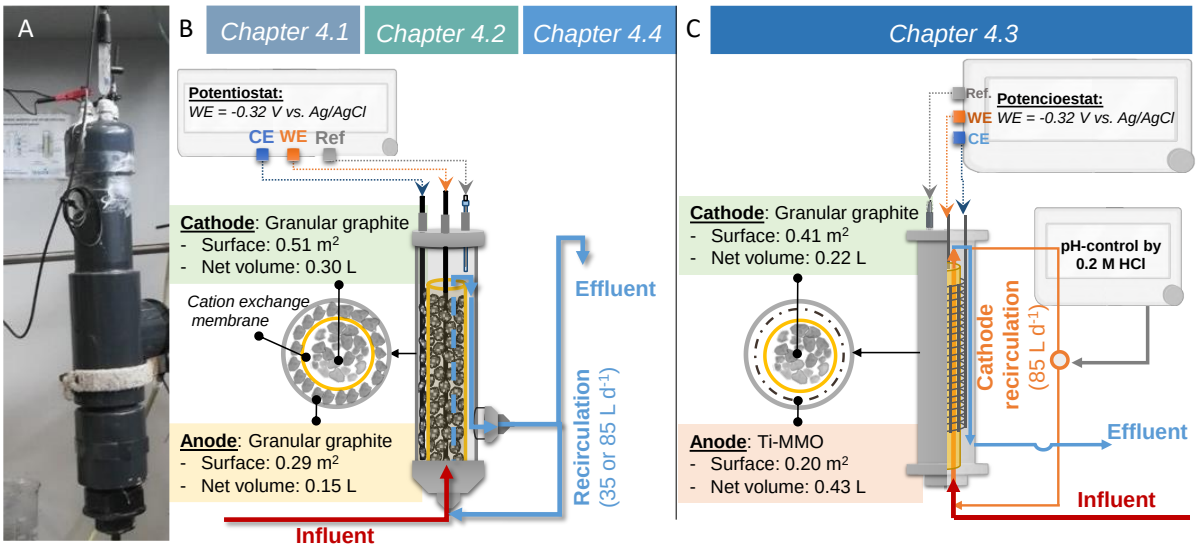

Figure 4: (A) Image of the tubular denitrifying bioelectrochemical reactor. (B) Process outline and scheme of the reactor that utilised granular graphite as both electrodes. (C) Process outline and scheme of the reactor that utilised granular graphite as the cathode and Ti-MMO as the anode electrode.

The cathode compartment was filled with granular graphite (diameter 1.5-5 mm, enViro-cell, Germany; previously washed with 1 M HCl and 1 M NaOH), and graphite rod (8 x 400 mm Mersen Ibérica, Spain) was used as the current collectors. As for the anode, two different electrode materials were used. Granular graphite was used in *Chapters* 4.1, 4.2 and 4.4 to sustain the biofilm formation or as a sacrificial anode. In contrast, cylindrical Ti-MMO mesh (45 mm diameter, 0.5 mm thickness and 200 mm length, Special Metals and Products, SL, Spain) was used in *Chapter* 4.3 to promote chlorine formation. The compartments filled with granular graphite had a fixed bed porosity of 50% in the initial reactor assembly. Consequently, in *Chapters* 4.1, 4.2 and 4.4, the net liquid volumes of the cathode (NCC) and anode (NAC) compartments were 0.30 L and 0.15 L, respectively. While in *Chapter* 4.3, where the anode was substituted with Ti-MMO, the NCC was 0.22 L, and the NAC was 0.43 L. For estimating the electrode surface area of the granular graphite, spherical particles with an average diameter of 3.25 mm and a fixed bed porosity of 50% were assumed. As a result, the cathode surface was estimated to be 0.51 m^2 in *Chapters* 4.1, 4.2, and 4.4, while in *Chapter* 4.3, it was 0.41 m^2. As for the anode of granular graphite in *Chapters* 4.1, 4.2, and 4.4, its surface area was determined to be 0.29 m^2. In *Chapter* 4.3, the Ti-MMO anode surface was 0.20 m^2.

Additionally, the reactors were equipped with an Ag/AgCl sat. KCl reference electrode (+0.197 V vs. standard hydrogen electrode, SHE, SE 11, Xylem Analytics Germany Sales GmbH & Co. KG Sensortechnik Meinsberg, Germany) resulting in a three-electrode setup (working electrode, WE; counter electrode, CE; and reference electrode, Ref). In *Chapters* 4.1 to 4.4, the cathode potential was poised at -0.32 V using a potentiostat (VSP, BioLogic, France) to drive complete nitrate reduction to dinitrogen gas, according to previous knowledge (Pous et al., 2015b).

The reactors were operated in continuous flow mode with various HRTs, treating synthetic groundwater (*Chapters* 4.1, 4.2 and 4.3) or real groundwater after the electrochemical softening (*Chapter* 4.4). Sampling was performed after a waiting period of 3 HRT to achieve pseudo-stationary conditions. . In addition, samples were consistently collected when the current density remained stable. Overall, each modification was run for at least 5 days, with a minimum of 3 samples recorded. The cathode and anode were hydraulically connected in all cases. The influent was pumped vertically upward through the cathode compartment and overflowed at the top into the anode compartment. Subsequently, it circulated from the top to the bottom of the anode compartment, where the effluent was located. In *Chapters* 4.1, 4.2, and 4.4, a fraction of the effluent was recirculated to the influent to increase internal flow (Figure 4) at a recirculation flow rate of 35 L d^{-1} or 85 L d^{-1}. In *Chapter* 4.3, a fraction of the cathodic effluent was recirculated to the cathodic influent at a flow rate of 85 L d^{-1}. In both scenarios, the increase of the internal fluid velocity reinforced the mass transfer of substrate and counter ions from the bulk liquid to the inner biofilm layers. It also decreased the possible dead zones, increasing homogeneity inside the reactor. In addition, *Chapter* 4.3 included the installation of a pH probe in the recirculation line to control the cathodic pH at 6.8 ± 0.2.

3.2.2 eClamp

In *Chapter* 4.1 and more extensively in *Chapter* 4.2, electrochemical analysis of the individual granules sampled from the operational denitrifying bioelectrochemical reactors was conducted using an adapted version of the eClamp (Figure 5). The eClamp was originally introduced by Quejigo et al. (2018) and later modified by Korth et al. (2022). The eClamp comprised four spring steel wires (1.4310, Febrotec GmbH, Germany) arranged to form a mechanically movable gripper encased by a PEEK tube. The eClamp was used to collect 3 to 5 granules from the upper part of the cathode compartment of the bioelectrochemical fixed-bed reactor. The electrochemical experiments were performed in a four-neck round-bottom flask (Lenz Laborglas GmbH & CO.KG, Germany) containing 300 mL of fresh medium. The eClamp was utilised as the working electrode, and a graphite rod (diameter 10 mm, length 50 mm, Mersen Ibéria, Spain) served as the counter electrode. The setup was complemented with an Ag/AgCl sat. KCl reference electrode (SE 11, Xylem Analytics Germany Sales GmbH & Co. KG Sensortechnik

Meinsberg, Germany). Additionally, a pH and temperature probe (Multimeter 44, Crison, Spain) were included. A magnetic stirrer was set at 120 rpm to avoid diffusion limitations, and continuous N_2 sparging was applied to maintain an anoxic environment. The temperature was controlled at 25 °C using an external heating circuit around the round-bottom flask.

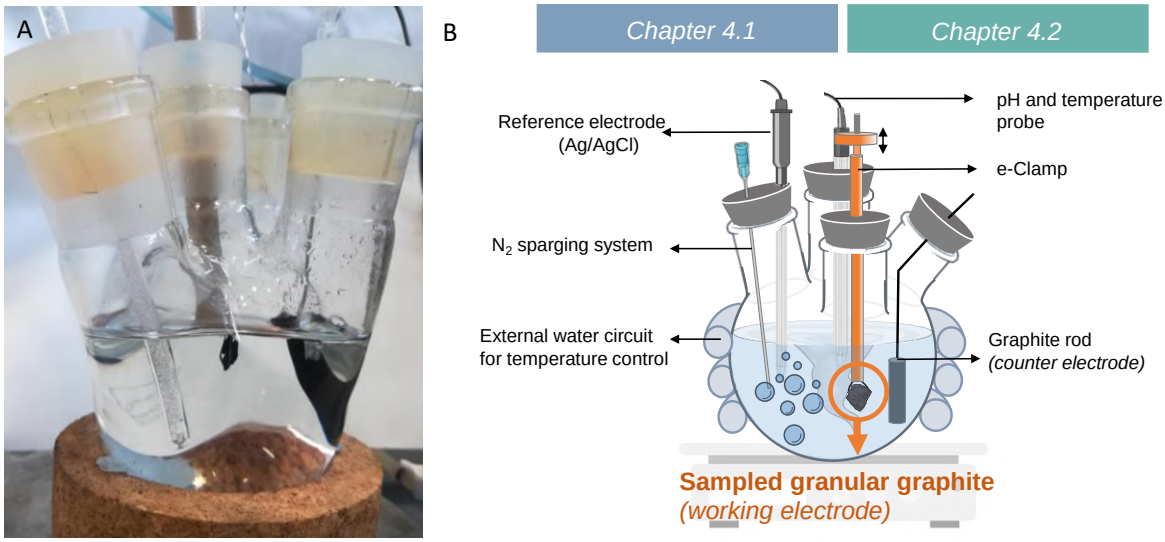

Figure 5: (A) Image and (B) process outline and scheme of the eClamp setup.

The electrochemical characterisation of the granular graphite was conducted using both non-turnover and turnover conditions under chronoamperometry (CA) and cyclic voltammetry (CV) techniques. In *Chapters* 4.1 and 4.2, the working electrode was poised at -0.32 V to study the denitrifying performance at this potential. Additionally, in *Chapter* 4.1, the arsenite oxidation was also studied at a potential of +0.30 V. These different potentials allowed for the investigation of specific electrochemical processes and behaviours related to denitrification and arsenite oxidation, respectively. Furthermore, CA was performed in both chapters until a stable current density was reached before conducting CVs. The CV experiments were carried out at a scan rate of 1 mV s^{-1}, scanning through different potential ranges to study the electrochemical behaviour and characteristics of the granular graphite electrodes.

3.2.3 Electrochemical reactor for water softening

In *Chapter* 4.4, electrochemical water softening was initially tested on a small scale as a preliminary study to gather information for reactor design. The preliminary study assembled different configurations: single- and two-chambers. For the single-chamber setup, a three-neck bottle with a total volume of 250 mL was utilised. In the two-chamber setup, an H-type configuration with a total volume of 250 mL was employed, where the anode and cathode were separated by a cation exchange membrane (2×10^{-4} m^2, CEM, CMI-7000, Membranes Int., USA). In both configurations, the cathode was constructed using stainless steel mesh with a surface area of 1.5×10^{-2} m^2 (1.0 mm of the light path

and 0.4 mm of wire diameter, CISA, Spain), while the anode was a Ti-MMO electrode rod (225 × 6 mm, NMT electrodes, South Africa). Recirculation flow of 15 L d^{-1} was applied to the whole setup (single-chamber setup) or to the cathodic chamber (two-chamber setup) to improve the hydrodynamics and promote mass transfer. The setups were equipped with an Ag/AgCl sat. KCl reference electrode (+0.197 V *vs*. SHE, SE 11, Xylem Analytics Germany Sales GmbH & Co. KG Sensortechnik Meinsberg, Germany). A power source (TENMA 72–2715, Farnell, Spain) was used to control the cathode potential at -0.60 V or -1.20 V, depending on the test.

Following the preliminary test results, a single-chamber reactor with internal dimensions of 20 x 20 x 3 cm and a working volume of 1.2 L was utilised for continuous electrochemical water softening in *Chapter* 4.4. Figure 6 provides a schematic representation of the reactor setup. The cathode and the anode were separated by an interelectrode gap of 15 mm. The cathode was constructed using two stainless steel mesh layers (20 x 20 cm^2 each layer, 1 mm mesh sizes, and 0.4 mm wire diameter, CISA, Spain) with a total surface area of 0.2 m^2. The anode consisted of titanium coated with mixed metal oxide mesh (Ti-MMO mesh, 10 x 10 cm^2, 2 mm light path, and 1 mm wire diameter, NMT electrodes, South Africa) with a total surface area of 6.3 10^{-2} m^2. The electrode surfaces were calculated by considering each individual mesh wire. The reactor was equipped with an Ag/AgCl sat. KCl reference electrode (+0.197 V vs. SHE, SE 11, Xylem Analytics Germany Sales GmbH & Co. KG Sensortechnik Meinsberg, Germany).

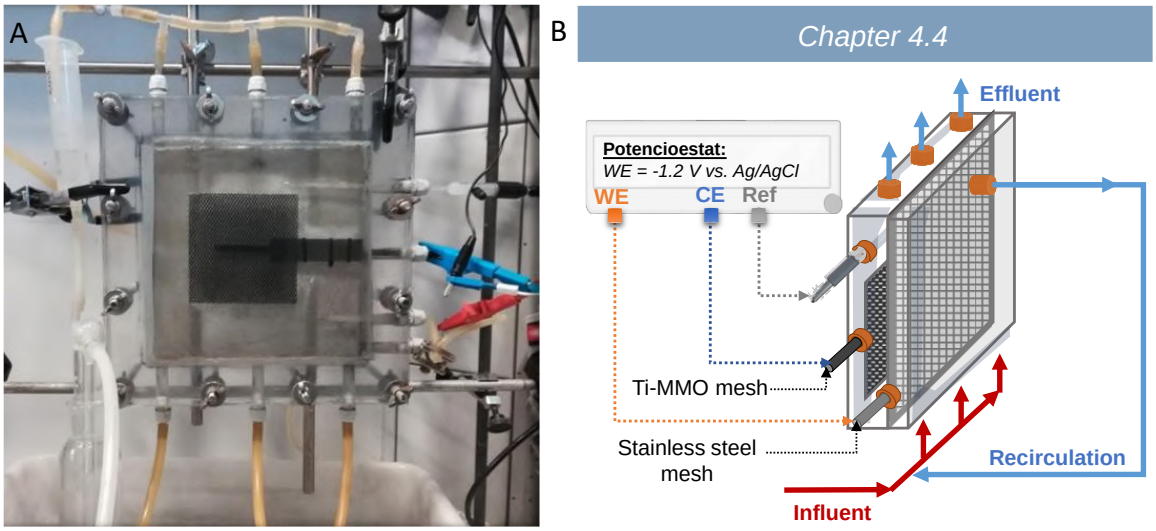

Figure 6: (A) Image and (B) process outline and scheme of the electrochemical softener.

The reactor was operated in continuous flow mode at an HRT of 4.1 h (flow rate of 7.1 L d^{-1}). The influent was pumped upward through three different points to ensure accurate flux distribution. Additionally, a recirculation flow rate of 50 L d^{-1} was applied to improve mass transfer and hydrodynamics. The operation consisted of two periods: (i) precipitation and (ii) detachment. During the precipitation

period, the system operated in chronoamperometry mode with a cathode potential of -1.20 V. In the detachment period, polarity reversal cycles were implemented to detach and recover the precipitates from the cathode surface. The working electrode (cathode) was switched to an anode to remove the precipitates formed on its surface. During polarity reversal, the influent was stopped, and the working electrode was poised at +1.20 V for 10 minutes. Following the detachment step, the medium was replaced with effluent to reset the operating conditions before starting the next precipitation period.

3.2.4 Denitrifying bioelectrochemical pilot plant

In *Chapter* 4.5, a denitrifying bioelectrochemical pilot plant was housed in a container located in Navata (Figure 7A), a rural area in Spain with a population of 1,465 inhabitants in 2022. The pilot plant consisted of two 1 m^3 tanks to store water directly extracted from a contaminated well. Additionally, a third 1 m^3 tank was used to store the water after undergoing softening treatment by an ion-exchange resin softener (Concept earth line +100, Concept, Spain) before the treatment in the denitrifying bioelectrochemical reactor.

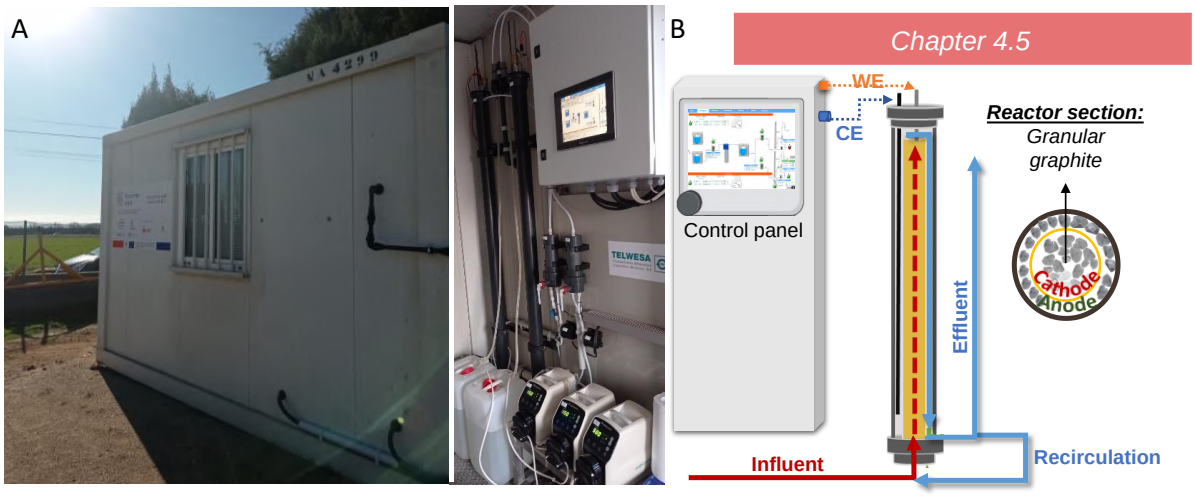

Figure 7: (A) Image and (B) process outline and scheme of the electrochemical pilot plant located in Navata.

The denitrifying bioelectrochemical reactor was a compact tubular fixed-bed reactor constructed using a polyvinyl chloride tubular structure (PVC, 6.0 cm diameter and 1.7 m length). The cathode (inner part) and anode (outer part) compartments were separated by a tubular cation-exchange membrane (diameter 4.5 cm, Catex membranes Ralex®, MEGA, Czech Republic) (Figure 7B). Both compartments were filled with granular graphite (average diameter of 3.25 mm, enViro-cell, Germany) with a bed porosity of 50%, resulting in a NCC of 1.2 L and a NAC of 0.9 L. The estimated cathode surface was 2.2 m^2, and the anode surface was 1.7 m^2, assuming that granular graphite was spheres with an average diameter of 3.25 mm. To ensure correct current and potential distribution along the column, a titanium

rod (6 x 2100 mm, Ti Gr1 ASTM B348, Special metals and products, Spain) and mesh (45 x 2000 mm, Ti Gr2 ASTM B265, Special metals and products, Spain) were installed in the cathode. Additionally, a titanium mixed metal oxide rod (Ti-MMO, Special metals and products, Spain) was introduced in the anode, serving as the anode current collector. The reactors were equipped with an Ag/AgCl sat. KCl reference electrode (+0.197 V vs. SHE, SE 11, Xylem Analytics Germany Sales GmbH & Co. KG Sensortechnik Meinsberg, Germany). The system was electrically operated by fixing the potential difference between the anode and the cathode using a power supply in the range of 1.20 to 1.77 V while keeping the cathode potential within a range from -0.23 ± 0.03 to -0.67 ± 0.03 V.

The reactor continuously treated real groundwater at different HRTs, each for a minimum duration of 7 days. Similar to the operation in the laboratory-scale, the cathode and the anode were hydraulically connected (Figure B). The influent was pumped directly upwards through the cathode compartment, and then it overflowed at the top, entering the anode compartment. It circulated from the top to the bottom of the anode compartment, where a recirculation tank (1.0 L) was positioned before the water was discharged from the system. A portion of the effluent was recirculated to the influent using a second pump at a flow rate of either 100 L d^{-1} or 150 L d^{-1}, depending on the operational period.

3.3 Inoculation procedures

As an inoculation medium, the effluent from a running denitrifying bioelectrochemical reactor was mixed with synthetic groundwater at different percentages (20% in *Chapters* 4.1 and 4.3 on the laboratory-scale and 50% in *Chapter* 4.5 on the pilot-scale). In *Chapter* 4.5, the effluent from this reactor was previously enriched by periodically sparging CO_2:H_2 (80:20%, AirLiquide, Spain). This enrichment process aimed to increase the microorganism content and reduce the inoculation period, ensuring a more efficient and effective start of the continuous operation. In *Chapter* 4.1, the objective was also to establish a community capable of oxidising arsenic. To achieve this, an autotrophic arsenite-oxidising inoculum was obtained by incubating samples from different contaminated sites in the province of Girona, Spain, under aerobic conditions with constant aeration.

The biological reactors were initially inoculated in batch mode before continuous operation by recirculating 2 L of medium containing denitrifying electroactive microorganisms (*Chapters* 4.1 and 4.3). The inoculums were mixed in different proportions with fresh medium (synthetic groundwater) depending on the specific reactor configuration and requirements. During the batch operation, the main objective was to develop a denitrifying microbiome. The cathode potential was poised at -0.32 V in *Chapters* 4.1 to 4.4 and -0.38 ± 0.19 V in *Chapter* 4.5. These potentials were previously established as sustainable to promote denitrification (Pous et al., 2015b). The performance of the inoculation was

monitored by following the concentration of target contaminants and the current density of the systems. To sustain denitrification, the medium in batch mode was either replaced or supplemented with additional nitrate, serving as the primary electron acceptor whenever low values were detected. The inoculation period concluded when the current density reached stable values, indicating the successful development of the denitrifying microbiome.

3.4 Synthetic groundwater and real groundwater characteristics

This Ph.D. thesis utilised various types of water for experimentation, including synthetic groundwater (both non-buffered and buffered) and real groundwater sourced from Navata, Spain.

In *Chapters* 4.1 to 4.4, non-buffered synthetic groundwater was utilised to simulate potential real-world scenarios. The composition of the non-buffered synthetic groundwater included 203.9 mg L^{-1} $NaNO_3$ (33 mg N-NO_3^- L^{-1}) as the main contaminant, 420.0 mg L^{-1} $NaHCO_3$ as inorganic carbon source, 7.5 mg L^{-1} KH_2PO_4, 1.9 mg L^{-1} Na_2HPO_4, 100.0 mg L^{-1} NaCl, 75.2 mg L^{-1} $MgSO_4 \times 7H_2O$, 10.0 mg L^{-1} NH_4Cl and 0.1 mL L^{-1} of a trace minerals solution (Balch et al., 1979). This resulted in a neutral pH and electrical conductivity of around 1.3 mS cm^{-1}. In addition, 10% effluent from a running denitrifying bioelectrochemical reactor was added to simulate the microorganism content of real groundwater. Besides, specific modifications were made to the medium for each experiment. In *Chapter* 4.1, the medium was supplemented with 8.7 mg L^{-1} of $AsNaO_2$ (equivalent to 5 mg As(III) L^{-1}). In *Chapter* 4.2, the electron acceptor (nitrate) underwent various changes, including alteration of concentration (from 0 to 50 mg N-NO_3^- L^{-1}) and testing of other denitrification intermediates, such as nitrite and nitrous oxide, either individually or together with nitrate.

In *Chapter* 4.2, more buffered synthetic groundwater was utilised as well to ensure optimal conditions, including stable pH and higher buffer capacity. The buffered synthetic groundwater solution comprised 1.05 g L^{-1} $NaHCO_3$ as an inorganic carbon source, 1.07 g L^{-1} KH_2PO_4, 0.16 g L^{-1} Na_2HPO_4, 0.25 g L^{-1} NaCl, 0.1 g L^{-1} $MgSO_4 \times 7H_2O$, 0.01 g L^{-1} NH_4Cl and 0.1 mL L^{-1} of a trace minerals solution (Balch et al., 1979), resulting in an initial pH of 7.0 and electric conductivity of 3.0 mS cm^{-1}.

Finally, in *Chapters* 4.4 and 4.5, real groundwater was treated. The main characteristics of the groundwater were as follows: 8.3 ± 0.4 pH, 0.8 ± 0.1 mS cm^{-1}, 92.0 ± 7.2 mg NO_3^- L^{-1}, 0.2 ± 0.4 mg NO_2^- L^{-1}, 35.5 ± 4.0 mg SO_4^{2-} L^{-1}, 1.4 ± 6.7 mg PO_4^{3-} L^{-1}, 0.2 ± 0.3 mg NH_4^+ L^{-1} and 4.2 ± 4.0 mg K^+ L^{-1}. In *Chapter* 4.5, the real groundwater was pretreated using an ion-exchange resin softener (Concept earth line +100, Concept, Spain) to reduce the water hardness from 300 to 45 ± 25 mg $CaCO_3$ L^{-1}.

3.5 Analytic methodologies

Liquid samples were collected periodically throughout the entire thesis, usually 2-3 times per week, and were analysed following the APHA standard water measurements (APHA, 2005). The pH and electrical conductivity of the samples were measured with a pH-meter (pH-meter basic 20+, Crison, Spain) and a conductivity meter (EC-meter basic 30+, Crison, Spain), respectively. The ion content of all samples, previously filtered through a 0.2 µm Nylon filter, was analysed using ionic chromatography (ICS 5000, Dionex, USA). Specifically, nitrate (NO_3^-), nitrite (NO_2^-), chloride (Cl^-), and arsenate (As(V)) were examined, while cations such as ammonium (NH_4^+), calcium (Ca^{2+}), and magnesium (Mg^{2+}) were analysed less frequently. In *Chapter* 4.1, total arsenic was analysed by adding an oxidising agent (100 mM $KMnO_4$) to oxidise all arsenic forms into arsenate fully. Arsenite (As(III)) concentration was calculated as the difference between total arsenic and arsenate. Three measurements of arsenic forms were obtained to ensure an accurate arsenic balance: Total arsenic, arsenite, and arsenate. Nitrous oxide (N_2O) was measured periodically using a N_2O liquid-phase microsensor (Unisense, Denmark) located in the effluent of the reactors.

Specific analyses were also performed in *Chapter* 4.2. Free chlorine was measured immediately after sampling using a specific kit (Free Chlorine DPD Reagent Powder Pillows, HACH Company, Loveland, CO, USA). Additionally, Total coliforms, *E. coli*, and *Enterococcus* concentrations were analysed externally at Cat-Gairín Laboratory, Girona. Finally, in *Chapters* 4.4 and 4.5, water hardness, calcium, and magnesium concentration were analysed by a DR2800 spectrophotometer using a specific water hardness kit (LCK327, HACH Company, Loveland, CO, USA).

3.6 Microbial community analysis

Chapters 4.1 and 4.5 determined the microbial community structure and taxonomical classification of relevant bacteria using barcoded amplicon-based Illumina sequencing of the partial 16S rRNA gene. For liquid samples, cells were recovered by centrifugation of 4 to 10 mL of the sample at 4000 rpm for 10 minutes at 4 °C. For the biofilm formed on the granular graphite, 0.5 g of crushed electrode material was used directly for DNA extraction. The extracted DNA was quantified using a NanoDrop ND-1000 spectrophotometer (NanoDrop Technologies Inc., Wilmington, USA) and stored at -20 °C. Illumina MiSeq flow cell (V2) sequencing was conducted at the RTSF Core facilities at Michigan State University, USA (https://rtsf.atsci.msu.edu/). The V4 region of the 16S rDNA was amplified using the primers 515F and 806R, following the method described by Kozich et al. (2013). Raw sequencing data were quality filtered, trimmed, dereplicated, merged, and, after a process of chimera removal, were clustered into amplicon sequence variants (ASVs) using the DADA2 Pipeline (Callahan et al., 2016). Afterwards, ASVs tabulation and taxonomy assignment were performed using the Silva taxonomic database: *Chapter* 4.1

used v132, and *Chapter* 4.5 used v138.1. Representative sequences for each amplicon sequence variant ASVs were assigned taxonomically using Blast searches at NCBI.

3.7 Calculations

3.7.1 Hydraulic retention time (HRT) and cathodic hydraulic retention time (HRT_{cat})

The HRT was calculated considering the total net reactor volume and the flow rates in each period of the experimentation. However, specifically, for the evaluation of denitrification performance, the focus was specifically on the cathode compartment, where denitrification was expected to occur. Therefore, only the NCC was considered, resulting in the HRT_{cat}. This approach allowed for a more accurate assessment of the denitrification process.

3.7.2 Removal rates

Nitrate reduction rate (rNO_3^-) and the reduction of denitrification intermediate rates (g N m^{-3} d^{-1}) to dinitrogen gas were calculated based on their different concentrations in the liquid phase between the influent and the effluent, using *Equations* 1 to 3. These equations provide a quantitative understanding of the denitrification process and allow for determining the conversion rates.

$$rNO_3^- = \frac{C_{NO_3^-\,influent} - C_{NO_3^-\,effluent}}{HRT_{cat}} \qquad \textit{Equation 1}$$

$$rNO_2^- = rNO_3^- + \frac{C_{NO_2^-\,influent} - C_{NO_2^-\,effluent}}{HRT_{cat}} \qquad \textit{Equation 2}$$

$$rN_2O = rNO_2^- + \frac{C_{N_2O\,influent} - C_{N_2O\,effluent}}{HRT_{cat}} \qquad \textit{Equation 3}$$

Where $C_{x\ influent}$ and $C_{x\ effluent}$ represent nitrate, nitrite, and nitrous oxide mass concentration in the influent and effluent (g N m^{-3}), and HRT_{cat} is expressed in days.

In *Chapter* 4.2, the theoretical nitrate reduction rate obtained from the analysis of isolated granules was also calculated from the current density (*j*, A m^{-2}), assuming the complete conversion of nitrate to dinitrogen gas, which requires 5 electrons.

$$r_{NO_3^-} = j \cdot \frac{1}{F} \cdot \frac{1mol\ N{-}NO_3^-}{5\ mol\ e^-} \cdot m_N \cdot t \qquad \textit{Equation 4}$$

Where *F* represents the Faraday constant (96,485 C mol^{-1}), m_N is the nitrogen molar mass (14 g mol^{-1}); and *t* is the time converting factor from day to seconds (86,400). The unit of the reduction rates is obtained as g N m^{-2} d^{-1}, but this rate may be normalised by the NCC to express the rate as g N m^{-3} d^{-1}.

This normalisation allows a more accurate comparison of the reduction rates across different reactor configurations and sizes.

In addition, other rates were calculated in this thesis to provide insight into other reactions of interest. In *Chapter* 4.1, where both nitrate reduction and arsenite oxidation coexisted, the arsenite oxidation rate was calculated using *Equation* 5.

$$rAs(III) = \frac{C_{As(III)_{influent}} - C_{As(III)_{effluent}}}{HRT} \qquad \textit{Equation 5}$$

Where $C_{As(III)influent}$ and $C_{As(III)effluent}$ represent arsenite mass concentration in the influent and effluent (g As(III) m^{-3}), and HRT is expressed in days. The unit of the oxidation rate is obtained as g As(III) m^{-3} d^{-1}.

In *Chapter* 4.4, the hardness removal rate of the electrochemical softener was calculated using *Equation* 6, normalised by the cathode surface area.

$$rCaCO_3 = \frac{C_{aco_{3_{influent}}} - C_{aco_{3_{effluent}}}}{HRT} \cdot \frac{V}{S} \qquad \textit{Equation 6}$$

Where $C_{CaCO3influent}$ and $C_{CaCO3effluent}$ represent hardness in the effluent and influent (mg $CaCO_3$ L^{-1}), *HRT* is the hydraulic retention time (h); V is the net volume of the reactor (L) and *S* is the cathode surface area (m^2). The unit of the rate was obtained as mg $CaCO_3$ m^{-2} h^{-1}.

3.7.3 Coulombic efficiency (CE)

The coulombic efficiency describes the efficiency with which a charge (electrons) is transferred in a system, facilitating an electrochemical reaction. In the entire Ph.D. thesis, the cathodic coulombic efficiency for the reduction of nitrate (CE_{cat}) was calculated as proposed by Pous et al. (2017), considering all reduction steps from nitrate to dinitrogen gas, including the accumulation of nitrite and nitrous oxide (*Equations* 7 and 8).In order to assess the efficiency of the oxidation of arsenite to arsenate (*Chapter* 4.1), the anodic coulombic efficiency (CE_{an}) was calculated as shown in *Equations* 9 and 10.

$$j_{NO_3^-} = \frac{V_{NCC} \cdot F \cdot HRT_{cat} \cdot (n_{NO_3^-/NO_2^-} \cdot rNO_3^- + n_{NO_2^-/N_2O} \cdot rNO_2^- + n_{N_2O/N_2} \cdot rN_2O)}{m_N \cdot t} \qquad \textit{Equation 7}$$

$$CE_{cat} = \frac{j}{j_{NO_3^-}} \cdot 100 \qquad \textit{Equation 8}$$

$$j_{As(III)} = \frac{(V_{NCC} + V_{NAC}) \cdot HRT \cdot F \cdot (n_{As(III)/As(V)} \cdot rAs(III))}{m_{As} \cdot t} \qquad \textit{Equation 9}$$

$$CE_{an} = \frac{j_{As(III)}}{j} \cdot 100 \qquad \textit{Equation 10}$$

Where V_{NCC} and V_{NAC} are net cathode and anode compartment volume in m^{-3}, respectively; *F* is the Faraday constant (96,485 C mol^{-1}); m_N and m_{As} are molar masses (14 g mol^{-1} for nitrogen and 75 g mol^{-}

[1] for arsenic); *HRT and* HRT_{cat} are the hydraulic retention time considering the net reactor volume and the net cathodic compartment in days, respectively; *t* is the time converting factor from day to seconds (86,400); *n* represent the equivalent electrons required for each redox reaction ($n_{NO_3^-/NO_2^-} = 2; n_{NO_2^-/N_2O} = 2; n_{N_2O/N_2} = 1;$ and $n_{As(III)/As(V)} = 2$); rNO_3^-, rNO_2^-, and rN_2O are the nitrogen reduction rate in g N m_{NCC}^{-3} d^{-1}, and *rAs(III)* is the arsenite oxidation rate in g As(III) m^{-3} d^{-1}. For coulombic efficiency, *j* is the current observed in reactors and jNO_3^- and *jAs(III)* are the theoretically calculated current for nitrate reduction and arsenite oxidation, respectively.

3.7.4 Energy consumption of an bio- and electrochemical reactor

The energy supplied by the power source (or the potentiostat) was calculated using *Equation* 11. To facilitate understanding and enable comparison, these consumption values were normalised to the total nitrate reduction (kWh kg^{-1} NO_3^-), hardness reduction (kWh kg^{-1} $CaCO_3$) or by volume of water treated (kWh m^{-3}), according to the objective of the discussion.

$$P = j \cdot Ecell \qquad \textit{Equation 11}$$

Where P is the power (W); *j* is the observed current (A); and *Ecell* is the observed cell voltage (V).

In addition to the power supply necessary to sustain the electrochemical reactors, the energy consumed by the pump was also taken into account to evaluate the total electricity consumption of the system comprehensively. Initially, in *Chapter* 4.4, a theoretical approach was adopted, following the method proposed by Zou and He (2018) (*Equation* 12). Subsequently, in *Chapter* 4.5, the estimation was pursued by considering the power specification of a centrifugal pump.

$$P_{pump} = \frac{Q_{pump} \cdot (H_{hydraulic} + H_{dynamic})}{1000\, x\, \eta} = \frac{v\, \pi\, d^2/4 \cdot (\rho\, g\, h + \rho\, v^2/2)}{1000 \cdot \eta} \qquad \textit{Equation 12}$$

Where $H_{hydraulic}$ (Pa) and $H_{dynamic}$ (Pa) are the hydraulic and dynamic heads provided by the pump, respectively; *v* (m s^{-1}) is the water velocity calculated from the flow rate divided into the section of the tube area; *d* (m) is the tube diameter; *h* (m) is the difference of water height before and after the pump; ρ (kg m^{-3}) is water density; and η (%) is the pump efficiency.

3.7.5 Statistical analyses

The results underwent various statistical tests using Microsoft Excel, including mean calculation and standard deviation. Additionally, in certain scenarios where results comparison was needed, an analysis of variance (t-test and ANOVA) was conducted with assumptions of normal distribution, two-sided analysis, heteroscedasticity, and a 95% confidence level. The linearity of the results was assessed through linear regression, calculating the coefficient of determination (R^2) and the Pearson correlation coefficient (r_{xy}).

CHAPTER 4:

Results

4.1 Electro-bioremediation of nitrate and arsenite polluted groundwater

Alba Ceballos-Escalera[1], Narcís Pous[1], Paola Chiluiza-Ramos[2], Benjamin Korth[3], Falk Harnisch[3], Lluís Bañeras[2], M. Dolors Balaguer[1], Sebastià Puig[1]

[1]LEQUiA, Institute of the Environment, University of Girona, C/ *Maria Aurèlia Capmany, 69*, E-17003, Girona, Spain.

[2]Group of Environmental Microbial Ecology, Institute of Aquatic Ecology, University of Girona, C/ *Maria Aurèlia Capmany, 40,* E-17003, Girona, Spain.

[3]Department of Environmental Microbiology, Helmholtz Centre for Environmental Research GmbH - UFZ, *Permoserstraße 15*, 04318 Leipzig, Germany.

Published on: Water Research, Volume 190, February 2021, 116748

DOI: https://doi.org/10.1016/j.watres.2020.116748

Graphical abstract:

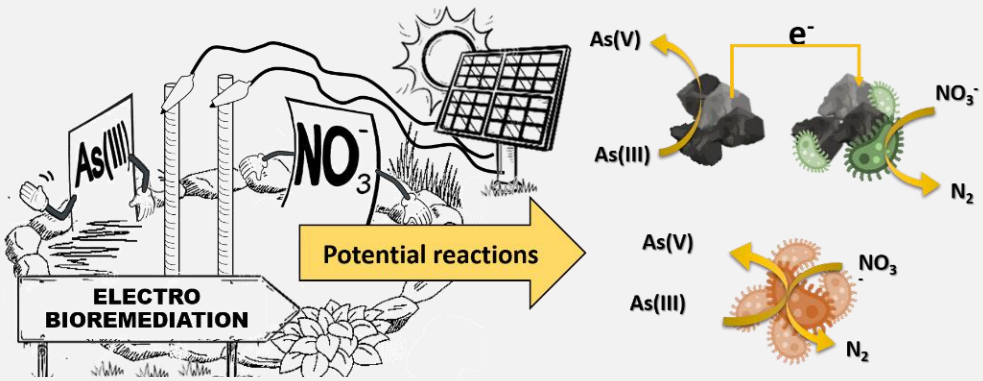

Highlights:

- Sustainable technology for efficient treatment of nitrate and arsenite.
- Bioelectrochemical NO_3^- reduction to N_2 with coulombic efficiency close to 100 %.
- Denitrifying biocathode formed by *Sideroxydans* sp. resistant to 5 mg As (III) L^{-1}.
- Arsenite oxidation catalytical and linked to denitrification by *Achromobacter* sp.

4.2 Ex-situ electrochemical characterisation of fixed-bed denitrification biocathodes: a promising strategy to improve bioelectrochemical denitrification

Alba Ceballos-Escalera[1], Narcís Pous[1], Benjamin Korth[2], Falk Harnisch[2], M. Dolors Balaguer[1], Sebastià Puig[1]

[1]LEQUiA, Institute of the Environment, University of Girona, C/ *Maria Aurèlia Capmany, 69*, E-17003, Girona, Spain.

[2]Department of Environmental Microbiology, Helmholtz Centre for Environmental Research GmbH - UFZ, *Permoserstraße 15*, 04318 Leipzig, Germany.

Accepted on: Chemosphere, November 2023

DOI: https://doi.org/10.1016/j.chemosphere.2023.140699

Graphical abstract:

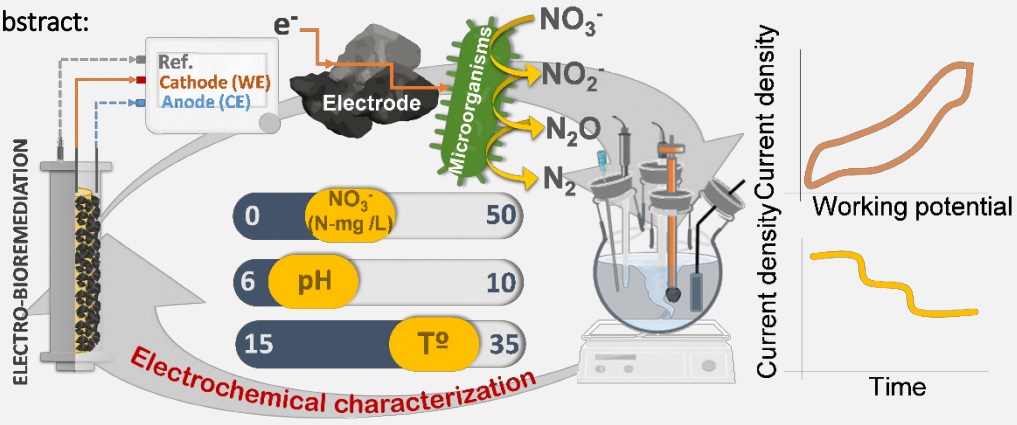

Highlights:

- Non-invasive electrochemical analysis allows denitrifying biocathode optimisation.
- A unique formal potential is detected regardless of the terminal electron acceptor.
- EET is identified as the main limiting step in bioelectrochemical denitrification.
- High nitrate affinity (0.7 ± 0.2 mg $N \cdot L^{-1}$) ensures a maximum treatment rate above drinking water standards.
- pH and temperature directly influence the performance, being optimal at pH 6 and 35 °C.

4.3 Nitrate electro-bioremediation and water disinfection for rural areas

Alba Ceballos-Escalera[1], Narcís Pous[1], M. Dolors Balaguer[1], Sebastià Puig[1]

[1]LEQUiA, Institute of the Environment, University of Girona, C/ *Maria Aurèlia Capmany, 69*, E-17003, Girona, Spain.

Submitted on: Chemosphere, July 2023

Graphical abstract:

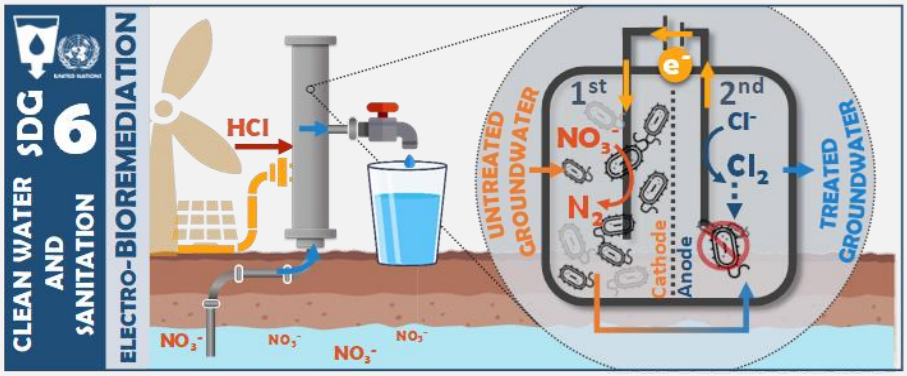

Highlights:

- Treated groundwater meets standards for nitrogen compounds and pathogens.
- Highest reported nitrate reduction rate of 5.0 kg NO_3^- m^{-3} d^{-1} at HRT_{cat} of 0.7 h.
- Water disinfection ensured through in-situ electrochemical chlorine evolution.
- Cost-effective treatment with an estimated competitive operational cost of 1.05 € m^{-3}

4.4 Electrochemical water softening as pretreatment for nitrate electro-bioremediation

Alba Ceballos-Escalera[1], Narcís Pous[1], M. Dolors Balaguer[1], Sebastià Puig[1]

[1]LEQUiA, Institute of the Environment, University of Girona, C/ *Maria Aurèlia Capmany, 69*, E-17003, Girona, Spain.

Published on: Science of The Total Environment, Volume 806, Part 1, February 2022, 150433

DOI: https://doi.org/10.1016/j.scitotenv.2021.150433

Graphical abstract:

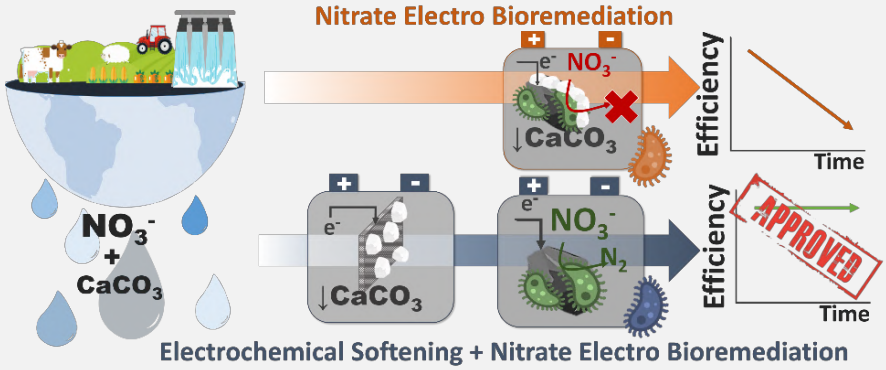

PHHighlights:

- Electrochemical softening reduced 90% the groundwater saturation index.
- Softened groundwater reached suitable properties for nitrate electro-bioremediation.
- Reversal polarity periods increased the electrochemical softening lifetime up to 48%.
- Electrochemical softening at a competitive operational cost.

4.5 Advancing towards electro-bioremediation scaling-up: on-site pilot plant for successful nitrate-contaminated

Alba Ceballos-Escalera[1], Narcís Pous[1], Lluís Bañeras[2], M. Dolors Balaguer[1], Sebastià Puig[1]

[1]LEQUiA, Institute of the Environment, University of Girona, C/ *Maria Aurèlia Capmany, 69*, E-17003, Girona, Spain.

[2]Group of Environmental Microbial Ecology, Institute of Aquatic Ecology, University of Girona, C/ *Maria Aurèlia Capmany, 40,* E-17003, Girona, Spain.

Submitted on*: Water Research, December 2023*

Graphical abstract:

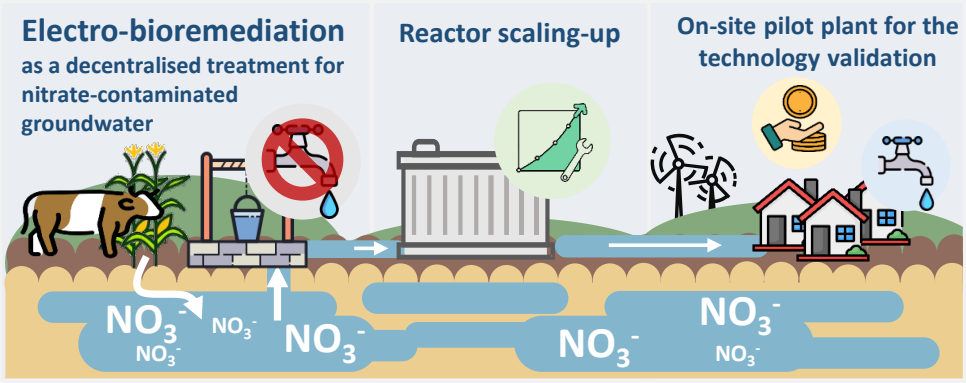

Highlights:

- Successful transition of electro-bioremediation from laboratory to on-site pilot plant
- Achieved maximum nitrate reduction rate of 0.89 ± 0.09 kg NO_3^- m^{-3} d^{-1} at 2.0 h HRT_{cat}
- Collaborative microbial community ensures full NO_3^- reduction to N_2
- Competitive operational cost of 0.4 € m^{-3} for on-site electro-bioremediation

CHAPTER 5:

General discussion

5

The research described in this Ph.D. thesis addressed key aspects related to the transition towards the implementation of nitrate-contaminated groundwater electro-bioremediation. Firstly, the Ph.D. thesis enquired at the laboratory-scale studies to gain valuable insights into the process and its optimisation as well as to assess its potential as a water treatment method. Subsequently, this valuable knowledge was utilised and successfully implemented at a pilot scale on-site. This discussion section delves into the challenges associated with scaling-up bioelectrochemical systems, as well as determining their economic feasibility. The insights provided here aim to bridge the gap in scaling-up this technology and evaluating its possible implementation in the water sector.

5.1 Nitrate reduction rate and efficiency: a roadmap from the different designs and scales

5.1.1 Advances in nitrate reduction rates: from the laboratory to an *on-site* pilot plant

One of the principal objectives of this Ph.D. thesis was to reach the highest possible nitrate reduction rate linked to the development of a compact system, all while ensuring that the effluent quality adhered to the stipulated nitrate and nitrite standards for potable water. Table 2 provides a concise overview of the outcomes derived from this research concerning nitrate treatment, encompassing both the maximum nitrate reduction rate and efficiency. A nitrate reduction rate of 2.3 ± 0.2 kg NO_3^- $m^{-3}d^{-1}$ and a high nitrate reduction efficiency of 90 ± 6 % were achieved by applying an HRT_{cat} of 1.5 ± 0.1 h and an external recirculation from the effluent to the influent at a rate of 85 L d^{-1} (Chapter 4.1). As a result, the treatment was able to reach the drinking water standards regarding nitrate and nitrite concentrations. Notably, the system was capable of fully oxidising arsenite into arsenate as a co-contaminant present in the same water matrix.

Despite having a good nitrate reduction rate compared with the state-of-the-art (Table 2), the research aimed to enhance it further. *Chapter* 4.3 implemented a pH control at 6.75 ± 0.25 to improve nitrate reduction based on the strong correlation found in *Chapter* 4.2 between pH and optimal nitrate reduction in the acidic range of 6-10 (discussed below). At the same time, the external recirculation from the anode to the cathode was replaced by internal cathodic recirculation to avoid the presence of oxygen and chlorine in the cathode. These modifications contributed to achieving a remarkable reduction rate of 5.0 ± 0.3 kg NO_3^- $m^{-3}d^{-1}$ at 0.7 h of HRT_{cat} while maintaining a high nitrate reduction efficiency of 90 ± 4%. This rate was reported as the maximum nitrate reduction rate in the electro-bioremediation field to date. Consequently, the effluent successfully met the appropriate drinking water quality standards in terms of nitrate and nitrite concentrations. Moreover, although this approach required continuous consumption of chemicals to sustain the pH control, this study effectively recovered the cost of the acid dosed by the production of free chlorine (disinfectant) in the anode compartment.

Table 3: Summary of the results from each chapter of this Ph.D. thesis compared to some of the main remarkable studies on nitrate electro-bioremediation. The water quality is shown in green when the nitrate and nitrite effluent content met the standards for drinking water (European Directive 2020/2184) and in yellow when not. The nitrate reduction rate values are represented with bars, with green indicating the observed rates in this study, orange representing the hypothetical maximum rate extracted from the current density in the study of isolated granules (Chapter 4.2), and blue indicating the values of the state-of-the-art studies.

References	Cathode potential (V)	Water matrix	Electric conductivity (mS cm^{-1}) and pH	Influent nitrate concentration (mg L^{-1})	Net cathode volume (L)	HRT_{cat} (h) [a]	Effluent quality: Nitrate and nitrite (mg L^{-1})	Nitrate reduction rate (kg NO3- $m^{-3}d^{-1}$)[a]	Nitrate removal efficiency (%)	Chemical consumption?
Present work										
Chapter 4.1	-0.32	Synthetic groundwater	EC: 1.0 ± 0.1 pH: 8.0 ±0.3	123 ± 26	0.30	1.5 ± 0.1	NO_3^-: 12.2 ± 9.3 NO_2^-: 0.4 ± 0.1	2.3 ± 0.2	90 ± 6	NO
Chapter 4.2			EC: 1.0 ± 0.1 pH: Not applicable	*145*	*Isolated granules*	Not applicable	Not applicable	9.5 ± 2.6 [b]	Not applicable	Not applicable
Chapter 4.3			EC: 1.3 ± 0.1 pH: 6.7 ± 0.3	169 ± 5	0.22	0.7 ± 0.0	NO_3^-: 15.1 ± 7.7 NO_2^-: 0.0 ± 0.0	5.0 ± 0.3	90 ± 4	Yes [d]
Chapter 4.4		Real groundwater from Navata (Spain)	EC: 0.4 ± 0.0 pH: 7.0 ± 0.2	114 ± 3	0.30	2.1 ± 0.1	NO_3^-: 3.3 ± 1.7 NO_2^-: 0.0 ± 0.0	1.3 ± 0.0	97 ± 1	NO
Chapter 4.5	-0.67 ± 0.03		EC: 0.8 ± 0.1 pH: 8.3 ± 0.4	92.0 ± 7.2	1.20	2.0 ± 0.0	NO_3^-: 15.9 ± 7.1 NO_2^-: 0.0 ± 0.0	0.9 ± 0.1	82 ± 18	NO
State of the art										
(Clauwaert et al., 2009)	-0.67	Synthetic medium	EC: 13.1 pH: 7.2	88 - 484	0.11	Not applicable [c]	n.d.	2.1	72	Yes [d]
(Pous et al., 2017)	-0.32	Synthetic groundwater	EC: 4.1 pH: n.d.	144 ± 1	0.24	0.5	NO_3^-: 72.2 NO_2^-: 0.0	3.7	50	NO
(Cecconet et al., 2018)	-0.50	Synthetic groundwater	EC: n.d. pH: 7.5	198	0.65	15.6	NO_3^-: 11.9 NO_2^-: n.d.	0.3	94 ± 4	NO
(Wang et al., 2021)	Periodic polarisation at -0.33	Synthetic groundwater	EC: n.d. pH: 7.0	145	0.15	3.3	NO_3^-: 24.2 NO_2^-: n.d.	0.9	83	NO
(Puggioni et al., 2021)	<-0.90	Synthetic groundwater	EC: 2.0 pH: 7.5	132	0.11	18	NO_3^-: 40.0 NO_2^-: 0.0	0.2	69±2	Yes [d]

[a] Values regarding the net cathodic compartment volume; [b] Theoretical rate extracted from the current density; [c] Batch mode; [d] Acid consumption for pH control; n.d. No data is available

The overall results presented in this Ph.D. thesis represent a significant advancement in improving nitrate reduction rates when compared to the state-of-the-art in the field of nitrate electro-bioremediation (Table 3). The results using synthetic groundwater, fall within the upper range of the maximum reported rates in the existing literature. Before this thesis, the electro-bioremediation process had a minimum HRT_{cat} of 0.5 h and a maximum nitrate reduction rate of 3.7 kg NO_3^- m^{-3} d^{-1} (Pous et al., 2017). However, it is important to note that these achievements were accompanied by a relatively low nitrate reduction efficiency of 50% (Table 3). In contrast, *Chapter* 4.1 of this study presented a nitrate reduction rate of approximately 2.3 ± 0.2 kg NO_3^- m^{-3} d^{-1}, and in the subsequent *Chapter* 4.3, this rate enhanced up to 5.0 ± 0.3 kg NO_3^- m^{-3} d^{-1}, both keeping a consistently high nitrate reduction efficiency of over 90%. Notably, *Chapter* 4.3 surpasses nitrate reduction rates reported in other laboratory-scale studies with similar pH control (Table 3) (Clauwaert et al., 2009; Puggioni et al., 2021).

The research moved a step forward by testing the process with real groundwater at a laboratory-scale (*Chapter* 4.4). The real groundwater treatment may present some challenges, including high hardness (325 ± 10 mg $CaCO_3$ L^{-1}) and low electric conductivity of the water (Table 3). Specifically, to avoid scale formation, the groundwater was first pretreated with an electrochemical softener before the treatment by electro-bioremediation. Despite having lower electrical conductivity (0.4 ± 0.0 mS cm^{-1}) compared to synthetic groundwater (1.3 ± 0.1 mS cm^{-1}), the nitrate reduction efficiency remained at 97 ± 1%, with no accumulation of nitrite or other intermediates. The system achieved a nitrate reduction rate of 1.3 ± 0.0 kg NO_3^- $m^{-3}d^{-1}$ at an HRT_{cat} of 2.1 ± 0.1 hours, which was slightly lower than that previous results due to the higher HRT_{cat} and lower nitrate concentration in the influent (Table 3). Nevertheless, these results demonstrate the viability of electro-bioremediation with real groundwater while maintaining the standards and efficiency achieved with synthetic groundwater.

Moving forward on electro-bioremediation scale-up and validation, *Chapter* 4.5 developed and operated a pilot plant treating real groundwater *on-site*. The pilot plant consisted of an ion exchange softener and an electro-bioremediation module. Results exhibited a nitrate reduction rate of 0.9 ± 0.1 kg NO_3^- $m^{-3}d^{-1}$ at HRT_{cat} of 2.0 ± 0.0 h and nitrate reduction efficiency was 82 ± 18 % while complying with the standards for nitrate and nitrite concentrations in drinking water, values similar to those observed at laboratory-scale when working with real groundwater. Besides, energy consumption in the pilot plant did not show significant differences between the laboratory and pilot plant scales (4.8 ± 0.5 kWh kg^{-1} NO_3^- in *Chapter* 4.1 *vs*. 4.3 ± 0.4 kWh kg^{-1} NO_3^- in *Chapter* 4.5). This suggests that the modifications made to ensure proper current distribution (using titanium current collectors) effectively addressed challenges associated with the poor electrical conductivity of granular graphite, exacerbated

by the larger reactor size. The outcomes of the pilot plant in terms of nitrate reduction rate and efficiency substantiated the successful technology transition into TRL 5.

Overall, lower nitrate reduction rates were observed when treating real groundwater in both the pilot plant (*Chapter* 4.5) and the laboratory scale (*Chapter* 4.4), in contrast to the treatment of synthetic groundwater (Table 3). Several plausible reasons could explain these differences, especially compared to the results obtained in *Chapter* 4.1 (i.e., the same reactor was used to further test the real groundwater and design the pilot plant). It is worth noting that the influent nitrate concentration was higher (up to 169 ± 5 $mgNO_3^-$ L^{-1}) in the studies carried out with synthetic groundwater, while it decreased (e.g., 92 ± 5 $mgNO_3^-$ L^{-1} in the operational pilot plant) in the studies developed with real nitrate-polluted groundwater from Navata site (specifics concentrations in Table 3). This is the reason why, at similar HRT, the nitrate removal rates were different. Simultaneously, other factors within the water matrix may have played a significant role. In particular, the lower electrical conductivity of the real groundwater (<0.8 mS cm^{-1} compared to >1.0 mS cm^{-1} in the synthetic groundwater, Table 3) could potentially limit denitrification (Puig et al., 2012). Moreover, some trace elements (e.g. Fe, Mn and Zn) added to the synthetic groundwater may not be present in the real groundwater, potentially affecting the denitrification process (Labbé et al., 2003). Conversely, the differences in the microbial communities between the reactors studied could significantly impact the denitrification capacity of the treatment. At the family level, the biocathodes in the laboratory reactors analysed in Chapter 4.1 were mainly composed of *Acidithiobacillaceae*, *Comamonadaceae*, and *Rhodocyclaceae*. Meanwhile, in the pilot plant (*Chapter* 4.5), the biocathode community was composed mainly of *Pseudomonadaceae*, *Rhizobiaceae*, *Gallionellaceae*, and *Xanthomonadaceae*. Finally, the larger scale referred to in *Chapter* 4.5 introduced several challenges that may have influenced the lower nitrate reduction rate, as discussed later. The main challenge was the heterogeneous distribution of redox potential along the reactor due to the low electrical conductivity of the granular graphite. This was exacerbated by the increased reactor length, which directly impacted the nitrate reduction rate.

Notably, the HRT_{cat}, and consequently the nitrate reduction rate, was demonstrated to play a key role in system performance and has a direct impact on the determination of water production costs, as discussed in *Chapter* 4.5. For instance, the hypothetical reduction of the HRT_{cat} from 2.0 h to 0.5 h, along with an increase in the nitrate reduction rate to sustain nitrate efficiency and the water quality, could potentially lead to a 75% reduction in the estimated total water production cost (considering OPEX and CAPEX). Therefore, improving this rate while retaining the advantages in terms of low energy consumption and low environmental impacts is a key aspect in advancing the field of nitrate electro-bioremediation. Despite the significant progress made in achieving high nitrate reduction rates in these

thesis sections (*Chapters* 4.1, 4.3, 4.4 and 4.5), a more comprehensive evaluation of possible approaches for nitrate reduction optimisation is required. Understanding system dynamics and operating parameters is critical for optimising nitrate electron-bioremediation. Thus, identifying the limiting step of the denitrifying biocathode, determining its redox potential, and considering factors such as substrate availability, pH, temperature, and co-contaminants are key to denitrification performance.

5.1.2 Electro-bioremediation characterisation and optimisation: from isolated granules to a running reactor

The establishment of a single dynamic model and optimal operating parameters for electro-bioremediation is challenging because it involves the coexistence of biological and electrochemical reactions. In addition, factors such as the diversity of electrode materials, reactor configurations and microorganisms add to the complexity. Thus, developing a swift methodology to characterise and subsequently optimise each system can open the door to increasing treatment capacity in different scenarios. In this field, electrochemical characterisation is a valuable tool for this purpose. However, its implementation in bioelectrochemical reactors is challenging due to various factors that can hide the results, including the distance from the reference electrode, variations in redox potential distribution due to the low electrical conductivity of certain electrodes (e.g., granular graphite), heterogeneity in the medium (e.g., pH), and variations in the distribution of the microbiome (Quejigo et al., 2021). To address these constraints, electrochemical characterisation can be conducted on a smaller scale by employing small and simple bioelectrochemical reactors (i.e., H-types). These can be inoculated using the same source as the reactor or its effluent. However, this methodology can be time-consuming, as it takes a significant amount of time to inoculate it. Additionally, the resulting biocathode may differ from those found in the running reactor. An alternative approach is to extract a portion of the biocathode from the reactor under study and analyse *ex-situ*. The Ph.D. thesis evaluated the extraction and *ex-situ* electrochemical characterisation of isolated granular graphite from a bioelectrochemical fixed-bed reactor. This methodology significantly reduces the analysis time from weeks or even months to hours by eliminating the need for an inoculation period. Moreover, it offers a snapshot of the biocathode's state precisely at the time of extraction from the operational reactor, all without influencing the reactor's ongoing operation.

The different steps of nitrate reduction in a biocathode, mostly composed of *Sideroxydans lithotrophicus* sp. were studied by the *ex-situ* electrochemical characterisation (*Chapter* 4.2). In this study, these different nitrate reduction intermediates (nitrate, nitrite and nitrous oxide) showed the same electroactive response in terms of gravimetric current density (-0.21 ± 0.06 mA g^{-1}). Besides, it

could be identified a single limiting step at a formal potential of -0.225 ± 0.007 V (pH 7 and 25°C) testing the different nitrate intermediates. This suggested that EET was the primary limiting step, independent of the denitrification step in that biocathode, highlighting the importance of maintaining consistent redox potential in the reactor to optimise denitrification performance. It also suggested that harmful denitrification intermediates such as nitrite and nitrous oxide would not accumulate significantly during the studied reactor. Nevertheless, the electrochemical characterisation in the literature revealed a wide range of formal potential reported in denitrifying biocathode. For instance, Pous et al. (2014) showed two formal potentials at -0.300 V for nitrate reduction and -0.700 V for nitrite reduction (pH 8.0) in a biocathode mainly formed by *Thiobacillus* spp. Similarly, Chaudhary et al. (2021) found formal potentials at -0.294 V and -0.724 V (pH 9.5) in a biofilm mainly formed by *Pseudomonas*, *Natronococcus,* and *Pseudoalteromonas* spp. Nevertheless, other studies reported electroactive redox sites at -0.374 V (pH 7.0) for a denitrifying biofilm mainly consisting of *Geobacter* (Pous et al., 2016), or -0.487 V and -0.406 V (pH 7.0) in the case of a microbiome composed of *Pseudomonas nitroreducens* and *Paracoccus versutus* (Korth et al., 2022). This variability in the results reported for the denitrifying biocathodes demonstrates the complexity of the systems. For this reason, the presented *ex-situ* methodology is an interesting tool for swift electrochemical characterisation to elucidate the dynamics of each biocathode that can impact on the final reactor performance.

In parallel, *the ex-situ* characterisation also provided evidence that a Michaelis-Menten kinetic model can accurately describe the nitrate reduction at a biocathode poised at -0.32 V, and it allowed the estimation of the corresponding apparent affinity constant (K_M^{app}) and maximum uptake rate (v_{max}^{app}). These parameters were considered "apparent parameters" as they are influenced by different factors that are difficult to measure in graphite granules, such as biofilm thickness, biofilm density, the surface area of granular graphite, and radial diffusion. A high nitrate affinity of the microbiome attached to the granular graphite was observed (K_M^{app} of 3.1 ± 0.9 mg NO_3^- L^{-1}), ensuring that nitrate uptake does not limit reactor operation even when nitrate concentrations are found below drinking water standards (NO_3^- < 50 mg NO_3^- L^{-1}; European Directive 2020/2184). This finding is crucial for the successful performance of the electro-bioremediation process in real-world scenarios aiming to remove the presence of nitrate. The v_{max}^{app} was determined at -0.37 ± 0.06 mA g^{-1}. This value could be used to estimate a potential maximum nitrate reduction rate up to 9.5 ± 2.6 kg NO_3^- m^{-3} d^{-1} in the reactor (Table 3), assuming the complete transformation of nitrate into nitrogen gas and 100% coulombic efficiency. This represents the highest potential capacity for removing nitrate within the system, assuming no substrate limitations, a homogenous redox potential, and full mixing. Thus, there is room for enhancing nitrate reduction rates compared to the reported rates in the literature as well as in the reactors discussed in this Ph.D. thesis (maximum reported rate up to 5.0 ± 0.3 kg NO_3^- $m^{-3}d^{-1}$). Additionally, these

kinetic parameters, which have not been previously reported in the literature, are indispensable for modelling denitrifying bioelectrochemical reactors in future investigations.

Ex-situ electrochemical characterisation is a valuable tool for assessing the effect of some operational parameters, such as the influence of pH and temperature on denitrification performance. The studied biocathode exhibited a strong linear correlation between the pH and the temperature with the electroactive response (i.e., nitrate reduction rate). Specifically, there was a positive correlation with temperature within the range of 15 to 35°C and a negative correlation with pH within the range of 6.0 to 9.0. The temperature correlation aligned with typical denitrifying activity, which is negligible below 5°C and increases linearly until reaching a maximum of approximately 25-30°C. However, determining the optimal pH value is more complex due to the different optimal values reported in the literature. For example, the *ex-situ* analysis of granular graphite of another biocathode demonstrated comparable rates of nitrate reduction within a pH range of 6 to 8 (Korth et al., 2022). In contrast, some denitrifying reactors have reported the optimal pH to be 7.2 (Clauwaert et al., 2009; Molognoni et al., 2017). The results presented in *Chapter* 4.2 demonstrate a potential enhancement of up to 36% in performance by increasing the reactor temperature from 25 °C (working temperature) to 35 °C. Similarly, the adjustment of the operating pH from 8.0 to 6.7 could theoretically result in a significant 65% increase in the nitrate reduction rate. *Chapter* 4.3 demonstrated the improved performance by adjusting the pH in the cathodic compartment compared to the performance in Chapter 4.1, both operating with the same biocathode studied *ex-situ* in *Chapter* 4.2. The nitrate reduction rate increased from 2.3 ± 0.2 kg NO_3^- m^{-3} d^{-1} when operating at an uncontrolled pH of 8.0 ± 0.2 (*Chapter* 4.1) to 5.0 ± 0.3 kg NO_3^- m^{-3} d^{-1} when operating at a controlled cathodic pH of 6.7 ± 0.3 (*Chapter* 4.3). The nitrate reduction rate increased by 117%, surpassing the expected increase due to pH adjustments. This substantial improvement suggests that other modifications to the system could also contribute to enhance the performance (discussed above).In parallel, it is important to consider the correlation between performance and pH, especially concerning potential gradients within the reactor. This is particularly significant in systems with low electrical conductivity, where proton diffusion between the anode and cathode, as well as within the biofilm, is limited. Therefore, balancing the pH between the anode and cathode by external recirculation to achieve a neutral pH (*Chapter* 4.1) or by implementing pH control (*Chapter* 4.3) was key to increasing the nitrate reduction rate. Moreover, the recirculation velocity significantly influenced the performance, as high velocities enhanced homogeneity along the reactor.

The gathered results suggest that the potential of electro-bioremediation is still not fully exploited and that there is room for enhancing the treatment in terms of nitrate reduction rate, which would allow an increase in the influent water flow rate. To achieve this, it is necessary to improve the reactor

configuration to achieve homogeneous substrate distribution and redox potential, and to select the optimal operating conditions. In parallel, *ex-situ* characterisation has proved valuable in understanding and optimising bioelectrochemical reactors, providing decisive guidance for scaling up the technology. Although initially tested on a laboratory-scale, implementation on a larger scale may be plausible with careful consideration of various factors. For example, in fixed-bed electrochemical reactors, issues such as redox potential heterogeneity and microbial stratification, as discussed in *Chapter* 4.5, will pose significant challenges to this characterisation. Overcoming these difficulties requires careful sampling of representative granules from the biocathode and accurate interpretation of this heterogeneity. Therefore, this tool could be used effectively on a larger scale with appropriate considerations to guide parameter selection during operation or to predict variations in treatment capacity in response to these parameters.

5.2 Insights and harnessing the versatility of electro-bioremediation through anodic reactions: counter reaction counts!

Nitrate contamination in groundwater is a widespread environmental issue that often coexists with various other pollutants, including inorganic/organic compounds and pathogens. These contaminants might be present in groundwater due to agricultural activities, industrial discharges, or natural processes. Contaminant coexistence may pose two significant challenges for water treatment and remediation processes. Firstly, how does this coexisting contaminant affect denitrification in electro-bioremediation? Secondly, can the co-contaminant also be effectively eliminated in the electro-bioremediation treatment?

Coexisting contaminants in groundwater can interfere with the denitrification process in electro-bioremediation. Some of these contaminants may compete with nitrate as electron acceptors during the denitrification process, potentially hindering the efficient reduction of nitrate. For instance, sulphate, frequently found in groundwater, could potentially interfere with the nitrate reduction process in electro-bioremediation by acting as an alternative electron acceptor (Nguyen et al., 2016a). Other potential competing electron acceptors include iron(III) and arsenic(V). Additionally, some contaminants might also exhibit inhibitory effects on denitrifying microorganisms such as heavy metals (Igiri et al., 2018), potentially impacting their efficiency and compromising the overall performance. Consequently, assessing the impact of these contaminants, along with the water matrix, in the context of electro-bioremediation becomes crucial.

Furthermore, investigating the potential for cocktails of contaminants within a single treatment could be essential for achieving a more sustainable treatment, leading to reduced costs and operational efforts. In the context of nitrate electro-bioremediation, the utilisation of certain anodic reactions may

offer a versatile strategy to treat multiple contaminants. However, the importance of anodic reactions in denitrifying bioelectrochemical systems has frequently been disregarded (Jia et al., 2008; Tong and He, 2013; Zhou et al., 2009), resulting in a missed opportunity to fully harness their potential benefits. Currently, the most commonly explored co-degradation involves organic matter oxidation, but there are numerous other possibilities to consider. This Ph.D. thesis explored the usage of anode oxidations to tackle two specific co-contaminants: arsenic (III) (*Chapter* 4.1) and pathogens (*Chapter* 4.3), both of which are discussed in detail below.

5.2.1 Challenges and opportunities of electro-bioremediation for nitrate and arsenic co-contaminated groundwater

In conventional arsenic removal methods, like precipitation or adsorption, the initial stage involves the oxidation of arsenic (III) to arsenic(V) because arsenic (V) is less soluble, less mobile, and less toxic than arsenic (III) (Banerjee et al., 2008; Borho and Wilderer, 1996). The biological oxidation of arsenic (III) offers relevant advantages compared to conventional chemical oxidation methods. Conventional chemical oxidants (e.g., ozone, iron and manganese oxide) have low selectivity, producing toxic by-products like nitroaromatic compounds (Ji et al., 2017). Furthermore, electro-bioremediation does not only eliminate the chemical requirements but also simplifies the entire treatment process. Integrating arsenic oxidation and nitrate reduction within a single reactor significantly reduces operational costs while enhancing treatment sustainability.

Co-treatment of nitrate with arsenic (III) was validated in a bioelectrochemical reactor (*Chapter* 4.1.). Remarkably, the study achieved complete oxidation of arsenic (III) to arsenic (V) (>99%) at a maximum rate of 90 g As(III) m^{-3} d^{-1} (HRT of 2.9 ± 0.1 h), while nitrate was reduced to dinitrogen gas with an efficiency of 90 ± 6% (Table 3). As a result, the subsequent ecotoxicity analysis demonstrated a reduction in toxicity when compared to the untreated synthetic groundwater (Fekete-Kertész et al., 2023). Furthermore, *ex-situ* characterisation of the biocathode ruled out any inhibitory effect of arsenic at a concentration of 5 mg L^{-1} on bioelectrochemical denitrification while achieving a high nitrate reduction rate in an operational reactor (Table 3).

Specifically, various arsenic oxidation pathways were identified within the studied denitrifying bioelectrochemical reactor, which emerged from intricate interactions among various electron acceptors (nitrate, oxygen and anode electrode), as well as electrochemical and biological reactions. These pathways included abiotic oxidation using the anode as the sole electron acceptor or utilising the oxygen generated from water splitting, particularly in the presence of granular graphite as a conductive material. However, the most plausible pathway appeared to be the biological oxidation of arsenic (III), involving nitrate as an electron acceptor. The biological hypothesis was substantiated by the microbial

characterisation, revealing the presence of *Achromobacter* spp., which can oxidise arsenic using oxygen (Nguyen et al., 2017), nitrate (Su et al., 2018) or an electrode as an electron acceptor (Nguyen et al., 2016b; Pous et al., 2015a). This capability of the treatment to achieve both arsenic (III) oxidation and nitrate reduction, alongside the resilience of the denitrification process in the presence of arsenic, underscores the versatility of electro-bioremediation.

5.2.2 Improving water quality through electro-bioremediation: a focus on water disinfection

Water disinfection is a critical step to ensure the absence of pathogens that can arise from punctual contamination (e.g., faecal and manure leaching) or during the water transport from the source to the point of use due to unhygienic practices (Chique et al., 2021; Peter-Varbanets et al., 2009). The European Directive 2020/2184 sets *Escherichia coli* and intestinal *Enterococcus* guideline values of 0 UFC mL^{-1} for drinking water. Chlorination has been a reliable disinfection method for controlling pathogen contamination for decades. However, it should be implemented carefully due to the potential generation of harmful by-products. For example, the reaction between chlorine and organic matter leads to the formation of disinfection by-products such as trihalomethanes, haloacetic acids and halogenated acetonitriles, all of which pose health risks to humans. Therefore, in the context of groundwater with low organic matter content, chlorination is considered a sustainable disinfection method with minimal risk of toxic by-product formation (Mazhar et al., 2020). Perchlorate is another toxic by-product that is important to consider in electrochemical disinfection (Long et al., 2021). However, its production can be minimised by using Ti-MMO anodes (e.g. Ti/IrO_2, Schaefer et al., 2015).

An innovative method was developed that simultaneously treated nitrate-contaminated groundwater by combining nitrate reduction and water disinfection in a single bioelectrochemical reactor (*Chapter* 4.3). The disinfection process involved *in-situ* chlorine production through anodic chloride oxidation using a Ti-MMO electrode. In terms of reactor operation, the external recirculation (between anode effluent and cathode influent) used in *Chapter* 4.1 has been replaced by internal cathodic recirculation to prevent biocathode damage caused by the accumulation of chlorine and oxygen in the anode compartment. Furthermore, a pH control was implemented to maintain a constant value of 6.75 ± 0.25 and ensure optimal denitrification performance, considering the significant correlation between pH and denitrification performance demonstrated in *Chapter* 4.2. This control was performed by the controlled addition of hydrochloric acid, which also contributed to an increase in the chloride concentration from 92 ± 1 mg Cl^- L^{-1} in the influent to 387 ± 24 mg Cl^- L^{-1}. The increase in chloride concentration had a direct impact on chlorine production. Consequently, a significant residual free chlorine concentration was achieved in the effluent, ranging from 0.3 ± 0.1 mg Cl_2 L^{-1} at HRT_{cat} of 2.4 h to 4.4 ± 1.4 mg Cl_2 L^{-1} at HRT_{cat} of 0.7 h. This variation corresponded to higher current intensities at lower $HRTs_{cat}$, increasing

from 35 ± 1 mA at HRT_{cat} of 2.4 h to 105 ± 5 mA at HRT_{cat} of 0.7 h. The residual free chlorine concentration effectively ensured disinfection and could have maintained water quality up to the point of use. This residual chlorine concentration aligns with levels typically found in conventional water treatment plants ranging from 0.2 to 2.0 mg Cl_2 L^{-1} (Brandt et al., 2017). Additionally, the disinfection process was evaluated regarding pathogen content for the first time, revealing the complete absence of Total coliforms, *E. coli,* and *Enterococcus* in the effluent.

Integrating water disinfection and nitrate reduction via electro-bioremediation simplifies the overall treatment, consolidating it into a single step for cost-effective potabilisation. For instance, the estimated operational cost of the electro-bioremediation addressing the nitrate reduction and the final disinfection was 0.9 ± 0.2 € m^{-3}, considering electricity consumption for powering the bio/electrochemical reactions (12% of the operating cost) and acid consumption (88% of the operational cost). This approach proved cost-effective when compared to other frequently used methods for nitrate removal, including reverse osmosis (0.04-2.67 € m^{-3}) and ion-exchange resin (0.07-2.85 € m^{-3}) (Jensen et al., 2012). Additionally, these nitrate removal treatments require a separate disinfection step. For instance, chlorination-based disinfection devices have a cost between 0.01 - 0.93 € m^{-3} (Dossegger et al., 2021). Hence, electro-bioremediation presented a competitive treatment by combining nitrate reduction and water disinfection, recovering chlorine from the HCl used to maintain the optimal pH for denitrification. Furthermore, *in-situ* chlorine production eliminates the need for transporting and handling hazardous disinfectant chemicals. Consequently, this simplification not only decreases overall operational expenses but also enhances the overall sustainability and safety of the treatment.

5.3 Decision-making for nitrate electro-bioremediation pilot plant development: from laboratory-scale to real implementation

The laboratory experimentation of this Ph.D. thesis validated and strengthened the use of electro-bioremediation for treating nitrate-contaminated groundwater (TRL 4-5). The subsequent phase involved the scaling-up of this technology and its validation in a real-world environment (TRL 6-7). There have been only a few attempts to apply METs for nitrogen removal at a pilot-scale so far (San-Martín et al., 2018; Lust et al., 2020; Vilajeliu-Pons et al., 2017). In addition, a previous project aimed at developing an *on-site* nitrate electro-bioremediation pilot plant was carried out within the group (NONIT, A BES for nitrate removal from contaminated groundwater, financed by Aqua Development Network, S.A. (ADNT). 067/14 24/11/2014). This underscores the urgent necessity to upscale this technology and validate its practical feasibility. The limited attempts at scaling-up highlight the complexity of this transition, exposing a notable gap between the promising results seen in laboratory-

scale experiments and the outcomes achieved at pilot-scale. It is crucial to interconnect the insights at the laboratory-scale with the factors that may come into play during scaling-up and real-world scenarios. Nevertheless, the information and findings obtained from pilot plant experiences will provide additional valuable knowledge that will contribute to the future advancement of METs (Figure 8).

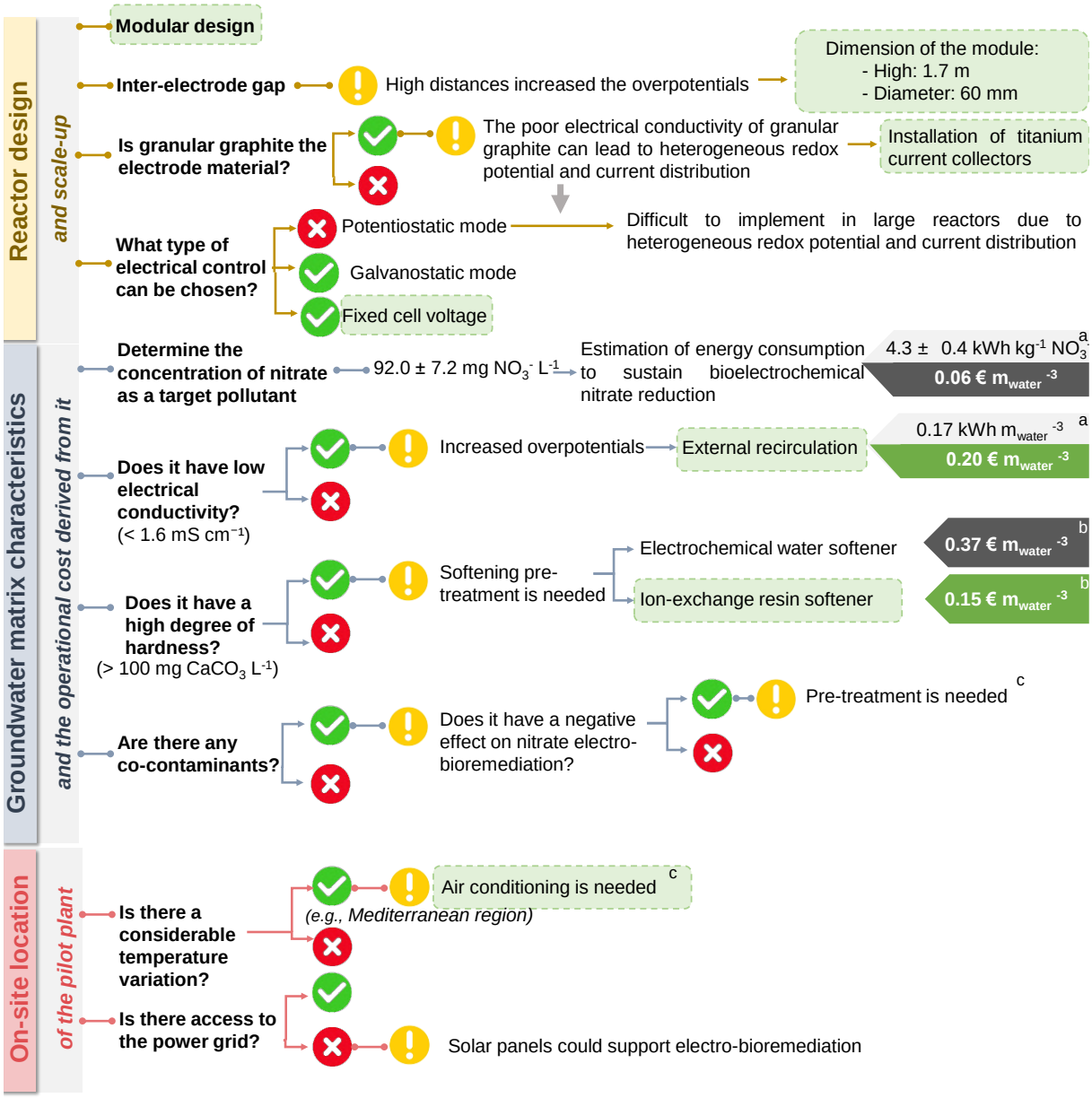

Figure 8: Decision-making tree outlining the main factors considered to develop an electro-bioremediation pilot plant and estimating its impact on operational costs. The green boxes represent the decisions made in the pilot plant developed in this Ph.D. thesis. [a] Extracted from Real Operations of the Pilot Plant in *Chapter* 4.5 at HRT_{cat} 2.0 h; [b] Extracted from *Chapter* 4.4.; and [c] The cost is not calculated due to the variability in the cost of each scenario.

5.3.1 Reactor design and scale-up

In the field of water treatment, scaling-up reactors typically involve increasing the volume while maintaining certain ratios, such as volume-to-surface area or volume-to-water flow rate. Nevertheless, this approach faces limitations in effectively addressing the scalability challenges of METs due to the intricate interplay between electrochemistry and microbiology (Jadhav et al., 2022a). Consequently, it is imperative to take into account various factors during the scaling-up process and assess their influence on reactor performance. Some of these factors include inter-electrode gap space, the distribution of redox potential across electrodes, electrode materials, and mass transfer between the liquid and electrode surface (Kadier et al., 2020; Rossi and Logan, 2022). As a result, the concept of developing modular units to better control these factors is considered a reasonable approach for scaling-up METs (Baeza et al., 2017; Dekker et al., 2009; Flimban et al., 2019). The different units can be connected either in series or parallel, creating a stacked system (Vilajeliu-Pons et al., 2017). A similar approach was implemented in the pilot plant developed in Navata. A modular tubular fixed-bed reactor was designed from the laboratory-scale designs by extending their reactor length but keeping the reactor diameter constant to keep the inter-electrode gap space from laboratory to pilot-scale.

Additionally, in prior laboratory studies (*Chapter* 4.2), the extracellular electron transfer was identified as a primary limiting step, underscoring the significance of maintaining a uniform redox potential and current density distribution to optimise denitrification performance. Nevertheless, granular graphite has a low electrical conductivity, leading to high electrical resistivity (approximately $1e^{-2}$ Ω m) together with a high redox potential and current distribution heterogeneity along the reactor. This is aggrieved by the considerable increase in reactor length (from 0.35 m at the laboratory-scale to 1.7 m at pilot-scale). The implementation of current collectors aimed to reduce these resistances to as low as $1e^{-3}$ Ω m, based on previous expertise within the group. While graphite rods were initially used as current collectors in the laboratory, their fragility led to the adoption of titanium-based current collectors in the pilot plant reactor in *Chapter* 4.5. In addition, titanium ($1e^{-6}$ Ω m) presented a lower electrical resistivity than graphite rod ($1e^{-3}$ Ω m). Hence, implementing a current collector holds the potential to mitigate heterogeneity in granular graphite electrodes. To ensure proper distribution within the cathode compartment in the pilot plant reactor (*Chapter* 4.5), an external cylindrical mesh of titanium was placed around the outer part of the cathode compartment. In addition, following the concept of a zero-gap electrode to minimise ohmic resistances (Baek et al., 2022), the titanium mesh was in contact with the cationic exchange membrane (i.e., the separator between the anode and cathode compartments). However, it is important to note that the current collectors in the pilot plant reactors represented 60% of the total reactor construction cost. Therefore, in order to properly allocate the investment in the reactor, their implementation requires careful consideration and evaluation.

Finally, replicating the same electrical control as in the laboratory-scale (potentiostatic) was not possible due to the electrical conductivity of granular graphite and the reactor's dimensions, which led to redox heterogeneity along the reactor (Figure 8). The cathode potential control at -0.32 V to support bioelectrochemical denitrification used at the laboratory-scale was switched to a cell voltage control. Thus, in the pilot plant, the cell voltage was regularly adjusted to keep the cathode potential within the range of -0.23 ± 0.03 to -0.67 ± 0.03 V. The cell voltage was raised from 1.22 ± 0.02 to 1.72 ± 0.05 V as denitrification rates increased during the experimental period to support the higher current density. Another alternative (not tested) would be a galvanostatic control, fixing the current density.

5.3.2 Influence of target groundwater matrix on pilot plant design and operation

The composition of groundwater during the treatment is a critical factor in all water treatment processes. Initially, the focus is on the concentration of the target contaminant (92.0 ± 7.2 mg NO_3^- L^{-1}). In electro-bioremediation, where a solid electrode replaces conventional chemicals, the quantity of contaminant to be removed is directly related to the current density needed to flow through the system and, thus, to the amount of energy required. The energy consumed by the system to facilitate bioelectrochemical nitrate reduction at the pilot-scale was 4.3 ± 0.3 kWh kg^{-1} NO_3^- (*Chapter* 4.5). Taking into account the influent nitrate concentration, the energy cost derived from denitrification in the pilot plant was 0.06 € m^{-3} (Figure 8).

Although considering the target contaminants is crucial, a comprehensive groundwater characterisation is essential to ensure the successful implementation of electro-bioremediation in the field. This includes parameters such as electrical conductivity, pH, and other ion content. This perspective was consistently applied throughout the entire Ph.D. thesis to gain valuable insights that could be later utilised in the development of the pilot plant. Normally, groundwater is characterised by low electrical conductivity (e.g., 0.8 mS cm^{-1} in Navata). This parameter leads to increased overpotentials within the system, affecting the transfer of charge-balancing ions. Specifically, the migration of protons outwards from the electroactive biofilm is impacted, consequently hindering the denitrification process by means of pH inhibition, as shown in *Chapter* 4.2. Prior work by Puig et al. (2012) already demonstrated the significant influence of low electrical conductivity (<1.6 mS cm^{-1}) on denitrification performance and selectivity. The laboratory studies (e.g., *Chapter* 4.1*)* demonstrated that implementing external recirculation to increase the internal flow velocity is essential in scenarios with low electrical conductivity to balance the pH and overcome mass transfer limitations. Subsequently, the pilot plant implemented an external recirculation, representing an energy cost that needs to be considered (0.20 € m^{-3}) (Figure 8).

The elevated presence of hardness ions (carbonate, calcium, and magnesium) is a common issue in water treatment plants due to scale deposition. However, this concern could be exacerbated in electro-bioremediation, where a higher local cathode pH might intensify scaling over the cathode electrode surface (Santini et al., 2017), which would reduce the effectiveness and lifespan of the treatment. Thus, a softening pretreatment is mandatory to operate with high-hardness groundwater (around 300 mg $CaCO_3$ L^{-1}). The pilot plant was equipped with a commercial softener (ion exchange resin softener, 0.15 € m^{-3}) for pretreating the groundwater. However, a more sustainable treatment option could be electrochemical water softening, as demonstrated at the laboratory-scale (0.37 € m^{-3}, as discussed in *Chapter* 4.4).

Another factor derived from the groundwater that may influence the performance is the presence of co-contaminants, which may come from various sources. These contaminants have the potential to influence denitrification performance in electro-bioremediation. Therefore, it is important to assess their impact on reactor performance during treatment through preliminary studies. Finally, one aspect that was not considered is the low abundance, even absence, of certain micronutrients in the real groundwater, which can have a significant impact on all biological treatment processes (e.g., phosphate content in Navata site was < 1 mg $P\text{-}PO_4^{3-}$ L^{-1}). Further evaluation of this aspect may introduce improvements in the treatment.

5.3.3 Electro-bioremediation pilot plant location: challenges of *on-site* treatment

The implementation of electro-bioremediation at real sites consistently poses challenges. While there are studies investigating the implementation of *in-situ* electro-bioremediation within the aquifer (Cecconet et al., 2020), more attention has been dedicated to *on-site* treatments (i.e., pump-and-treat). In-situ implementation requires a more detailed study of the characteristics of each aquifer to be treated and its surroundings. Meanwhile, *on-site* treatment is promising due to its potential for standardisation across multiple sites. Therefore, this Ph.D. thesis includes various designs and scales relevant to *on-site* treatment, culminating in the installation of an electro-bioremediation pilot plant for the *on-site* treatment of nitrate-contaminated groundwater.

The performance of the pilot plant and its *on-site* operation are directly influenced by its location. For instance, fluctuations in water quality might occur during the treatment process. Climatic conditions can also impact denitrification performance within the electro-bioremediation. For example, the Mediterranean climate is characterised by temperatures ranging between 35°C (maximum in summer) and 0°C (minimum in winter), with significant temperature variations between day and night. Given the temperature dependence of biological denitrification, with the optimal activity around 25-30°C and negligible activity below 5°C (Skiba, 2008), these temperature fluctuations can indeed affect the

performance of the denitrification process in electro-bioremediation. This impact was further explored in *Chapter* 4.2, revealing a linear dependency between the electroactivity of the denitrifying biocathode and temperature, with the highest activity observed at the higher tested temperature of 35°C. As a result, effective temperature control becomes imperative to ensure the successful operation of an *on-site* electro-bioremediation treatment. Consequently, the pilot plant was equipped with an air conditioning system to maintain a constant temperature throughout the experimental period.

Finally, when considering the perspective of employing electro-bioremediation as a decentralised water treatment approach, it becomes imperative to take into account the intricate challenge of electricity grid accessibility in remote regions. While this treatment method may indeed be entirely independent of reagents, the demand for energy remains indispensable in electro-bioremediation. Nevertheless, notable research has demonstrated the resilience of METs during periods of electricity interruption (Rovira-Alsina et al., 2021; Wang et al., 2021). This suggests the potential utilisation of solar panels as an energy source. However, further investigation is needed to fully explore the feasibility of this approach, particularly through studies carried out at the pilot plant level.

5.4 Current and future perspectives of nitrate electro-bioremediation for decentralised water treatment

While this Ph.D. thesis introduces nitrate electro-bioremediation as a decentralised solution for treating nitrate-contaminated groundwater, some key questions arise: Can it effectively compete with conventional treatments? Is electro-bioremediation sufficiently developed for real-world implementation and commercialisation?

Energy consumption is a crucial factor in the implementation of water treatment technologies and their competitiveness with conventional methods. This Ph.D. thesis showcases various designs and scales, and in all cases, nitrate electro-bioremediation has demonstrated a consistent energy consumption rate of 4-6 kWh kg^{-1} NO_3^-, equivalent to 0.3 kWh m^{-3} in the pilot plant (influent nitrate content of 92.0 ± 7.2 mg NO_3^- L^{-1}). This energy consumption is comparable to that of conventional treatments like reverse osmosis and electrodialysis, which usually range from 0.3 to 2.06 kWh m^{-3} (Aliaskari and Schäfer, 2021; Twomey et al., 2010). The lower energy consumption provides an advantage for possibly implementing the technology in remote areas with limited access to the electricity grid through the use of solar panels to provide this low energy demand. Furthermore, decentralised treatment offers additional advantages over conventional treatment with regard to chemical independence and the lack of concentrated and hazardous brine production. Electro-bioremediation goes even further by achieving efficient and selective nitrate removal, with over 99% conversion to N_2, a significant benefit demonstrated throughout the entirety of this Ph.D. thesis.

The advantages of electro-bioremediation over conventional treatments are considerable. However, an important aspect to consider in the evaluation for its future implementation is the water production cost. The operating cost of electro-bioremediation, estimated from the pilot plant operation, was 0.4 € m^{-3} at an HRT_{cat} of 2.0 hours (*Chapter* 4.5). This cost includes the energy consumed by the reactor to support the bio/electrochemical reactions, the recirculation pump and maintenance. However, if the CAPEX is considered, assuming a reactor lifetime of 30 years, the TOTEX increases to 7.05 € m^{-3}. This is still high in comparison with conventional treatment. For example, reverse osmosis can range between 0.04-2.67 € m^{-3} and ion exchange resin between 0.07-2.85 € m^{-3} (Jensen et al., 2012). This is an indication that the technology is still under development and needs further improvements before commercialisation. One effective approach involves the reduction of HRT_{cat} alongside an increase in the volume treated within a single module, resulting in reduced water production costs, thereby enhancing its competitiveness in the market. In this sense, conventional treatments still have higher treatment capacities with shorter HRT (in the range of seconds to minutes) (Xu et al., 2018). If the HRT_{cat} were reduced to 0.5 h (the lower value reported in the literature, Table 3), the TOTEX could be reduced to 1.80 € m^{-3}. This emphasises the necessity for additional work at the pilot plant level to achieve cost-effective treatment and make electro-bioremediation commercially viable.

In particular, the bioelectrochemical reactor in the pilot plant costs around 1400€, but there is considerable scope for cost reduction through materials research to develop new electrodes and reactor design. On one hand, the titanium current collectors have proved to be a key component of the reactor, accounting for 60% of the reactor cost. On the other hand, in this thesis, cationic exchange membranes were chosen for all bioelectrochemical reactors. In addition, the cationic exchange membrane used to separate the anodic and cathodic compartments in the pilot plant accounted for 26% of the total reactor cost (*Chapter* 4.5). This membrane is commonly used in bioelectrochemical reactors, particularly in scenarios where compounds formed in one compartment could potentially influence the other (e.g. anodic oxygen production potentially affecting denitrification). Therefore, in this Ph.D. thesis, the use of cation exchange membranes was chosen for all bioelectrochemical reactors. However, in the laboratory-scale bioelectrochemical reactor presented in *Chapter* 4.1 and in the pilot plant presented in *Chapter* 4.5, the effluent from the anode was recirculated to the cathode. Thus, both compartments were hydraulically connected, which is possible due to the low oxygen production in the anode compartment and to promote proton balance between both compartments. Consequently, in these scenarios, the membrane only provides physical separation, allowing it to be replaced by other low-cost materials such as plastic (Dell'Armi et al., 2022).

Towards the future implementation of electro-bioremediation, this Ph.D. thesis focused on using a modular bioelectrochemical reactor. The pilot plant presented in *Chapter* 4.5 used a single module to validate electro-bioremediation for nitrate-contaminated groundwater on a larger scale in a real-world environment. These individual modules can be easily connected in parallel to increase water treatment capacity while maintaining consistent performance in terms of nitrate reduction rate and effluent quality. Assuming the use of the same reactors as in *Chapter* 4.5 and an improvement of the HRT_{cat} to 0.5 h (treatment capacity of 57 L d^{-1} for each module), it can be estimated that 18 modules would be required to supply 1 m^3 d^{-1}. This represents an initial investment cost of around 25,000 € for the stack reactors, while the expected TOTEX remains at 1.80 € m^{-3} with an amortisation period of 30 years (as mentioned above). In addition to the reactors, the initial investment must consider other equipment such as the tanks, the potentiostat, the control panel and, if necessary, other supporting equipment such as the water softener or the air conditioner. Nevertheless, it is important to explore the potential for reducing the cost of reactor construction. Overall, electro-bioremediation is promising in terms of cost-effectiveness. Future advances in reactor design and ongoing research efforts to optimise operating parameters are key to achieve its full potential as a reliable and efficient technology for the remediation of nitrate-contaminated groundwater.

Other important factors to consider for the future development of electro-bioremediation as a decentralised system include automation of the treatment process to ensure simple operation by non-specialised users. The pilot plant presented and developed in *Chapter* 4.5 included remote control and monitoring. In addition, the pilot plant was able to achieve a very resilient treatment without any maintenance tasks, thus reducing the personal requirements. Nevertheless, the automation of the entire treatment should be given further attention. Finally, gaining social and administrative acceptance is key as electro-bioremediation moves towards wider implementation. Administrations often have specific requirements in addition to meeting drinking water standards, and these may vary from region to region. Identifying and addressing these different requirements through future research will be critical to the successful adoption of electro-bioremediation.

CHAPTER 6:

Conclusions

6

The issue of water stress, particularly water pollution, has become a global concern. There is an urgent need to regenerate contaminated groundwater reserves. However, existing remediation treatments are often associated with significant environmental impacts and economic costs. Therefore, it is necessary to develop novel technologies able to treat contaminated groundwater with minimised environmental impacts and economic expenses. This Ph.D. thesis validates and provides insights that highlight the significant potential of electro-bioremediation as a decentralised water treatment for nitrate-contaminated groundwater. With promising results obtained at laboratory-scale (TRL 3-4), this Ph.D. thesis progressed to validate the technology through the implementation of an on-site pilot plant (TRL 5). In particular, this Ph.D. thesis achieved the following milestones:

(i) The improvement of the nitrate reduction rates and efficiencies was the primary focus. The laboratory-scale study started with a nitrate reduction rate of 2.3 kg NO_3^- $m^{-3}d^{-1}$ (HRT_{cat} 1.5 h), and it was increased to 5.0 kg NO_3^- $m^{-3}d^{-1}$ (HRT_{cat} 0.7 h) by introducing pH control at 6.75 ± 0.25. Notably, this achievement represents the highest nitrate reduction rate reported to date, to the best of the author's knowledge. When the technology was evaluated at a pilot-scale level treating nitrate-contaminated groundwater *on-site*, a substantial nitrate reduction rate of around 1.0 kg NO_3^- $m^{-3}d^{-1}$ (HRT_{cat} 2.0 h) was achieved. The different studies performed in this Ph.D. thesis underscored the pivotal role of hydrodynamics in circumventing the constraints posed by the low ionic strength of groundwater. Consistently through all the chapters, significant advantages over conventional treatments were demonstrated, including reduced environmental impacts (e.g., no sludge generation) and competitive energy requirements (4-6 kWh kg^{-1} NO_3^-).

(ii) Electro-bioremediation was demonstrated to be a versatile treatment method. For example, it was shown to be effective in dealing with the coexistence of arsenite and nitrate contamination. Arsenite was efficiently oxidised to arsenate as a critical step for its removal, thereby reducing its toxicity. Remarkably, even at a high concentration of 5 mg L^{-1}, arsenic did not adversely affect the bioelectrochemical nitrate reduction rate nor the end-product selectivity (i.e., nitrate conversion to dinitrogen gas).

(iii) *Ex-situ* biocathode characterisation using the eClamp setup allowed the fast electrochemical characterisation of running reactors. These studies revealed that EET was the limiting step in the electroactive denitrifying biofilm throughout the reduction of the different denitrification intermediates. The nitrate removal kinetics fitted to an adapted Michaelis-Menten model, yielding a K_M^{app} of 3.8 ± 0.9 mg N-NO_3^- L^{-1} and a v_{max}^{app} of 9.5 ± 2.6 kg NO_3^- $m^{-3}d^{-1}$. These results demonstrated: i) the capability of electroactive denitrifying biofilms to fully remove nitrate from water without

compromising microbial activity, and ii) the potential of these biofilms to remove nitrates at rates exceeding those observed in the running reactors. Finally, this methodology also provided an efficient screening of pH and temperature that can be used to further increase the nitrate reduction rates, as well as to anticipate the biocathode response to fluctuations. Specifically, in the denitrifying biocathode studied, optimal nitrate removal occurred at pH 6 and 35°C.

(iv) Electrochemical disinfection was integrated into a single-step electro-bioremediation system, allowing for the achievement of an effluent that met drinking water standards not only in terms of nitrates and nitrites but also with regard to pathogens. This system involved the addition of hydrochloric acid, which enhanced denitrification in the biocathode compartments, while chloride was recovered and oxidised to chlorine in the anode. The treated water showed free chlorine concentrations ranging from 0.3 ± 0.1 mg Cl_2 L^{-1} at HRT_{cat} of 2.4 h to 4.4 ± 1.4 mg Cl_2 L^{-1} at HRT_{cat} of 0.7 h. Pathogen analysis confirmed the absence of Total coliforms, *E. coli*, and *Enterococcus* in the effluent. Thus, the system proved to be a competitive and environmentally friendly decentralised treatment option with competitive operating costs.

(v) The presence of hardness in the groundwater matrix can significantly affect electro-bioremediation performance due to scale formation over the cathode. This Ph.D. thesis developed an electrochemical water softening membrane-less reactor that was shown to be a suitable pretreatment method for nitrate electro-bioremediation.

(vi) Scale-up of electro-bioremediation is the main challenge for advancing towards real-world implementation. This Ph.D. thesis successfully transitioned electro-bioremediation from the laboratory to an *on-site* pilot plant. The process of scaling-up addressed the challenges related to reactor design, the water matrix, and *on-site* operation. The technology was validated in a real-world environment (TRL 5), achieving a nitrate reduction rate of 0.9 kg NO_3^- $m^{-3}d^{-1}$ (efficiency 82.5 ± 17.9%) at an HRT_{cat} of 2.0 h and keeping energy consumption at 4.3 ± 0.4 kWh kg^{-1} NO_3^-. In addition, the competitive OPEX cost of 0.40 € m^{-3} encourages further exploration in this area.

In conclusion, this Ph.D. thesis represents a significant step towards unlocking the full potential of electro-bioremediation in addressing the pressing challenges of nitrate-groundwater contamination. The results encourage further research in this area due to its significant advantages, including its versatility in treating different contaminants. This Ph.D. thesis paves the way for further development of electro-bioremediation at a pilot-scale level to enable the implementation and future commercialisation of this technology.

References

Alavijeh, H.N., Sadeghi, M., Ghahremanfard, A., 2023. Experimental and economic evaluation of nitrate removal by a nanofiltration membrane. Environ. Sci. Pollut. Res. 30, 40783–40798. https://doi.org/10.1007/s11356-022-24972-9

Albina, P., Durban, N., Bertron, A., Albrecht, A., Robinet, J.C., Erable, B., 2021. Nitrate and nitrite bacterial reduction at alkaline pH and high nitrate concentrations, comparison of acetate versus dihydrogen as electron donors. J. Environ. Manage. 280, 111859. https://doi.org/10.1016/j.jenvman.2020.111859

Aliaskari, M., Schäfer, A.I., 2021. Nitrate, arsenic and fluoride removal by electrodialysis from brackish groundwater. Water Res. 190, 116683. https://doi.org/10.1016/j.watres.2020.116683

Anraku, Y., 1988. Bacterial electron transport chains. Annu. Rev. Biochem. 57, 101–132. https://doi.org/10.1146/annurev.bi.57.070188.000533

APHA, 2005. Standard Methods for the Examination of Water and Wastewater, 19th ed, American Public Healt Association, Washington DC, USA.

Ariono, D., Purwasasmita, M., Wenten, I.G., 2016. Brine effluents: Characteristics, environmental impacts, and their handling. Journal of Engineering and Technological Sciences 48(9), 367 – 387. https://doi.org/10.5614/j.eng.technol.sci.2016.48.4.1

Ashbolt, N.J., 2004. Microbial contamination of drinking water and disease outcomes in developing regions. Toxicology 198, 229–238. https://doi.org/10.1016/j.tox.2004.01.030

Aulenta, F., Reale, P., Canosa, A., Rossetti, S., Panero, S., Majone, M., 2010. Characterization of an electro-active biocathode capable of dechlorinating trichloroethene and cis-dichloroethene to ethene. Biosens. Bioelectron. 25, 1796–1802. https://doi.org/10.1016/j.bios.2009.12.033

Bachate, S.P., Khapare, R.M., Kodam, K.M., 2012. Oxidation of arsenite by two β-proteobacteria isolated from soil. Appl. Microbiol. Biotechnol. https://doi.org/10.1007/s00253-011-3606-7

Baek, G., Rossi, R., Saikaly, P.E., Logan, B.E., 2022. High-rate microbial electrosynthesis using a zero-gap flow cell and vapor-fed anode design. Water Res. 219, 118597. https://doi.org/10.1016/J.WATRES.2022.118597

Baeza, J.A., Martínez-Miró, À., Guerrero, J., Ruiz, Y., Guisasola, A., 2017. Bioelectrochemical hydrogen production from urban wastewater on a pilot scale. J. Power Sources 356, 500–509. https://doi.org/10.1016/j.jpowsour.2017.02.087

Balch, W.E., Fox, G.E., Magrum, L.J., Woese, C.R., Wolfe, R.S., 1979. Methanogens: reevaluation of a unique biological group. Microbiol. Rev. 43, 260–296. https://doi.org/10.1128/mr.43.2.260-296.1979

Banerjee, K., Amy, G.L., Prevost, M., Nour, S., Jekel, M., Gallagher, P.M., Blumenschein, C.D., 2008. Kinetic and thermodynamic aspects of adsorption of arsenic onto granular ferric hydroxide (GFH). Water Res. 42, 3371–3378. https://doi.org/10.1016/j.watres.2008.04.019

Barba, S., López-Vizcaíno, R., Saez, C., Villaseñor, J., Cañizares, P., Navarro, V., Rodrigo, M.A., 2018. Electro-bioremediation at the prototype scale: What it should be learned for the scale-up. Chemical Engineering Journal 334, 2030–2038. https://doi.org/10.1016/J.CEJ.2017.11.172

Bard, A.J., Faulkner, L.R., 2001. Electrochemical Methods: Fundamentals and Applications, 2nd Edition, Electrochemical Methods - Fundamentals and Applications. https://doi.org/https://doi.org/10.1023/A:1021637209564

Bardon, C., Poly, F., Piola, F., Pancton, M., Comte, G., Meiffren, G., Haichar, F. el Z., 2016. Mechanism of biological denitrification inhibition: procyanidins induce an allosteric transition of the membrane-bound nitrate reductase through membrane alteration. FEMS Microbiol. Ecol. 92, fiw034. https://doi.org/10.1093/FEMSEC/FIW034

Batlle-Vilanova, P., Puig, S., Gonzalez-Olmos, R., Vilajeliu-Pons, A., Bañeras, L., Balaguer, M.D., Colprim, J., 2014. Assessment of biotic and abiotic graphite cathodes for hydrogen production in microbial electrolysis cells. Int. J. Hydrogen Energy 39, 1294–1305. https://doi.org/10.1016/j.ijhydene.2013.11.017

Battistuzzi, G., Borsari, M., Sola, M., 2001. Medium and Temperature Effects on the Redox Chemistry of Cytochrome c. Eur. J. Inorg. Chem 2001, 2989–3004. https://doi.org/10.1002/1099-0682

Bereiter, R., Vescoli, D., Antonio Liebminger, L., 2021. Disinfection in Water and Used Water Purification. Handb. Water Used Water Purif. 1–32. https://doi.org/10.1007/978-3-319-66382-1_65-1

Bergmann, H., 2021. Electrochemical disinfection – State of the art and tendencies. Curr. Opin. Electrochem. 28, 100694. https://doi.org/10.1016/J.COELEC.2021.100694

Bissen, M., Frimmel, F.H., 2003. Arsenic - A review. Part II: Oxidation of arsenic and its removal in water treatment. Acta Hydrochim. Hydrobiol. 31, 97–107. https://doi.org/10.1002/aheh.200300485

Blázquez, E., Gabriel, D., Baeza, J.A., Guisasola, A., Ledezma, P., Freguia, S., 2021. Implementation of a sulfide–air fuel cell coupled to a sulfate-reducing biocathode for elemental sulfur recovery. Int. J. Environ. Res. Public Health 18, 5571. https://doi.org/10.3390/ijerph18115571

Bleam, W., 2017. Chapter 9: Reduction-Oxidation Chemistry, in: Soil and Environmental Chemistry. Academic Press, pp. 445–489. https://doi.org/10.1016/B978-0-12-804178-9.00009-4

Borho, M., Wilderer, P., 1996. Optimized removal of arsenate(III) by adaptation of oxidation and precipitation processes to the filtration step. Water Sci. Technol. 34, 25–31. https://doi.org/10.1016/S0273-1223(96)00783-4

Borsje, C., Liu, D., Sleutels, T.H.J.A., Buisman, C.J.N., ter Heijne, A., 2016. Performance of single carbon granules as perspective for larger scale capacitive bioanodes. J. Power Sources. https://doi.org/10.1016/j.jpowsour.2016.06.092

Bosko, M.L., Rodrigues, M.A.S., Ferreira, J.Z., Miró, E.E., Bernardes, A.M., 2014. Nitrate reduction of brines from water desalination plants by membrane electrolysis. J. Memb. Sci. 451, 276–284. https://doi.org/10.1016/J.MEMSCI.2013.10.004

Botti, A., Pous, N., Cheng, H.Y., Colprim, J., Zanaroli, G., Puig, S., 2023. Electrifying secondary settlers to enhance nitrogen and pathogens removals. Chem. Eng. J. 451(3), 138949. https://doi.org/10.1016/j.cej.2022.138949

Brandt, M.J., Johnson, K.M., Elphinston, A.J., Ratnayaka, D.D., 2017. Chapter 11 - Disinfection of Water, in: Twort's Water Supply. Butterworth-Heinemann, pp. 475–511. https://doi.org/10.1016/B978-0-08-100025-0.00011-9

Brutinel, E.D., Gralnick, J.A., 2012. Shuttling happens: Soluble flavin mediators of extracellular electron transfer in Shewanella. Appl. Microbiol. Biotechnol. 93, 41–48. https://doi.org/10.1007/S00253-011-3653-0/FIGURES/3

Caizán-Juanarena, L., Servin-Balderas, I., Chen, X., Buisman, C.J.N., ter Heijne, A., 2019. Electrochemical and microbiological characterization of single carbon granules in a multi-anode microbial fuel cell. J. Power Sources. https://doi.org/10.1016/j.jpowsour.2019.04.042

Callahan, B.J., McMurdie, P.J., Rosen, M.J., Han, A.W., Johnson, A.J.A., Holmes, S.P., 2016. DADA2: High-resolution sample inference from Illumina amplicon data. Nat. Methods 13, 581–583. https://doi.org/10.1038/nmeth.3869

Cao, X., Huang, X., Liang, P., Xiao, K., Zhou, Y., Zhang, X., Logan, B.E., 2009. A new method for water desalination using microbial desalination cells. Environ. Sci. Technol. 43, 114–1120. https://doi.org/10.1021/es901950j

Ceballos-Escalera, A., Pous, N., Balaguer, M.D., Puig, S., 2022. Electrochemical water softening as pretreatment for nitrate electro bioremediation. Sci. Total Environ. 806, 150433. https://doi.org/10.1016/J.SCITOTENV.2021.150433

Ceballos-Escalera, A., Pous, N., Chiluiza-Ramos, P., Korth, B., Harnisch, F., Bañeras, L., Balaguer, M.D., Puig, S., 2021. Electro-bioremediation of nitrate and arsenite polluted groundwater. Water Res. 190, 116748. https://doi.org/10.1016/j.watres.2020.116748

Cecconet, D., Devecseri, M., Callegari, A., Capodaglio, A.G., 2018a. Effects of process operating conditions on the autotrophic denitrification of nitrate-contaminated groundwater using bioelectrochemical systems. Sci. Total Environ. 613–614, 663–671. https://doi.org/10.1016/j.scitotenv.2017.09.149

Cecconet, D., Sabba, F., Devecseri, M., Callegari, A., Capodaglio, A.G., 2020. In situ groundwater remediation with bioelectrochemical systems: A critical review and future perspectives. Environ. Int. 137, 105550. https://doi.org/10.1016/j.envint.2020.105550

Cecconet, D., Zou, S., Capodaglio, A.G., He, Z., 2018b. Evaluation of energy consumption of treating nitrate-contaminated groundwater by bioelectrochemical systems. Sci. Total Environ. 636, 881–890. https://doi.org/10.1016/j.scitotenv.2018.04.336

Chakraborty, A., DasGupta, C.K., Bhadury, P., 2020. Diversity of Betaproteobacteria revealed by novel primers suggests their role in arsenic cycling. Heliyon. https://doi.org/10.1016/j.heliyon.2019.e03089

Chaudhary, S., Singh, R., Yadav, S., Patil, S.A., 2021. Electrochemical enrichment of haloalkaliphilic nitrate-reducing microbial biofilm at the cathode of bioelectrochemical systems. iScience 24, 102682. https://doi.org/10.1016/j.isci.2021.102682

Chen, F., Xia, Q., Ju, L.K., 2006. Competition between oxygen and nitrate respirations in continuous culture of Pseudomonas aeruginosa performing aerobic denitrification. Biotechnol. Bioeng. 93, 1069–1078. https://doi.org/10.1002/bit.20812

Chen, W., Parette, R., Zou, J., Cannon, F.S., Dempsey, B.A., 2007. Arsenic removal by iron-modified activated carbon. Water Res. https://doi.org/10.1016/j.watres.2007.01.052

Chique, C., Hynds, P., Burke, L.P., Morris, D., Ryan, M.P., O'Dwyer, J., 2021. Contamination of domestic groundwater systems by verotoxigenic escherichia coli (VTEC), 2003–2019: A global scoping review. Water Res. 188, 116496. https://doi.org/10.1016/J.WATRES.2020.116496

Choi, J.H., Maruthamuthu, S., Lee, H.G., Ha, T.H., Bae, J.H., 2009. Nitrate removal by electro-bioremediation technology in Korean soil. J. Hazard. Mater. 168, 1208–1216. https://doi.org/10.1016/j.jhazmat.2009.02.162

Chu, L., Wang, J., 2017. Denitrification of groundwater using a biodegradable polymer as a carbon source: Long-term performance and microbial diversity. RSC Adv. 7, 53454. https://doi.org/10.1039/c7ra11151g

Clauwaert, P., De Paepe, J., Jiang, F., Alonso-Fariñas, B., Vaiopoulou, E., Verliefde, A., Rabaey, K., 2020. Electrochemical tap water softening: A zero chemical input approach. Water Research 169, 115263 https://doi.org/10.1016/j.watres.2019.115263

Clauwaert, P., Desloover, J., Shea, C., Nerenberg, R., Boon, N., Verstraete, W., 2009. Enhanced nitrogen removal in bio-electrochemical systems by pH control. Biotechnol. Lett. 31, 1537–1543. https://doi.org/10.1007/s10529-009-0048-8

Clauwaert, P., Rabaey, K., Aelterman, P., De Schamphelaire, L., Pham, T.H., Boeckx, P., Boon, N., Verstraete, W., 2007. Biological denitrification in microbial fuel cells. Environ. Sci. Technol. 41, 3354–3360. https://doi.org/10.1021/es062580r

Costa, A.R., de Pinho, M.N., 2006. Performance and cost estimation of nanofiltration for surface water treatment in drinking water production. Desalination 196, 55–65. https://doi.org/10.1016/J.DESAL.2005.08.030

Costa, N.L., Clarke, T.A., Philipp, L.A., Gescher, J., Louro, R.O., Paquete, C.M., 2018. Electron transfer process in microbial electrochemical technologies: The role of cell-surface exposed conductive proteins. Bioresour. Technol. 255, 308–317. https://doi.org/10.1016/J.BIORTECH.2018.01.133

Crognale, S., Amalfitano, S., Casentini, B., Fazi, S., Petruccioli, M., Rossetti, S., 2017. Arsenic-related microorganisms in groundwater: a review on distribution, metabolic activities and potential use in arsenic removal processes. Rev. Environ. Sci. Biotechnol. 16, 647–665. https://doi.org/10.1007/s11157-017-9448-8

Cusick, R.D., Bryan, B., Parker, D.S., Merrill, M.D., Mehanna, M., Kiely, P.D., Liu, G., Logan, B.E., 2011. Performance of a pilot-scale continuous flow microbial electrolysis cell fed winery wastewater. Appl. Microbiol. Biotechnol. 89, 2053–2063. https://doi.org/10.1007/s00253-011-3130-9

de Smit, S.M., Buisman, C.J.N., Bitter, J.H., Strik, D.P.B.T.B., 2021. Cyclic Voltammetry is Invasive on Microbial Electrosynthesis. ChemElectroChem 8, 3384–3396. https://doi.org/10.1002/CELC.202100914

Dekker, A., Ter Heijne, A., Saakes, M., Hamelers, H.V.M., Buisman, C.J.N., 2009. Analysis and improvement of a scaled-up and stacked microbial fuel cell. Environ. Sci. Technol. 43, 9038–9042. https://doi.org/10.1021/ES901939R

Dell'Armi, E., Rossi, M.M., Zeppilli, M., Majone, M., Papini, M.P., 2022. Bioelectrochemical Chlorinated Aliphatic Hydrocarbons Reduction in Synthetic and Real Contaminated Groundwaters. Chem. Eng. Trans. 93, 217–222. https://doi.org/10.3303/CET2293037

Deslouis, C., Gabrielli, C., Keddam, M., Khalil, A., Rosset, R., Tribollet, B., Zidoune, M., 1997. Impedance techniques at partially blocked electrodes by scale deposition. Electrochimica Acta 42(8), 1219-1233 https://doi.org/10.1016/S0013-4686(96)00290-3

Dessì, P., Rovira-Alsina, L., Sánchez, C., Dinesh, G.K., Tong, W., Chatterjee, P., Tedesco, M., Farràs, P., Hamelers, H.M.V., Puig, S., 2021. Microbial electrosynthesis: Towards sustainable biorefineries for production of green chemicals from CO2 emissions. Biotechnol. Adv. 46, 107675. https://doi.org/10.1016/j.biotechadv.2020.107675

Di Capua, F., Milone, I., Lakaniemi, A.M., Lens, P.N.L., Esposito, G., 2017. High-rate autotrophic denitrification in a fluidized-bed reactor at psychrophilic temperatures. Chem. Eng. J. 313, 591–598. https://doi.org/10.1016/J.CEJ.2016.12.106

Dirany, A., Drogui, P., El Khakani, M.A., 2016. Clean electrochemical deposition of calcium carbonate to prevent scale formation in cooling water systems. Environmental Chemistry Letters volume 14, 507-514 https://doi.org/10.1007/s10311-016-0579-x

Donald E., C., Alexander N., G., Paul G., F., 2010. Nitrogen's Past and Future. Science 330, 192–196. https://doi.org/10.1126/science.330.6001.147-b

Dossegger, L., Tournefier, A., Germann, L., Gartner, N., Huonder, T., Wanyama, K., Ouma, H., Meierhofer, R., 2021. Assessment of low-cost, non-electrically powered chlorination devices for gravity-driven membrane water kiosks in eastern Uganda. Waterlines 40, 92–106. https://doi.org/http:/ /dx.doi.org/ 10. 3 362/ 1756-3488.20-00014

EEA, 2018. European waters - assessment of status and pressures 2018. https://doi.org/0.2800/303664

Emerson, D., Field, E.K., Chertkov, O., Davenport, K.W., Goodwin, L., Munk, C., Nolan, M., Woyke, T., 2013. Comparative genomics of freshwater Fe-oxidizing bacteria: implications for physiology, ecology, and systematics. Front. Microbiol. 4, 254. https://doi.org/10.3389/FMICB.2013.00254

Entezari, M.H., Tahmasbi, M., 2009. Water softening by combination of ultrasound and ion exchange. Ultrasonics Sonochemistry 16(3), 356-360 https://doi.org/10.1016/j.ultsonch.2008.09.008

EurEau, 2020. The governance of water services in Europe, National Guidelines for Infection Prevention and Control in Viral Hemorrhagic Fevers (VHF).

European Commission, 2008. Groundwater protection in Europe: The new groundwater directive - consolidating the EU regulatory framework. Office for Official Publications of the European Communities. https://doi.org/10.2779/84304

European Commission, 2021. Report from the comission to the council and the european parliament on the implementation of Council Directive 91/676/EEC concerning the protection of waters against pollution caused by nitrates from agricultural sources based on Member State reports for the period 2016–2019.

Eurostat. Statistics Explained: Electricity price statistics second period 2020. https://ec.europa.eu/eurostat/statistics-explained/index.php?title=Electricity_price_statistics (accessed 7.13.21).

Fanning, J.C., 2000. The chemical reduction of nitrate in aqueous solution. Coord. Chem. Rev. 199, 159–179. https://doi.org/10.1016/S0010-8545(99)00143-5

FAO AQUAMAPS, Level of water stress (SDG 6.4.2) by major river basin [WWW Document], 2022. URL https://data.apps.fao.org/aquamaps/ (accessed 5.17.23).

FAO, U.W., 2021. Progress on level of water stress. Global status and acceleration needs for SDG Indicator 6.4.2. https://doi.org/10.4060/cb6241en

Fekete-Kertész, I., Pous, N., Feigl, V., Berkl, Z., Ceballos-Escalera, A., Balaguer, M.D., Puig, S., Molnár, M., 2023. Ecotoxicity characterization assisted performance assessment of electro-bioremediation reactors for nitrate and arsenite elimination. Biotechnol. Bioeng. 1–16. https://doi.org/10.1002/bit.28580

Feng, J., Lang, G., Li, Tingting, Zhang, J., Li, Tengyue, Jiang, Z., 2022. Enhanced removal performance of zero-valent iron towards heavy metal ions by assembling Fe-tannin coating. J. Environ. Manage. 319, 115619. https://doi.org/10.1016/J.JENVMAN.2022.115619

Fewtrell, L., 2004. Drinking-water nitrate, methemoglobinemia, and global burden of disease: A discussion. Environmental Health Perspectives 112 (14) https://doi.org/10.1289/ehp.7216

Flimban, S.G.A., Ismail, I.M.I., Kim, T., Oh, S.E., 2019. Overview of recent advancements in the microbial fuel cell from fundamentals to applications: Design, major elements, and scalability. Energies 12, 3390. https://doi.org/10.3390/en12173390

Fourmond, V., Hoke, K., Heering, H.A., Baffert, C., Leroux, F., Bertrand, P., Léger, C., 2009. SOAS: A free program to analyze electrochemical data and other one-dimensional signals. Bioelectrochemistry 76, 141–147. https://doi.org/10.1016/j.bioelechem.2009.02.010

Fujii, K., Yoshida, N., Miyazaki, K., 2021. Michaelis–Menten equation considering flow velocity reveals how microbial fuel cell fluid design affects electricity recovery from sewage wastewater. Bioelectrochemistry 140, 107821. https://doi.org/10.1016/j.bioelechem.2021.107821

Gabrielli, C., Keddam, M., Khalil, A., Rosset, R., Zidoune, M., 1997. Study of calcium carbonate scales by electrochemical impedance spectroscopy. Electrochimica Acta 42(8), 1207-1218 https://doi.org/10.1016/S0013-4686(96)00289-7

Gabrielli, C., Keddam, M., Perrot, H., Khalil, A., Rosset, R., Zidoune, M., 1996. Characterization of the efficiency of antiscale treatments of water. Part I: Chemical processes. Journal of Applied Electrochemistry 26, 1125-1132 https://doi.org/10.1007/BF00243737

Gabrielli, C., Maurin, G., Francy-Chausson, H., Thery, P., Tran, T.T.M., Tlili, M., 2006. Electrochemical water softening: principle and application. Desalination 201(1-3), 150–163 https://doi.org/10.1016/j.desal.2006.02.012

Gadegaonkar, S.S., Mander, Ü., Espenberg, M., 2023. A state-of-the-art review and guidelines for enhancing nitrate removal in bio-electrochemical systems (BES). J. Water Process Eng. 53, 103788. https://doi.org/10.1016/J.JWPE.2023.103788

Gai, M., Yano, T., Tamegai, H., Fukumori, Y., Yamanaka, T., 1992. Thiobacillus ferrooxidans cytochrome c oxidase: Purification, and molecular and enzymatic features. J. Biochem. 112, 816–821. https://doi.org/10.1093/oxfordjournals.jbchem.a123982

García-Lledó, A., Vilar-Sanz, A., Trias, R., Hallin, S., Bañeras, L., 2011. Genetic potential for N2O emissions from the sediment of a free water surface constructed wetland. Water Res. 45, 5621–5632. https://doi.org/10.1016/j.watres.2011.08.025

García-Ruiz, R., Pattinson, S.N., Whitton, B.A., 1998. Kinetic parameters of denitrification in a river continuum. Appl. Environ. Microbiol. 64, 2533–2538. https://doi.org/10.1128/aem.64.7.2533-2538.1998

Gerba, C.P., 2015. Environmentally Transmitted Pathogens, in: Environmental Microbiology. pp. 509–550. https://doi.org/10.1016/B978-0-12-394626-3.00022-3

Ghosh, R., Chatterjee, S., Mandal, N.C., 2020. Stenotrophomonas, in: Beneficial Microbes in Agro-Ecology: Bacteria and Fungi. Academic Press, pp. 427–442. https://doi.org/10.1016/B978-0-12-823414-3.00020-4

Glass, C., Silverstein, J., 1998. Denitrification kinetics of high nitrate concentration water: pH effect on inhibition and nitrite accumulation. Water Res. https://doi.org/10.1016/S0043-1354(97)00260-1

Gregoire, K.P., Glaven, S.M., Hervey, J., Lin, B., Tender, L.M., 2014. Enrichment of a High-Current Density Denitrifying Microbial Biocathode. J. Electrochem. Soc. 161, H3049–H3057. https://doi.org/10.1149/2.0101413jes

Gregory, K.B., Bond, D.R., Lovley, D.R., 2004. Graphite electrodes as electron donors for anaerobic respiration. Environ. Microbiol. https://doi.org/10.1111/j.1462-2920.2004.00593.x

Gu, Z., Liu, Z., Cheng, Y., Zhu, Z., Tian, J., Hu, C., Qu, J., 2024. Intensified denitrification in a fluidized-bed reactor with suspended sulfur autotrophic microbial fillers. Bioresour. Technol. 391, 129965. https://doi.org/10.1016/J.BIORTECH.2023.129965

Hassan, H., Dai, S., Jin, B., 2019. Bioelectrochemical Reaction Kinetics, Mechanisms, and Pathways of Chlorophenol Degradation in MFC Using Different Microbial Consortia. ACS Sustain. Chem. Eng. 7, 17263–17272. https://doi.org/10.1021/acssuschemeng.9b04038

Hasson, D., Sidorenko, G., Semiat, R., 2010. Calcium carbonate hardness removal by a novel electrochemical seeds system. Desalination 263(1-3), 285-289 https://doi.org/10.1016/j.desal.2010.06.036

He, S., Tominski, C., Kappler, A., Behrens, S., Roden, E.E., 2016. Metagenomic analyses of the autotrophic Fe(II)-oxidizing, nitrate-reducing enrichment culture KS. Appl. Environ. Microbiol. 82, 2656–2668. https://doi.org/10.1128/AEM.03493-15

Hosono, T., Nakano, T., Shimizu, Y., Onodera, S. ichi, Taniguchi, M., 2011. Hydrogeological constraint on nitrate and arsenic contamination in Asian metropolitan groundwater. Hydrol. Process. https://doi.org/10.1002/hyp.8015

Hu, L., Wang, X., Chen, C., Chen, Jianmeng, Wang, Z., Chen, Jun, Hrynshpan, D., Savitskaya, T., 2022. NosZ gene cloning, reduction performance and structure of Pseudomonas citronellolis WXP-4 nitrous oxide reductase. RSC Adv. 12, 2549. https://doi.org/10.1039/d1ra09008a

Igiri, B.E., Okoduwa, S.I.R., Idoko, G.O., Akabuogu, E.P., Adeyi, A.O., Ejiogu, I.K., 2018. Toxicity and Bioremediation of Heavy Metals Contaminated Ecosystem from Tannery Wastewater: A Review. J. Toxicol. 2018, D 2568038. https://doi.org/10.1155/2018/2568038

Isabel San-Martín, M., Mateos, R., Carracedo, B., Escapa, A., Morán, A., 2018. Pilot-scale bioelectrochemical system for simultaneous nitrogen and carbon removal in urban wastewater treatment plants. J. Biosci. Bioeng. 126, 758–763. https://doi.org/10.1016/J.JBIOSC.2018.06.008

Jadhav, D.A., Chendake, A.D., Vinayak, V., Atabani, A., Ali Abdelkareem, M., Chae, K.J., 2022a. Scale-up of the bioelectrochemical system: Strategic perspectives and normalization of performance indices. Bioresour. Technol. 363, 127935. https://doi.org/10.1016/j.biortech.2022.127935

Jadhav, D.A., Das, I., Ghangrekar, M.M., Pant, D., 2020. Moving towards practical applications of microbial fuel cells for sanitation and resource recovery. J. Water Process Eng. 38, 101566. https://doi.org/10.1016/j.jwpe.2020.101566

Jadhav, D.A., Park, S.G., Pandit, S., Yang, E., Ali Abdelkareem, M., Jang, J.K., Chae, K.J., 2022b. Scalability of microbial electrochemical technologies: Applications and challenges. Bioresour. Technol. 345, 126498. https://doi.org/10.1016/j.biortech.2021.126498

Jang, Y.-C., Somanna, Y., Kim, H., 2016. Source, Distribution, Toxicity and Remediation of Arsenic in the Environment – A review. Int. J. Appl. Environ. Sci. ISSN.

Jensen, V.B., Darby, J.L., Seidel, C., Gorman, C., 2012. Drinking Water Treatment for Nitrate. Technical Report 6, California State Water Resources Control Board.

Ji, Y., Wang, L., Jiang, M., Lu, J., Ferronato, C., Chovelon, J.M., 2017. The role of nitrite in sulfate radical-based degradation of phenolic compounds: An unexpected nitration process relevant to groundwater remediation by in-situ chemical oxidation (ISCO). Water Res. https://doi.org/10.1016/j.watres.2017.06.081

Jia, Y.H., Tran, H.T., Kim, D.H., Oh, S.J., Park, D.H., Zhang, R.H., Ahn, D.H., 2008. Simultaneous organics removal and bio-electrochemical denitrification in microbial fuel cells. Bioprocess Biosyst. Eng. 31, 315–321. https://doi.org/10.1007/S00449-007-0164-6/FIGURES/8

Jin, H., Yu, Y., Zhang, L., Yan, R., Chen, X., 2019. Polarity reversal electrochemical process for water softening. Separation and Purification Technology 210, 943-949 https://doi.org/10.1016/j.seppur.2018.09.009

Jourdin, L., Sousa, J., Stralen, N. van, Strik, D.P.B.T.B., 2020. Techno-economic assessment of microbial electrosynthesis from CO2 and/or organics: An interdisciplinary roadmap towards future research and application. Appl. Energy 279, 115775. https://doi.org/10.1016/J.APENERGY.2020.115775

Kadier, A., Chaurasia, A.K., Sapuan, S.M., Ilyas, R.A., Ma, P.C., Alabbosh, K.F.S., Rai, P.K., Logroño, W., Hamid, A.A., Hasan, H.A., 2020. Essential Factors for Performance Improvement and the Implementation of Microbial Electrolysis Cells (MECs), in: Bioelectrochemical Systems. Springer Singapore, pp. 139–168. https://doi.org/10.1007/978-981-15-6872-5_7

Kadier, A., Chaurasia, A.K., Sapuan, S.M., Ilyas, R.A., Ma, P.C., Alabbosh, K.F.S., Rai, P.K., Logroño, W., Hamid, A.A., Hasan, H.A., 2020. Essential Factors for Performance Improvement and the Implementation of Microbial Electrolysis Cells (MECs), in: Bioelectrochemical Systems. Springer Singapore, pp. 139–168. https://doi.org/10.1007/978-981-15-6872-5_7

Kaur, A., Kim, J.R., Michie, I., Dinsdale, R.M., Guwy, A.J., Premier, G.C., 2013. Microbial fuel cell type biosensor for specific volatile fatty acids using acclimated bacterial communities. Biosens. Bioelectron. 47, 50–55. https://doi.org/10.1016/j.bios.2013.02.033

Kim, D.U., Lee, H., Kim, H., Kim, S.G., Ka, J.O., 2016. Dongia soli sp. nov., isolated from soil from Dokdo, Korea. Antonie van Leeuwenhoek, Int. J. Gen. Mol. Microbiol. 109, 1397–1402. https://doi.org/10.1007/S10482-016-0738-X/FIGURES/3

Knowles, R., 1982. Denitrification. Microbiol. Rev. 46, 43–70. https://doi.org/10.1128/mr.46.1.43-70.1982

Kokabian, B., Gude, V.G., 2015. Role of membranes in bioelectrochemical systems. Membrane Water Treatment 6(1), 53-75 https://doi.org/10.12989/mwt.2015.6.1.053

Kondaveeti, S., Moon, J.M., Min, B., 2017. Optimum spacing between electrodes in an air-cathode single chamber microbial fuel cell with a low-cost polypropylene separator. Bioprocess Biosyst. Eng. 40, 1851–1858. https://doi.org/10.1007/s00449-017-1838-3

Korth, B., Harnisch, F., 2019. Spotlight on the energy harvest of electroactive microorganisms: The impact of the applied anode potential. Front. Microbiol. 10, 1352. https://doi.org/10.3389/fmicb.2019.01352

Korth, B., Pous, N., Hönig, R., Haus, P., Corrêa, F.B., Nunes da Rocha, U., Puig, S., Harnisch, F., 2022. Electrochemical and Microbial Dissection of Electrified Biotrickling Filters. Front. Microbiol. 13, 869474. https://doi.org/10.3389/FMICB.2022.869474/BIBTEX

Kozich, J.J., Westcott, S.L., Baxter, N.T., Highlander, S.K., Schloss, P.D., 2013. Development of a dual-index sequencing strategy and curation pipeline for analyzing amplicon sequence data on the miseq illumina sequencing platform. Appl. Environ. Microbiol. 79, 5112–5120. https://doi.org/10.1128/AEM.01043-13

Kracke, F., Vassilev, I., Krömer, J.O., 2015. Microbial electron transport and energy conservation - The foundation for optimizing bioelectrochemical systems. Front. Microbiol. 6, 575. https://doi.org/10.3389/fmicb.2015.00575

Labbé, N., Parent, S., Villemur, R., 2003. Addition of trace metals increases denitrification rate in closed marine systems. Water Res. 37, 914–920. https://doi.org/10.1016/S0043-1354(02)00383-4

Lai, A., Aulenta, F., Mingazzini, M., Palumbo, M.T., Papini, M.P., Verdini, R., Majone, M., 2017. Bioelectrochemical approach for reductive and oxidative dechlorination of chlorinated aliphatic hydrocarbons (CAHs). Chemosphere. https://doi.org/10.1016/j.chemosphere.2016.11.072

Lai, A., Verdini, R., Aulenta, F., Majone, M., 2015. Influence of nitrate and sulfate reduction in the bioelectrochemically assisted dechlorination of cis-DCE. Chemosphere 125, 145–154. https://doi.org/10.1016/j.chemosphere.2014.12.023

Li, P., Karunanidhi, D., Subramani, T., Srinivasamoorthy, K., 2021. Sources and Consequences of Groundwater Contamination. Arch. Environ. Contam. Toxicol. https://doi.org/10.1007/s00244-020-00805-z

Li, Yunlong, Zhang, B., Cheng, M., Li, Yalong, Hao, L., Guo, H., 2016. Spontaneous arsenic (III) oxidation with bioelectricity generation in single-chamber microbial fuel cells. J. Hazard. Mater. https://doi.org/10.1016/j.jhazmat.2015.12.003

Lin, W., Wang, Z., Wang, W., Chen, Q., Xu, J., Yu, J., 2021. Comparative analysis the performance of electrochemical water softening between high frequency electric fields and direct current electric fields based on orthogonal experimental methods. Water Science and Technology 83, 1677–1690. https://doi.org/10.2166/WST.2021.084

Liu, H., Logan, B.E., 2004. Electricity generation using an air-cathode single chamber microbial fuel cell in the presence and absence of a proton exchange membrane. Environ. Sci. Technol. 38, 4040–4046. https://doi.org/10.1021/es0499344

Liu, J., Wang, Z., Belchik, S.M., Edwards, M.J., Liu, C., Kennedy, D.W., Merkley, E.D., Lipton, M.S., Butt, J.N., Richardson, D.J., Zachara, J.M., Fredrickson, J.K., Rosso, K.M., Shi, L., 2012. Identification and

characterization of M to A: A decaheme c-type cytochrome of the neutrophilic Fe(II)-oxidizing bacterium Sideroxydans lithotrophicus ES-1. Front. Microbiol. 3, 37. https://doi.org/10.3389/fmicb.2012.00037

Liu, R., Wang, Y., Wu, G., Luo, J., Wang, S., 2017. Development of a selective electrodialysis for nutrient recovery and desalination during secondary effluent treatment. Chem. Eng. J. 322, 224–233. https://doi.org/10.1016/J.CEJ.2017.03.149

Liu, X., Huang, M., Bao, S., Tang, W., Fang, T., 2020. Nitrate removal from low carbon-to-nitrogen ratio wastewater by combining iron-based chemical reduction and autotrophic denitrification. Bioresour. Technol. 301, 122731. https://doi.org/10.1016/j.biortech.2019.122731

Long, Y., Li, H., Jin, H., Ni, J., 2021. Interpretation of high perchlorate generated during electrochemical disinfection in presence of chloride at BDD anodes. Chemosphere 284, 131418. https://doi.org/10.1016/J.CHEMOSPHERE.2021.131418

Logan, B.E., Hamelers, B., Rozendal, R., Schroder, U., Keller, J., Freguia, S., Aelterman, P., Verstraete, W., Rabaey, K., 2006. Microbial Fuel Cells : Methodology and Technology. Environ. Sci. Technol. 40, 5181–5192. https://doi.org/10.1021/es0605016

Logan, B.E., Rossi, R., Ragab, A., Saikaly, P.E., 2019. Electroactive microorganisms in bioelectrochemical systems. Nat. Rev. Microbiol. https://doi.org/10.1038/s41579-019-0173-x

Lovley, D.R., 2008. The microbe electric: conversion of organic matter to electricity. Curr. Opin. Biotechnol. 19, 564–571. https://doi.org/10.1016/j.copbio.2008.10.005

Luan, J., Wang, L., Sun, W., Li, X., Zhu, T., Zhou, Y., Deng, H., Chen, S., He, S., Liu, G., 2019. Multi-meshes coupled cathodes enhanced performance of electrochemical water softening system. Separation and Purification Technology 217(15), 128-136 https://doi.org/10.1016/j.seppur.2019.01.054

Lust, R., Nerut, J., Kasak, K., Mander, Ü., 2020. Enhancing nitrate removal from waters with low organic carbon concentration using a bioelectrochemical system-a pilot-scale study. Water 12, 516. https://doi.org/10.3390/w12020516

Lycus, P., Bøthun, K.L., Bergaust, L., Shapleigh, J.P., Bakken, L.R., Frostegård, Å., 2017. Phenotypic and genotypic richness of denitrifiers revealed by a novel isolation strategy. ISME J. 11, 2219–2232. https://doi.org/10.1038/ismej.2017.82

Majone, M., Verdini, R., Aulenta, F., Rossetti, S., Tandoi, V., Kalogerakis, N., Agathos, S., Puig, S., Zanaroli, G., Fava, F., 2015. In situ groundwater and sediment bioremediation: Barriers and perspectives at European contaminated sites. New Biotechnology 32(1), 133-146 https://doi.org/10.1016/j.nbt.2014.02.011

Mazhar, M.A., Khan, N.A., Ahmed, S., Khan, A.H., Hussain, A., Rahisuddin, Changani, F., Yousefi, M., Ahmadi, S., Vambol, V., 2020. Chlorination disinfection by-products in municipal drinking water – A review. J. Clean. Prod. 273, 123159. https://doi.org/10.1016/J.JCLEPRO.2020.123159

McMurdie, P.J., Holmes, S., 2013. Phyloseq: An R Package for Reproducible Interactive Analysis and Graphics of Microbiome Census Data. PLoS One 8, e61217. https://doi.org/10.1371/journal.pone.0061217

Mohsenipour, M., Shahid, S., Ebrahimi, K., 2014. Removal techniques of nitrate from water. Asian J. Chem. 26, 7881–7886. https://doi.org/10.14233/ajchem.2014.17136

Molognoni, D., Devecseri, M., Cecconet, D., Capodaglio, A.G., 2017. Cathodic groundwater denitrification with a bioelectrochemical system. J. Water Process Eng. 19, 67–73. https://doi.org/10.1016/j.jwpe.2017.07.013

Morgado, L., Paixão, V.B., Schiffer, M., Pokkuluri, P.R., Bruix, M., Salgueiro, C.A., 2012. Revealing the structural origin of the redox-Bohr effect: The first solution structure of a cytochrome from Geobacter sulfurreducens. Biochem. J. 441, 179–187. https://doi.org/10.1042/BJ20111103

Nguyen, V.K., Park, Y., Yang, H., Yu, J., Lee, T., 2016a. Effect of the cathode potential and sulfate ions on nitrate reduction in a microbial electrochemical denitrification system. J. Ind. Microbiol. Biotechnol. 43, 783–793. https://doi.org/10.1007/S10295-016-1762-6

Nguyen, V.K., Park, Y., Yu, J., Lee, T., 2016b. Simultaneous arsenite oxidation and nitrate reduction at the electrodes of bioelectrochemical systems. Environ. Sci. Pollut. Res. 23, 19978–19988. https://doi.org/10.1007/s11356-016-7225-9

Nguyen, V.K., Park, Y., Yu, J., Lee, T., 2016c. Bioelectrochemical denitrification on biocathode buried in simulated aquifer saturated with nitrate-contaminated groundwater. Environ. Sci. Pollut. Res. 23, 15443–15451. https://doi.org/10.1007/S11356-016-6709-Y/FIGURES/5

Nguyen, V.K., Tran, H.T., Park, Y., Yu, J., Lee, T., 2017. Microbial arsenite oxidation with oxygen, nitrate, or an electrode as the sole electron acceptor. J. Ind. Microbiol. Biotechnol. 44, 857–868. https://doi.org/10.1007/s10295-017-1910-7

Oren, Y., Katz, V., Daltrophe, N.C., 2001. Improved compact accelerated precipitation softening (CAPS). Desalination 139(1-3), 155-159 https://doi.org/10.1016/S0011-9164(01)00305-8

Palma, E., Daghio, M., Franzetti, A., Petrangeli Papini, M., Aulenta, F., 2018. The bioelectric well: a novel approach for in situ treatment of hydrocarbon-contaminated groundwater. Microbial Biotechnology 11, 112–118 https://doi.org/10.1111/1751-7915.12760

Papillon, J., Ondel, O., Maire, É., 2021. Scale up of single-chamber microbial fuel cells with stainless steel 3D anode: Effect of electrode surface areas and electrode spacing. Bioresour. Technol. Reports 13, 100632. https://doi.org/10.1016/J.BITEB.2021.100632

Paquete, C.M., Rusconi, G., Silva, A. V., Soares, R., Louro, R.O., 2019. A brief survey of the "cytochromome." Adv. Microb. Physiol. 75, 69–135. https://doi.org/10.1016/BS.AMPBS.2019.07.005

Pasinszki, T., Krebsz, M., 2020. Synthesis and Application of Zero-Valent Iron Nanoparticles in Water Treatment, Environmental Remediation, Catalysis, and Their Biological Effects. Nanomaterials 10, 917. https://doi.org/10.3390/nano10050917

Peter-Varbanets, M., Zurbrügg, C., Swartz, C., Pronk, W., 2009. Decentralised systems for potable water and the potential of membrane technology. Water Res. 43, 245–265. https://doi.org/10.1016/j.watres.2008.10.030

Peter-Varbanets, M., Zurbrügg, C., Swartz, C., Pronk, W., 2009. Decentralized systems for potable water and the potential of membrane technology. Water Res. 43, 245–265. https://doi.org/10.1016/j.watres.2008.10.030

Picetti, R., Deeney, M., Pastorino, S., Miller, M.R., Shah, A., Leon, D.A., Dangour, A.D., Green, R., 2022. Nitrate and nitrite contamination in drinking water and cancer risk: A systematic review with meta-analysis. Environ. Res. 210, 112988. https://doi.org/10.1016/J.ENVRES.2022.112988

Piqué, À., Grandia, F., Canals, À., 2010. Processes releasing arsenic to groundwater in the Caldes de Malavella geothermal area, NE Spain. Water Res. https://doi.org/10.1016/j.watres.2010.07.012

Pous, N., Balaguer, M.D., Colprim, J., Puig, S., 2018. Opportunities for groundwater microbial electro-remediation. Microb. Biotechnol. 11, 119–135. https://doi.org/10.1111/1751-7915.12866

Pous, N., Carmona-Martínez, A.A., Vilajeliu-Pons, A., Fiset, E., Bañeras, L., Trably, E., Balaguer, M.D., Colprim, J., Bernet, N., Puig, S., 2016. Bidirectional microbial electron transfer: Switching an acetate oxidizing biofilm to nitrate reducing conditions. Biosens. Bioelectron. 75, 352–358. https://doi.org/10.1016/j.bios.2015.08.035

Pous, N., Casentini, B., Rossetti, S., Fazi, S., Puig, S., Aulenta, F., 2015a. Anaerobic arsenite oxidation with an electrode serving as the sole electron acceptor: A novel approach to the bioremediation of arsenic-polluted groundwater. J. Hazard. Mater. 283, 617–622. https://doi.org/10.1016/j.jhazmat.2014.10.014

Pous, N., Koch, C., Colprim, J., Puig, S., Harnisch, F., 2014. Extracellular electron transfer of biocathodes: Revealing the potentials for nitrate and nitrite reduction of denitrifying microbiomes dominated by Thiobacillus sp. Electrochem. commun. 49, 93–97. https://doi.org/10.1016/j.elecom.2014.10.011

Pous, N., Puig, S., Balaguer, M.D., Colprim, J., 2017. Effect of hydraulic retention time and substrate availability in denitrifying bioelectrochemical systems. Environ. Sci. Water Res. Technol. 3, 922–929. https://doi.org/10.1039/c7ew00145b

Pous, N., Puig, S., Coma, M., Balaguer, M.D., Colprim, J., 2013. Bioremediation of nitrate-polluted groundwater in a microbial fuel cell. J. Chem. Technol. Biotechnol. 88, 1690–1696. https://doi.org/10.1002/jctb.4020

Pous, N., Puig, S., Coma, M., Balaguer, M.D., Colprim, J., 2013. Bioremediation of nitrate-polluted groundwater in a microbial fuel cell. J. Chem. Technol. Biotechnol. https://doi.org/10.1002/jctb.4020

Pous, N., Puig, S., Dolors Balaguer, M., Colprim, J., 2015b. Cathode potential and anode electron donor evaluation for a suitable treatment of nitrate-contaminated groundwater in bioelectrochemical systems. Chem. Eng. J. 263, 151–159. https://doi.org/10.1016/j.cej.2014.11.002

Pradhan, B., Chand, Sujata, Chand, Sasmita, Rout, P.R., Naik, S.K., 2023. Emerging groundwater contaminants: A comprehensive review on their health hazards and remediation technologies. Groundw. Sustain. Dev. 20, 100868. https://doi.org/10.1016/j.gsd.2022.100868

Prado de Nicolás, A., Berenguer, R., Esteve-Núñez, A., 2022. Evaluating bioelectrochemically-assisted constructed wetland (METland®) for treating wastewater: Analysis of materials, performance and electroactive communities. Chem. Eng. J. 440, 135748. https://doi.org/10.1016/j.cej.2022.135748

Puggioni, G., Milia, S., Dessì, E., Unali, V., Pous, N., Balaguer, M.D., Puig, S., Carucci, A., 2021. Combining electro-bioremediation of nitrate in saline groundwater with concomitant chlorine production. Water Res. 206, 117736. https://doi.org/10.1016/j.watres.2021.117736

Puggioni, G., Milia, S., Unali, V., Ardu, R., Tamburini, E., Balaguer, M.D., Pous, N., Carucci, A., Puig, S., 2022. Effect of hydraulic retention time on the electro-bioremediation of nitrate in saline groundwater. Sci. Total Environ. 845, 157236. https://doi.org/10.1016/j.scitotenv.2022.157236

Puig, S., Coma, M., Desloover, J., Boon, N., Colprim, J., Balaguer, M.D., 2012. Autotrophic denitrification in microbial fuel cells treating low ionic strength waters. Environ. Sci. Technol. 46, 2309–2315. https://doi.org/10.1021/es2030609

Quejigo, J.R., Korth, B., Kuchenbuch, A., Harnisch, F., 2021. Redox Potential Heterogeneity in Fixed-Bed Electrodes Leads to Microbial Stratification and Inhomogeneous Performance. ChemSusChem 14, 1155–1165. https://doi.org/10.1002/cssc.202002611

Quejigo, J.R., Rosa, L.F.M., Harnisch, F., 2018. Electrochemical characterization of bed electrodes using voltammetry of single granules. Electrochem. commun. 90, 78–82. https://doi.org/10.1016/j.elecom.2018.04.009

Rabaey, K., Angenent, L., Schröder, U., Keller, J., 2009. Bioelectrochemical Systems: From Extracellular Electron Transfer to Biotechnological Application, Water Intelligence Online. IWA Publishing, London. https://doi.org/10.2166/9781780401621

Rabaey, K., Vandekerckhove, T., de Walle, A. V, Sedlak, D.L., 2020. The third route: Using extreme decentralization to create resilient urban water systems. Water Res. 185, 116276. https://doi.org/10.1016/j.watres.2020.116276

Rezvani, F., Sarrafzadeh, M.H., Ebrahimi, S., Oh, H.M., 2019. Nitrate removal from drinking water with a focus on biological methods: a review. Environ. Sci. Pollut. Res. 26, 1124–1141. https://doi.org/10.1007/s11356-017-9185-0

Rivett, M.O., Buss, S.R., Morgan, P., Smith, J.W.N., Bemment, C.D., 2008. Nitrate attenuation in groundwater: A review of biogeochemical controlling processes. Water Res. 42, 4215–4232. https://doi.org/10.1016/j.watres.2008.07.020

Rogińska, J., Philippon, T., Hoareau, M., Jorand, F.P.A., Barrière, F., Etienne, M., 2023. Challenges and applications of nitrate-reducing microbial biocathodes. Bioelectrochemistry 152, 108436. https://doi.org/10.1016/J.BIOELECHEM.2023.108436

Rosenbaum, M., Aulenta, F., Villano, M., Angenent, L.T., 2011. Cathodes as electron donors for microbial metabolism: Which extracellular electron transfer mechanisms are involved? Bioresour. Technol. 102, 324–333. https://doi.org/10.1016/j.biortech.2010.07.008

Rossi, R., Logan, B.E., 2022. Impact of reactor configuration on pilot-scale microbial fuel cell performance. Water Res. 225, 119179. https://doi.org/10.1016/J.WATRES.2022.119179

Rovira-Alsina, L., Balaguer, M.D., Puig, S., 2021. Thermophilic bio-electro carbon dioxide recycling harnessing renewable energy surplus. Bioresour. Technol. 321, 124423. https://doi.org/10.1016/J.BIORTECH.2020.124423

Sanjuán, I., Benavente, D., Expósito, E., Montiel, V., 2019. Electrochemical water softening: Influence of water composition on the precipitation behaviour. Separation and Purification Technology 211, 857-865 https://doi.org/10.1016/j.seppur.2018.10.044

Santini, M., Marzorati, S., Fest-Santini, S., Trasatti, S., Cristiani, P., 2017. Carbonate scale deactivating the biocathode in a microbial fuel cell. J. Power Sources 356, 400–407. https://doi.org/10.1016/j.jpowsour.2017.02.088

Schaefer, C.E., Andaya, C., Urtiaga, A., 2015. Assessment of disinfection and by-product formation during electrochemical treatment of surface water using a Ti/IrO2 anode. Chem. Eng. J. 264, 411–416. https://doi.org/10.1016/j.cej.2014.11.082

Schröder, U., Harnisch, F., Angenent, L.T., 2015. Microbial electrochemistry and technology: Terminology and classification. Energy Environ. Sci. 8, 513–519. https://doi.org/10.1039/c4ee03359k

Sevda, S., Sreekishnan, T.R., Pous, N., Puig, S., Pant, D., 2018. Bioelectroremediation of perchlorate and nitrate contaminated water: A review. Bioresour. Technol. 255, 331–339. https://doi.org/10.1016/j.biortech.2018.02.005

Shelobolina, E., Xu, H., Konishi, H., Kukkadapu, R., Wu, T., Blöthe, M., Roden, E., 2012. Microbial lithotrophic oxidation of structural Fe(II) in biotite. Appl. Environ. Microbiol. 78. https://doi.org/10.1128/AEM.01034-12

Shukla, S., Saxena, A., 2020. Sources and leaching of nitrate contamination in groundwater. Curr. Sci. 118, 883–891. https://doi.org/10.18520/cs/v118/i6/883-891

Skiba, U., 2008. Denitrification, in: Jørgensen, S.E., Fath, B.D. (Eds.), Encyclopedia of Ecology. Academic Press, Oxford, pp. 866–871. https://doi.org/10.1016/B978-008045405-4.00264-0

Solera, J.S., Castaño, M.J., 2008. Brucellosis, in: International Encyclopedia of Public Health. Academic Press, pp. 357–369. https://doi.org/10.1016/B978-012373960-5.00560-8

Stevens, R.J., Laughlin, R.J., Malone, J.P., 1998. Soil pH affects the processes reducing nitrate to nitrous oxide and di-nitrogen. Soil Biol. Biochem. 30, 1119–1126. https://doi.org/10.1016/S0038-0717(97)00227-7

Su, J., Liang, D., Lian, T., 2018. Comparison of denitrification performance by bacterium Achromobacter sp. A14 under different electron donor conditions. Chem. Eng. J. 333, 320–326. https://doi.org/10.1016/j.cej.2017.09.129

Sun, W., Sierra, R., Field, J.A., 2008. Anoxic oxidation of arsenite linked to denitrification in sludges and sediments. Water Res. https://doi.org/10.1016/j.watres.2008.08.004

Sun, W., Sierra-Alvarez, R., Hsu, I., Rowlette, P., Field, J.A., 2009. Anoxic oxidation of arsenite linked to chemolithotrophic denitrification in continuous bioreactors. Biotechnol. Bioeng. https://doi.org/10.1002/bit.22611

Suthar, S., Bishnoi, P., Singh, S., Mutiyar, P.K., Nema, A.K., Patil, N.S., 2009. Nitrate contamination in groundwater of some rural areas of Rajasthan, India. J. Hazard. Mater. 171, 189–199. https://doi.org/10.1016/J.JHAZMAT.2009.05.111

Tissen, C., Benz, S.A., Menberg, K., Bayer, P., Blum, P., 2019. Groundwater temperature anomalies in central Europe. Environ. Res. Lett. 14, 104012. https://doi.org/10.1088/1748-9326/ab4240

Tong, Y., He, Z., 2013. Nitrate removal from groundwater driven by electricity generation and heterotrophic denitrification in a bioelectrochemical system. J. Hazard. Mater. 262, 614–619. https://doi.org/10.1016/J.JHAZMAT.2013.09.008

Tournassat, C., Charlet, L., Bosbach, D., Manceau, A., 2002. Arsenic(III) oxidation by birnessite and precipitation of manganese(II) arsenate. Environ. Sci. Technol. https://doi.org/10.1021/es0109500

Tucci, M., Carolina, C.V., Resitano, M., Matturro, B., Crognale, S., Pietrini, I., Rossetti, S., Harnisch, F., Aulenta, F., 2021. Simultaneous removal of hydrocarbons and sulfate from groundwater using a "bioelectric well." Electrochimica Acta 388, 138636. https://doi.org/10.1016/J.ELECTACTA.2021.138636

Tugaoen, H.O.N., Garcia-Segura, S., Hristovski, K., Westerhoff, P., 2017. Challenges in photocatalytic reduction of nitrate as a water treatment technology. Sci. Total Environ. 599–600, 1524–15551. https://doi.org/10.1016/j.scitotenv.2017.04.238

Twomey, K.M., Stillwell, A.S., Webber, M.E., 2010. The unintended energy impacts of increased nitrate contamination from biofuels production. J. Environ. Monit. 12, 218–224. https://doi.org/10.1039/b913137j

UN Water, 2021. Summary Progress Update 2021: SDG 6-water and sanitation for all. Geneve, Switzeland.

UNICEF, 2021. Water security for all, Nueva York: UNICEF.

UNICEF, n.d. Water scarcity [WWW Document]. URL https://www.unicef.org/wash/water-scarcity (accessed 5.16.23).

Van der Bruggen, B., Goossens, H., Everard, P.A., Stemgée, K., Rogge, W., 2009. Cost-benefit analysis of central softening for production of drinking water. Journal of Environmental Management 91, 541–549. https://doi.org/10.1016/j.jenvman.2009.09.024

Van Doan, T., Lee, T.K., Shukla, S.K., Tiedje, J.M., Park, J., 2013. Increased nitrous oxide accumulation by bioelectrochemical denitrification under autotrophic conditions: Kinetics and expression ofdenitrification pathway genes. Water Res. 47, 7087–7097. https://doi.org/10.1016/j.watres.2013.08.041

Van Halem, D., Bakker, S.A., Amy, G.L., Van Dijk, J.C., 2009. Arsenic in drinking water: A worldwide water quality concern for water supply companies. Drink. Water Eng. Sci. 2, 29–34. https://doi.org/10.5194/dwes-2-29-2009

Vandekerckhove, T.G.L., De Mulder, C., Boon, N., Vlaeminck, S.E., 2018. Temperature impact on sludge yield, settleability and kinetics of three heterotrophic conversions corroborates the prospect of thermophilic biological nitrogen removal. Bioresour. Technol. 269, 104–112. https://doi.org/10.1016/j.biortech.2018.08.012

Ventura-Houle, R., Font, X., Heyer, L., 2018. Groundwater arsenic contamination and their variations on episode of drought: Ter River delta in Catalonia, Spain. Appl. Water Sci. https://doi.org/10.1007/s13201-018-0772-0

Vilajeliu-Pons, A., Bañeras, L., Puig, S., Molognoni, D., Vilà-Rovira, A., Amo, E.H. Del, Balaguer, M.D., Colprim, J., 2016. External resistances applied to MFC affect core microbiome and swine manure treatment efficiencies. PLoS One. https://doi.org/10.1371/journal.pone.0164044

Vilajeliu-Pons, A., Puig, S., Salcedo-Dávila, I., Balaguer, M.D., Colprim, J., 2017. Long-term assessment of six-stacked scaled-up MFCs treating swine manure with different electrode materials. Environ. Sci. Water Res. Technol. 3, 947–959. https://doi.org/10.1039/C7EW00079K

Vilardi, G., 2019. Mathematical modelling of simultaneous nitrate and dissolved oxygen reduction by Cu-nZVI using a bi-component shrinking core model. Powder Technology 343, 613–618 https://doi.org/10.1016/J.POWTEC.2018.11.082

Vilardi, G., De Caprariis, B., Stoller, M., Di Palma, L., Verdone, N., 2020. Intensified water denitrification by means of a spinning disk reactor and stirred tank in series: Kinetic modelling and computational fluid dynamics. Journal of Water Process Engineering 34, 101147 https://doi.org/10.1016/J.JWPE.2020.101147

Vilà-Rovira, A., Puig, S., Balaguer, M.D., Colprim, J., 2015. Anode hydrodynamics in bioelectrochemical systems. RSC Adv. 5, 78994–79000. https://doi.org/10.1039/c5ra11995b

Vilar-Sanz, A., Pous, N., Puig, S., Balaguer, M.D., Colprim, J., Bañeras, L., 2018. Denitrifying nirK-containing alphaproteobacteria exhibit different electrode driven nitrite reduction capacities. Bioelectrochemistry 121, 74–83. https://doi.org/10.1016/j.bioelechem.2018.01.007

Vilar-Sanz, A., Puig, S., García-Lledó, A., Trias, R., Balaguer, M.D., Colprim, J., Bañeras, L., 2013. Denitrifying bacterial communities affect current production and nitrous oxide accumulation in a microbial fuel cell. PLoS One 8, e63460. https://doi.org/10.1371/journal.pone.0063460

Villano, M., Aulenta, F., Ciucci, C., Ferri, T., Giuliano, A., Majone, M., 2010. Bioelectrochemical reduction of CO2 to CH4 via direct and indirect extracellular electron transfer by a hydrogenophilic methanogenic culture. Bioresour. Technol. 101, 3085–3090. https://doi.org/10.1016/j.biortech.2009.12.077

Virdis, B., Rabaey, K., Yuan, Z., Keller, J., 2008. Microbial fuel cells for simultaneous carbon and nitrogen removal. Water Res. 42, 3013–3024. https://doi.org/10.1016/j.watres.2008.03.017

Wang, H., Zhang, S., Wang, J., Song, Q., Zhang, W., He, Q., Song, J., Ma, F., 2018. Comparison of performance and microbial communities in a bioelectrochemical system for simultaneous denitrification and chromium removal: Effects of pH. Process Biochem. https://doi.org/10.1016/j.procbio.2018.08.007

Wang, J., Song, X., Wang, Y., Abayneh, B., Li, Y., Yan, D., Bai, J., 2016. Nitrate removal and bioenergy production in constructed wetland coupled with microbial fuel cell: Establishment of electrochemically active bacteria community on anode. Bioresour. Technol. 221, 358–356. https://doi.org/10.1016/j.biortech.2016.09.054

Wang, J., Wan, J., Wu, Z., Li, Hongli, Li, Haisong, Dagot, C., Wang, Y., 2017. Flexible biological arsenite oxidation utilizing NOx and O2 as alternative electron acceptors. Chemosphere. https://doi.org/10.1016/j.chemosphere.2017.03.044

Wang, K., Zhang, S., 2019. Extracellular electron transfer modes and rate-limiting steps in denitrifying biocathodes. Environ. Sci. Pollut. Res. 26, 16378–16387. https://doi.org/10.1007/s11356-019-05117-x

Wang, J., Chu, L., 2016. Biological nitrate removal from water and wastewater by solid-phase denitrification process. Biotechnol. Adv. 34, 1103–1112. https://doi.org/10.1016/J.BIOTECHADV.2016.07.001

Wang, S., Zhao, X., 2009. On the potential of biological treatment for arsenic contaminated soils and groundwater. J. Environ. Manage. https://doi.org/10.1016/j.jenvman.2009.02.001

Wang, W., Chen, Q., Lin, W., Zheng, X., Xu, J., Yu, J., 2021. Effect of operational parameters and material properties on hardness removal efficiency by electrochemical technique. Water Supply https://doi.org/10.2166/WS.2021.105

Wang, X., Aulenta, F., Puig, S., Esteve-Núñez, A., He, Y., Mu, Y., Rabaey, K., 2020. Microbial electrochemistry for bioremediation. Environ. Sci. Ecotechnology 1, 100013. https://doi.org/10.1016/j.ese.2020.100013

Wang, X., Prévoteau, A., Rabaey, K., 2021. Impact of Periodic Polarisation on Groundwater Denitrification in Bioelectrochemical Systems. Environ. Sci. Technol. 55, 15371–15379. https://doi.org/10.1021/acs.est.1c03586

Wang, X., Prévoteau, A., Rabaey, K., 2021. Impact of Periodic Polarization on Groundwater Denitrification in Bioelectrochemical Systems. Environ. Sci. Technol. 55, 15371–15379. https://doi.org/10.1021/acs.est.1c03586

Wang, Y.X., Hou, N., Liu, X.L., Mu, Y., 2022. Advances in interfacial engineering for enhanced microbial extracellular electron transfer. Bioresour. Technol. 345, 126562. https://doi.org/10.1016/J.BIORTECH.2021.126562

Ward, M.H., Jones, R.R., Brender, J.D., de Kok, T.M., Weyer, P.J., Nolan, B.T., Villanueva, C.M., van Breda, S.G., 2018. Drinking Water Nitrate and Human Health: An Updated Review. Int. J. Environ. Res. Public Heal. 2018, Vol. 15, Page 1557 15, 1557. https://doi.org/10.3390/IJERPH15071557

WHO, 2017. Guidelines for drinking-water quality: fourth edition incorporating the first addendum. World Health Organization https://doi.org/10.5942/jawwa.2017.109.0087

WHO, 2017. Guidelines for drinking-water quality: fourth edition incorporating the first addendum., World Health Organization. https://doi.org/10.5942/jawwa.2017.109.0087

WHO, UNICEF, 2021. Progress on household drinking water, sanitation and hygiene 2000-2020: Five years into the SDGs, Geneva: World Health Organization (WHO) and the United Nations Children's Fund (UNICEF).

Wrighton, K.C., Virdis, B., Clauwaert, P., Read, S.T., Daly, R.A., Boon, N., Piceno, Y., Andersen, G.L., Coates, J.D., Rabaey, K., 2010. Bacterial community structure corresponds to performance during cathodic nitrate reduction. ISME J. 4, 1443–1455. https://doi.org/10.1038/ismej.2010.66

Wu, L., Wei, W., Xu, J., Chen, X., Liu, Y., Peng, L., Wang, D., Ni, B.J., 2021. Denitrifying biofilm processes for wastewater treatment: Developments and perspectives. Environ. Sci. Water Res. Technol. 7, 40–67. https://doi.org/10.1039/d0ew00576b

Wu, Q., Liu, J., Li, Q., Mo, W., Wan, R., Peng, S., 2022. Effect of Electrode Distances on Remediation of Eutrophic Water and Sediment by Sediment Microbial Fuel Cell Coupled Floating Beds. Int. J. Environ. Res. Public Health 19, 10423. https://doi.org/10.3390/ijerph191610423

Xiao, Y., Zhang, E., Zhang, J., Dai, Y., Yang, Z., Christensen, H.E.M., Ulstrup, J., Zhao, F., 2017. Extracellular polymeric substances are transient media for microbial extracellular electron transfer. Sci. Adv. 3, e1700623. https://doi.org/10.1126/SCIADV.1700623/SUPPL_FILE/1700623_SM.PDF

Xin, J., Wang, Y., Shen, Z., Liu, Y., Wang, H., Zheng, X., 2021. Critical review of measures and decision support tools for groundwater nitrate management: A surface-to-groundwater profile perspective. J. Hydrol. 598, 126386. https://doi.org/10.1016/J.JHYDROL.2021.126386

Xu, J., Hao, Z., Xie, C., Lv, X., Yang, Y., Xu, X., 2012. Promotion effect of Fe2+ and Fe3O4 on nitrate reduction using zero-valent iron. Desalination 284, 9–13. https://doi.org/10.1016/J.DESAL.2011.08.029

Xu, X., He, Q., Ma, G., Wang, H., Nirmalakhandan, N., Xu, P., 2018. Selective separation of mono- and di-valent cations in electrodialysis during brackish water desalination: Bench and pilot-scale studies. Desalination 428, 146–160. https://doi.org/10.1016/J.DESAL.2017.11.015

Yang, N., Zhan, G., Wu, T., Zhang, Y., Jiang, Q., Li, D., Xiang, Y., 2018. Effect of air-exposed biocathode on the performance of a Thauera-dominated membraneless single-chamber microbial fuel cell (SCMFC). J. Environ. Sci. 66, 216–226. https://doi.org/10.1016/j.jes.2017.05.013

Yang, W., Wang, J., Chen, R., Xiao, L., Shen, S., Li, J., Dong, F., 2022. Reaction mechanism and selectivity regulation of photocatalytic nitrate reduction for wastewater purification: progress and challenges. J. Mater. Chem. A 10, 17357–17376. https://doi.org/10.1039/D2TA04611C

Yu, G., Wang, J., Liu, L., Li, Y., Zhang, Y., Wang, S., 2020. The analysis of groundwater nitrate pollution and health risk assessment in rural areas of Yantai, China. BMC Public Health 20, 1–6. https://doi.org/10.1186/S12889-020-08583-Y/TABLES/5

Yu, Y., Jin, H., Jin, X., Yan, R., Zhang, L., Chen, X., 2018a. Current pulsated electrochemical precipitation for water softening. Industrial & Engineering Chemistry Research 57(18), 6585-6593 https://doi.org/10.1021/acs.iecr.8b00448

Yu, Y., Jin, H., Quan, X., Hong, B., Chen, X., 2019. Continuous multistage electrochemical precipitation reactor for water softening. Industrial & Engineering Chemistry Research 58(1), 461-468 https://doi.org/10.1021/acs.iecr.8b04200

Zeppilli, M., Dell'Armi, E., Di Franca, M.L., Matturro, B., Feigl, V., Molnár, M., Berkl, Z., Németh, I., Rossetti, S., Papini, M.P., Majone, M., 2022. Evaluation of a Bioelectrochemical Reductive/Oxidative Sequential Process for Chlorinated Aliphatic Hydrocarbons (Cahs) Removal from a Real Contaminated Groundwater. SSRN Electron. J. 49, 103101. https://doi.org/10.2139/ssrn.3981653

Zhai, S., Zhao, Y., Ji, M., Qi, W., 2017. Simultaneous removal of nitrate and chromate in groundwater by a spiral fiber based biofilm reactor. Bioresour. Technol. 232, 278–284. https://doi.org/10.1016/J.BIORTECH.2017.01.076

Zhang, C., Tang, J., Zhao, G., Tang, Y., Li, J., Li, F., Zhuang, H., Chen, J., Lin, H., Zhang, Y., 2020. Investigation on an electrochemical pilot equipment for water softening with an automatic descaling system: Parameter optimization and energy consumption analysis. Journal of Cleaner Production 276, 123178 https://doi.org/10.1016/j.jclepro.2020.123178

Zhang, D., Liu, Y., Han, Y., Zhang, Y., Jia, X., Li, W., Li, D., Jing, L., 2021. Nitrate removal from low C/N wastewater at low temperature by immobilized Pseudomonas sp. Y39-6 with versatile nitrate metabolism pathways. Bioresour. Technol. 326, 124794. https://doi.org/10.1016/J.BIORTECH.2021.124794

Zhang, S., Mao, G., Crittenden, J., Liu, X., Du, H., 2017. Groundwater remediation from the past to the future: A bibliometric analysis. Water Res. https://doi.org/10.1016/j.watres.2017.01.029

Zhang, X., Li, X., Zhao, X., Li, Y., 2019. Factors affecting the efficiency of a bioelectrochemical system: a review. RSC Adv. 9, 19748–19761. https://doi.org/10.1039/C9RA03605A

Zhao, F., Xin, J., Yuan, M., Wang, L., Wang, X., 2022. A critical review of existing mechanisms and strategies to enhance N2 selectivity in groundwater nitrate reduction. Water Res. 209, 117889. https://doi.org/10.1016/j.watres.2021.117889

Zhao, J., Li, F., Cao, Y., Zhang, X., Chen, T., Song, H., Wang, Z., 2021. Microbial extracellular electron transfer and strategies for engineering electroactive microorganisms. Biotechnol. Adv. 53, 107682. https://doi.org/10.1016/j.biotechadv.2020.107682

Zhao, X., Zhang, G., Zhang, Z., 2020. TiO2-based catalysts for photocatalytic reduction of aqueous oxyanions: State-of-the-art and future prospects. Environ. Int. 136, 105453. https://doi.org/10.1016/J.ENVINT.2019.105453

Zhong, L., Yang, S.S., Ding, J., Wang, G.Y., Chen, C.X., Xie, G.J., Xu, W., Yuan, F., Ren, N.Q., 2021. Enhanced nitrogen removal in an electrochemically coupled biochar-amended constructed wetland microcosms: The interactive effects of biochar and electrochemistry. Sci. Total Environ. 789, 147761. https://doi.org/10.1016/J.SCITOTENV.2021.147761

Zhou, M., Wang, W., Chi, M., 2009. Enhancement on the simultaneous removal of nitrate and organic pollutants from groundwater by a three-dimensional bio-electrochemical reactor. Bioresour. Technol. 100, 4662–4668. https://doi.org/10.1016/J.BIORTECH.2009.05.002

Zhu, I., Getting, T., 2012. A review of nitrate reduction using inorganic materials. Environ. Technol. Rev. 1, 46–58. https://doi.org/10.1080/09593330.2012.706646

Zou, S., He, Z., 2018. Efficiently "pumping out" value-added resources from wastewater by bioelectrochemical systems: A review from energy perspectives. Water Res. 131, 62–73. https://doi.org/10.1016/j.watres.2017.12.026

Zumft, W.G., 1997. Cell biology and molecular basis of denitrification. Microbiol. Mol. Biol. Rev. 61, 533–616. https://doi.org/10.1128/MMBR.61.4.533-616.1997

Appendix

Supplementary data: Chapter 4.1

Electro-bioremediation of nitrate and arsenite polluted groundwater

Alba Ceballos-Escalera[1], Narcis Pous[1], Paola Chiluiza-Ramos[2], Benjamin Korth[3], Falk Harnisch[3], Lluís Bañeras[2], M. Dolors Balaguer[1], Sebastià Puig[1]*

[1]LEQUiA, Institute of the Environment, University of Girona, C/ *Maria Aurèlia Capmany, 69*, E-17003, Girona, Spain.

[2]Group of Environmental Microbial Ecology, Institute of Aquatic Ecology, University of Girona, C/ *Maria Aurèlia Capmany, 40,* E-17003, Girona, Spain.

[3]Department of Environmental Microbiology, Helmholtz Centre for Environmental Research GmbH - UFZ, *Permoserstraße 15*, 04318 Leipzig, Germany.

Supplementary data 1: Additional figures

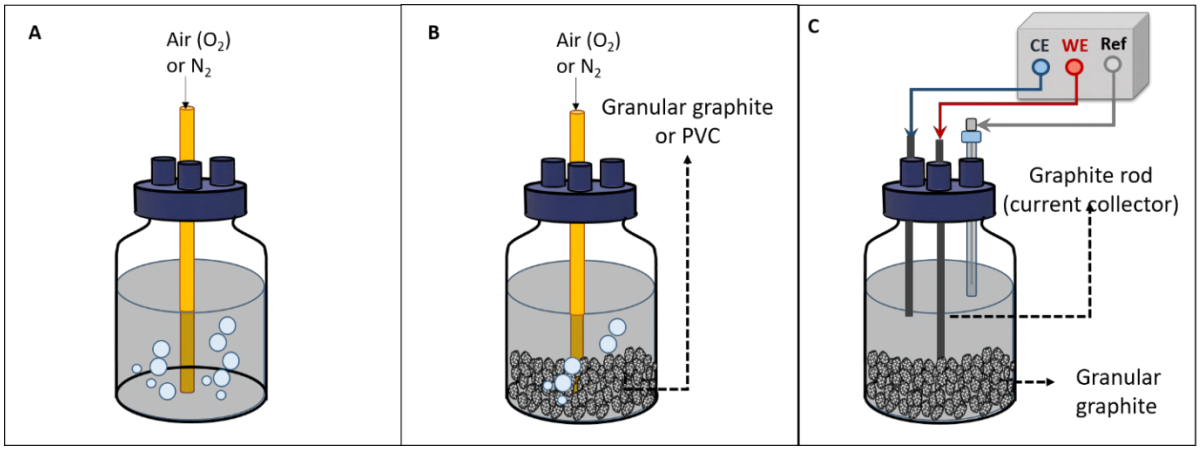

Figure S8: Scheme of abiotic arsenite oxidation test. A) Aerobic (flushed with air) and anoxic (flushed with dinitrogen gas) conditions without any granules; B) aerobic (flushed with air) and anoxic (flushed with dinitrogen gas) conditions with granular graphite or PVC granules; and C) three-electrode setup with the working electrode (WE, anode) with granular graphite poised at 1.15 V vs. SHE.

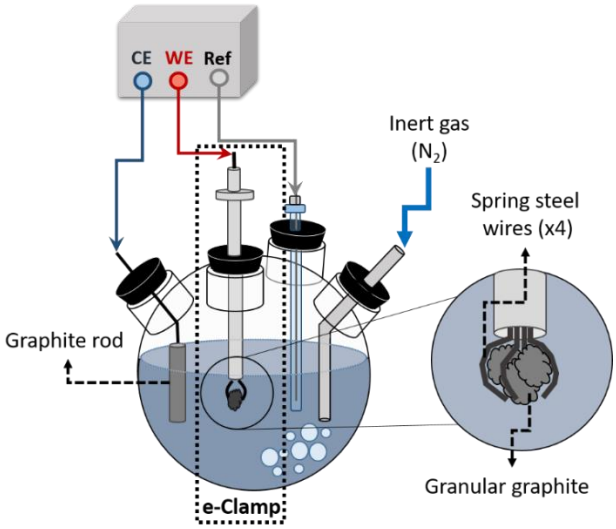

Figure S9: Scheme of the setup for electrochemical characterization of graphite granules with the e-clamp.

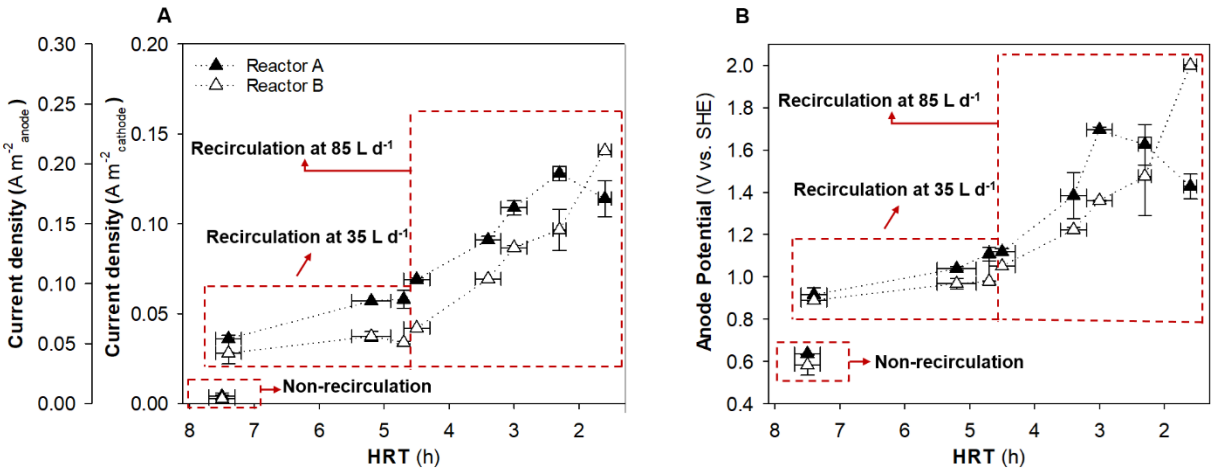

Figure S10: A) Current density of anode and cathode electrode considering the different reactor sizes and B) anode potentials at different hydraulic retention times (HRTs) and effluent recirculation flows. Results represent mean values and error bars represent standard deviation of analytical replicates during each operational condition (n≥3).

Supplementary data 2: Equations for the calculation of reaction rates and coulombic efficiencies.

$$rNO_3^- = \frac{C_{NO_3^-}{}_{influent} - C_{NO_3^-}{}_{effluent}}{HRT_{cat}} \quad \text{(S1)}$$

$$rNO_2^- = rNO_3^- + \frac{C_{NO_2^-}{}_{influent} - C_{NO_2^-}{}_{effluent}}{HRT_{cat}} \quad \text{(S2)}$$

$$rN_2O = rNO_2^- + \frac{C_{N_2O}{}_{influent} - C_{N_2O}{}_{effluent}}{HRT_{cat}} \quad \text{(S3)}$$

$$rAs(III) = \frac{C_{As(III)}{}_{influent} - C_{As(III)}{}_{effluent}}{HRT} \quad \text{(S4)}$$

where $Cx_{influent}$ and $Cx_{effluent}$ represent nitrate, nitrite, nitrous oxide, and arsenite mass concentration in the effluent and influent (either in g N m^{-3} or in g As m^{-3}).

$$q_{NO_3^-} = \frac{V_{NCC} \cdot F \cdot HRT_{cat} \cdot (n_{NO_3^-/NO_2^-} \cdot rNO_3^- + n_{NO_2^-/N_2O} \cdot rNO_2^- + n_{N_2O/N_2} \cdot rN_2O)}{m_N} \quad \text{(S5)}$$

$$CE_{cat} = \frac{q}{q_{NO_3^-}} \quad \text{(S6)}$$

$$q_{As(III)} = \frac{(V_{NCC} + V_{NAC}) \cdot HRT \cdot F \cdot (n_{As(III)/As(V)} \cdot rAs(III))}{m_{As}} \quad \text{(S7)}$$

$$CE_{an} = \frac{q_{As(III)}}{q} \quad \text{(S8)}$$

V_{NCC} and V_{NAC} are net cathode and anode compartment volume in m^{-3}, respectively; F is the Faraday constant (96 485 C mol^{-1}); m_N and m_{As} are molar masses (14 g mol^{-1} for nitrogen and 75 g mol^{-1} for arsenic); HRT and HRT_{cat} are the hydraulic retention time considering the net reactor volume and the net cathodic compartment in days, respectively; n represent the equivalent electrons required for each redox reaction ($n_{NO_3^-/NO_2^-} = 2; n_{NO_2^-/N_2O} = 2; n_{N_2O/N_2} = 1;$ and $n_{As(III)/As(V)} = 2$); rNO_3^-, rNO_2^-, and rN_2O are the nitrogen reduction rate in g N m_{NCC}^{-3} d^{-1}; and $rAs(III)$ is the arsenite oxidation rate in g As(III) $m_{NCC+NAC}^{-3}$ d^{-1}. For coulombic efficiency, q is the charge observed in reactors and qNO_3^- and $qAs(III)$ are the theoretical calculated charged for nitrate reduction and arsenite oxidation, respectively.

APPENDIX
Supplementary data: Chapter 4.1

Supplementary data 3: Additional tables

Table S3: Summary of results for denitrification performance under different HRTs and effluent recirculation. Results are represented as mean values with standard deviations of the corresponding operational conditions (analytical replicates during the operational condition, n≥3; except in the case of nitrous oxide, n=1).

Reactor	Effluent recirculation (L^{-1})	Period (days)	HRT (h)	HRT_{cat} (h)	Arsenite oxidation rate ($g\ As\ m^{-3}_{NCC+NAC} d^{-1}$)	Nitrate reduction rate ($g\ N\ m^{-3}_{NCC} d^{-1}$)	Arsenic and nitrogen content in the effluent					CE_{cat} (%)	CE_{an} (%)
							Arsenite ($mg\ As\ L^{-1}$)	Arsenate ($mg\ As\ L^{-1}$)	Nitrate ($mg\ N\ L^{-1}$)	Nitrite ($mg\ N\ L^{-1}$)	Nitrous oxide ($mg\ N\ L^{-1}$)		
A	0	0-25	7.5±0.2	5.0±0.2	10±0	24±10	0.0±0.1	7.0±0.3	32.3±4.3	0.2±0.1	0.0±0.0	86±20	6±5
	35	69-76	7.4±0.2	4.9±0.1	12±9	166±22	0.0±0.3	6.5±0.3	0.1±0.1	0.0±0.0	0.0±0.0	91±12	1±0
		77-83	5.2±0.3	3.5±0.2	-	262±20	-	-	0.3±0.3	0.1±0.1	0.0±0.0	91±7	-
		106-113	4.4±0.0	2.9±0.0	35±1	220±21	0.0±0.2	6.7±0.1	8.1±1.6	0.0±0.0	4.9±0.0	110±10	2±0
	85	114-123	4.5±0.3	3.0±0.2	-	278±23	-	-	0.2±0.2	0.0±0.0	0.0±0.0	105±9	-
		124-131	3.4±0.2	2.3±0.2	46±5	367±17	0.0±0.2	6.8±0.3	0.2±0.2	0.0±0.0	0.0±0.0	101±7	1±0
		132-139*	2.9±0.1	1.9±0.0	59±1	43±11	0.0±0.1	6.3±0.0	32.7±1.4	0.1±0.2	0.6±0.0		
		149-173	2.9±0.1	1.9±0.1	-	427±26	-	-	1.6±1.2	0.1±0.0	0.3±0.0	104±7	-
		174-186	2.3±0.1	1.5±0.1	66±4	519±53	0.0±0.3	7.3±0.3	2.8±2.1	0.1±0.1	0.8±0.0	101±8	2±0
		187-194	1.6±0.1	1.1±0.1	94±7	495±83	0.0±0.1	6.5±0.3	17.0±4.7	0.3±0.3	0.6±0.0	98±16	2±0
B	0	0-25	7.7±0.3	5.1±0.2	12±5	24±10	0.0±0.2	7.5±0.4	32.8±4.6	0.2±0.2	0.6±0.0	66±15	10±10
	35	69-76	7.5±0.3	5.0±0.2	9±6	166±22	0.0±0.1	6.4±0.4	0.1±0.1	0.0±0.0	0.0±0.0	87±15	1±0
		77-83	5.7±0.2	3.8±0.1	-	232±10	-	-	0.1±0.1	0.0±0.0	0.0±0.0	92±2	-
		106-113	4.7±0.4	3.1±0.2	34±4	167±12	0.0±0.1	7.0±0.2	11.8±1.5	0.0±0.0	6.3±0.0	104±2	2±0
	85	114-123	4.7±0.4	3.1±0.1	-	260±13	-	-	0.2±0.1	0.0±0.0	0.0±0.0	109±11	-
		124-131	3.7±0.3	2.5±0.2	41±7	329±39	0.0±0.2	7.0±0.1	1.1±1.3	0.1±0.1	0.0±0.0	98±10	1±0
		161-173	2.8±0.1	1.8±0.1	50±8	342±27	-	-	14.3±1.7	0.1±0.0	7.0±0.0	99.2±7	-
		174-186	2.2±0.1	1.5±0.1	63±5	456±61	0.0±0.1	6.3±0.5	10.0±5.5	0.1±0.1	1.3±0.0	92±17	1±0
		187-194	1.7±0.1	1.1±0.1	90±3	394±76	0.1±0.1	7.2±0.2	18.0±3.8	0.1±0.1	0.4±0.0	97±23	3±0

**Period tested under OCV condition.*

Table S4: Concentrations of the major impurities (>1 mg Kg $_{granular\ graphite}^{-1}$) present in the granular graphite after washing with 1 M HCl and 1 M NaOH. The analysis was performed by Inductively coupled plasma mass spectrometry (ICP-MS)

Impurities	**Concentration** (mg Kg $_{granular\ graphite}^{-1}$)	**Impurities**	**Concentration** (mg Kg $_{granular\ graphite}^{-1}$)
Silicon	235.1 ± 4.8	Aluminum	8.0 ± 1.3
Boron	72.8 ± 10.9	Sodium	5.8 ± 0.6
Sulfur	58.1 ± 2.2	Iron	5.7 ±0.2
Calcium	46.1 ± 2.6	Magnesium	2.0 ±0.0
Lithium	33.5 ± 0.8	Titanium	1.4 ± 0.3
Potassium	11.7 ± 1.0	Arsenic	1.5 ± 0.0
Phosphorous	11.6 ± 1.5	Barium	1.3 ± 1.5
Bromine	10.3 ±0.6	Strontium	1.1 ± 0.0

Supplementary data: Chapter 4.2

Ex-Situ electrochemical characterisation of fixed-bed denitrification biocathodes: a promising strategy to improve nitrate removal

Alba Ceballos-Escalera[1], Narcís Pous[1], Benjamin Korth[2], Falk Harnisch[2], M. Dolors Balaguer[1] and Sebastià Puig[1*]

[1] LEQUiA, Institute of the Environment, University of Girona, C/ Maria Aurèlia Capmany, 69, E-17003, Girona, Spain

[2] Department of Environmental Microbiology, Helmholtz Centre for Environmental Research GmbH - UFZ, Permoserstraße 15, 04318 Leipzig, Germany

Calculations:

Theoretical maximum nitrate reduction rate: it assumes the complete conversion of nitrate to nitrogen gas that requires 5 electrons. To calculate the current density (j_s, A m^{-2}), the current was divided by the surface area of the granules. It was assumed that each granule had an average surface area of 3.32 × 10^{-5} m^{-2}, and each sample contained 3 to 5 granules.

$$j_s \cdot \frac{1}{F} \cdot \frac{1mol\ N{-}NO_3^-}{5\ mol\ e^-} \cdot \frac{14g\ N{-}NO_3^-}{1mol\ N{-}NO_3^-} \cdot \frac{86400\ s}{1\ d} = r_{NO_3^-} \quad \text{(S1)}$$

- $r_{NO_3^-}$ (g $N\text{-}NO_3^-$ m^{-2} d^{-1}): theoretical maximum nitrate reduction rate.
- j_g: current density.
- F: Faraday constant (96485 C mol^{-1}).

Michaelis–Menten kinetics is adapted assuming that the recorded gravimetric current density (j_g, mA g^{-1}) represents the reaction rate (v). Consequently, j_g is also connected to the maximum reaction rate $\mathrm{v_{max}}$.

$$\mathrm{v} = \mathrm{v_{max}} \cdot \frac{[S]}{K_M + [S]} \quad \text{(S2)}$$

- v (mA g^{-1}): corresponds to j_g (mA g^{-1}) calculated by normalising the obtained current the dry weight of the sampled granules.
- $\mathrm{v_{max}}$ (mA g^{-1}): maximum reaction rate at saturating substrate concentration. In this study, it was assumed to be apparent ($\mathrm{v_{max}^{app}}$) as it is influenced by factors such as biofilm thickness, biofilm density, the surface area of granular graphite, and radial diffusion.
- $\mathrm{K_M}$ (mg $N\text{-}NO_3^-$ L^{-1}): affinity constant or Michaelis constant, corresponding to the concentration that is necessary to reach half of $\mathrm{v_{max}}$. In this study, it was assumed to be apparent ($\mathrm{K_M^{app}}$) as they are influenced by factors such as biofilm thickness, biofilm density, the surface area of granular graphite, and radial diffusion.
- $[S]$ (mg $N\text{-}NO_3^-$ L^{-1}): nitrate concentration.

Nernst equation:

$$E = E^o + \frac{RT}{zF} \ln Q \quad \text{(S3)}$$

$$Q = \frac{[\text{product}]^b}{[\text{reactant}]^a} \quad \text{(S4)}$$

- E (V): redox potential
- E^o (V): standard redox potential (298.15 K, 1 atm, and 1 M).
- R: Universal gas constant (8.314 J K^{-1} mol^{-1})
- T (K): temperature
- z: number of electrons exchanged.
- F: Faraday constant (96485 C mol^{-1}).
- Q: reaction quotient calculated by multiplying the activities (approximated by concentrations) of products and dividing by the reactants; all concentrations of reactants/products raised to the coefficients in the balanced chemical equation.

Figures:

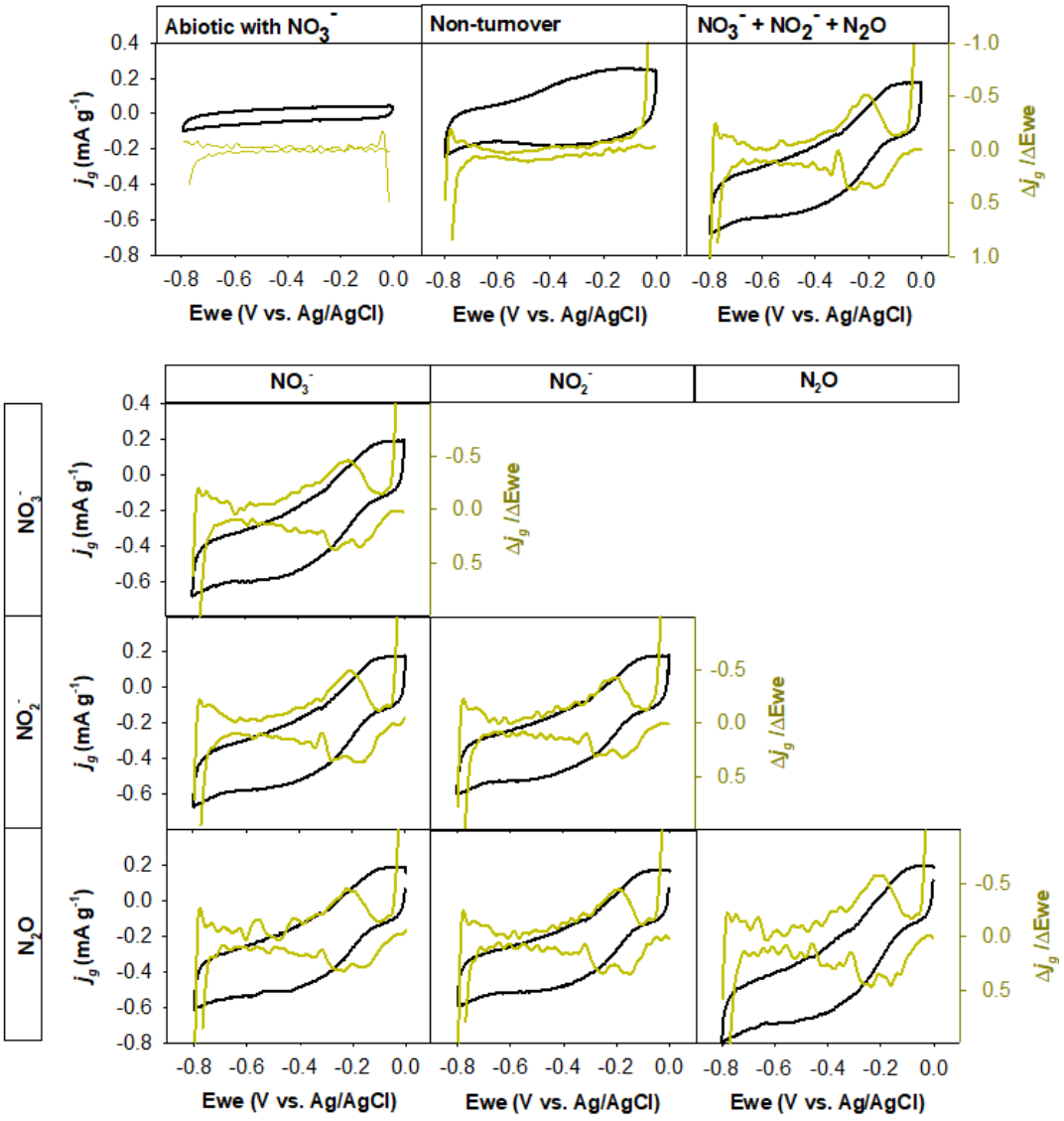

Figure S11: Representative voltammograms (black line) and corresponding first derivatives (green line) of granular graphite under abiotic, non-turnover, and turnover conditions at pH 7 and 25ºC. The turnover voltammograms were recorded in the presence of different electron acceptors (nitrate, nitrite and nitrous oxide) as well as a combination thereof.

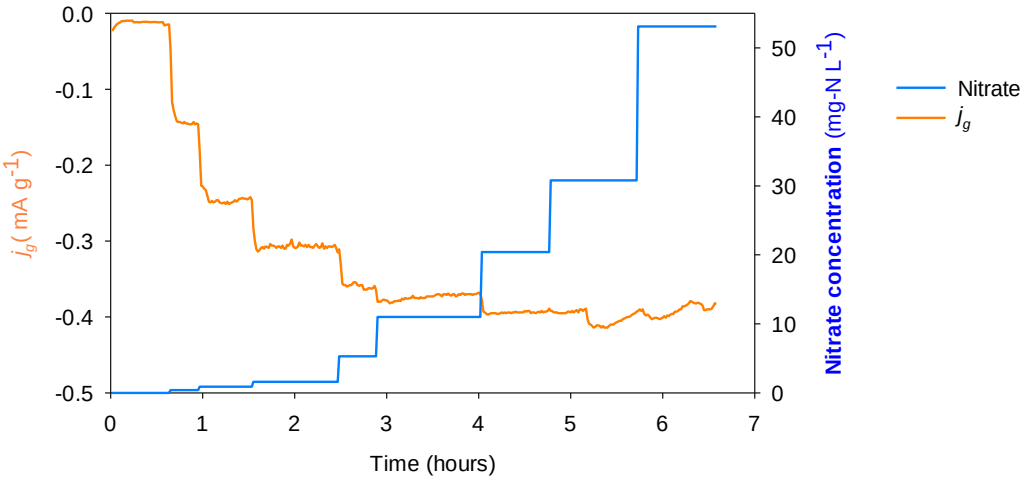

Figure S2: Representative course of the gravimetric current density at varying nitrate concentrations (replicate 3).

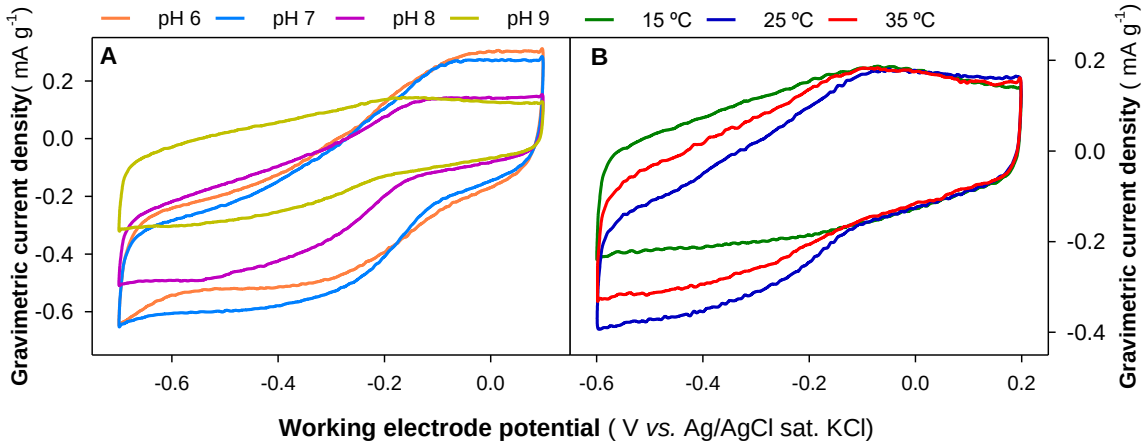

Figure S3: Representative voltammograms (replicate 3) used to determine the effect of pH and temperature on the formal potential (E^f). (A) The pH effect was evaluated at a constant temperature of 25°C. (B) The temperature effect was evaluated at a constant pH of 7.

APPENDIX
Supplementary data: Chapter 4.2

Tables:

Table S1: Most abundant amplicon sequence variant (ASVs) at a genus level after comparison of sequences with the NCBI GenBank database.

Number ASVs	Most probable identification	Sequence Similarity (% similarity)	Relative abundance (% of sequences)	
			Reactor A	
			Biofilm Anode	Biofilm Cathode
Betaproteobacteriales				
ASV1	(NR_152013.1) *Achromobacter agilis* strain LMG 3411	100	73.8 ± 8.5	2.2 ± 1.8
ASV8	(NR_152013.1) *Achromobacter agilis* strain LMG 3411	99.6	2.9 ± 04	<0.1
ASV2	(NR_074731.1) *Sideroxydans lithotrophicus* ES-1	96.44	<0.1	70.7 ± 2.7
ASV10	(NR_074731.1) *Sideroxydans lithotrophicus* ES-1	96.05	ND	2.6 ± 0.0
ASV5	(NR_043249.1) *Denitratisoma oestradiolicum* strain AcBE2-1	96.05	ND	4.3 ± 0.5
Rhizobiales				
ASV6	(NR_133841.1) *Rhizobium azibense* strain 23C2	99.6	1.6 ± 2.3	<0.1
ASV3	(NR_074219.1) *Starkeya novella* DSM 506	98.81	3.7 ± 5.2	0.4 ± 0.3
Actinobacteria				
ASV9	(NR_115708.1) *Rhodococcus qingshengii* strain djl-6-2	100	4.7 ± 1.7	0.3 ± 0.2
Bacteroidia				
ASV4	(NR_117435.1) *Ohtaekwangia koreensis* strain 3B-2	95.2	<0.1	7.5 ± 0.4

Table S2. Average gravimetric current density during chronoamperometry at -0.320 V vs. Ag/AgCl sat. KCl and formal potential at pH 7 and 25ºC were obtained by electrochemical characterisation of sampled granules.

			Chronoamperometry	Cyclic voltammetry
			Stable current density (mA g^{-1})	Formal potential (V vs. Ag/AgCl)
Non-turnover			0.01 ± 0.00	n.d.
Turnover				
NO_3^-			-0.22 ± 0.04	-0.229 ± 0.008
	NO_2^-		-0.19 ± 0.08	-0.222 ± 0.002
		N_2O	-0.21 ± 0.10	-0.222 ± 0.005
NO_3^-	NO_2^-	N_2O	-0.21 ± 0.05	-0.231 ± 0.004
NO_3^-	NO_2^-		-0.25 ± 0.05	-0.218 ± 0.012
NO_3^-		N_2O	-0.20 ± 0.07	-0.219 ± 0.008
	NO_2^-	N_2O	-0.21 ± 0.09	-0.228 ± 0.003

† n.d.: not detected

Supplementary data: Chapter 4.3

Nitrate electro-bioremediation and water disinfection for rural areas

Alba Ceballos-Escalera, Narcís Pous, M. Dolors Balaguer and Sebastià Puig*

LEQUiA, Institute of the Environment, University of Girona, C/ Maria Aurèlia Capmany, 69, E-17003, Girona, Spain

Calculations:

Equations for the calculation of reaction rates and coulombic efficiencies.

$$rNO_3^- = \frac{C_{NO_3^-}{}_{influent} - C_{NO_3^-}{}_{effluent}}{HRT_{cat}} \quad \text{(S1)}$$

$$rNO_2^- = rNO_3^- + \frac{C_{NO_2^-}{}_{influent} - C_{NO_2^-}{}_{effluent}}{HRT_{cat}} \quad \text{(S2)}$$

$$rN_2O = rNO_2^- + \frac{C_{N_2O}{}_{influent} - C_{N_2O}{}_{effluent}}{HRT_{cat}} \quad \text{(S3)}$$

where $Cx_{influent}$ and $Cx_{effluent}$ represent nitrate, nitrite and nitrous oxide mass concentration in the effluent and influent (either in g N m^{-3}). By the molar mass of nitrate (62 mg mol^{-1}) nitrate was converted to kg N-NO_3- m^{-3} d^{-1}.

$$j_{NO_3^-} = \frac{V_{NCC} \cdot F \cdot HRT_{cat} \cdot (n_{NO_3^-/NO_2^-} \cdot rNO_3^- + n_{NO_2^-/N_2} \cdot rNO_2^-)}{m_N \cdot t} \quad \text{(S4)}$$

$$Energy = j \cdot E_{cell} \cdot 24 \quad \text{(S5)}$$

$$CE_{cat} = \frac{j}{j_{NO_3^-}} \cdot 100 \quad \text{(S6)}$$

For the theoretical current for nitrate reduction (jNO_3^-, A): V_{NCC} is net cathode compartment volume in m^{-3}; F is the Faraday constant (96 485 C mol^{-1}); m_N is molar masses (14 g mol^{-1} for nitrogen); t is the time converting factor between day and seconds (86,400); HRT_{cat} is the hydraulic retention time considering the net cathodic compartment in days, respectively; n represent the equivalent electrons required for each redox reaction ($n_{NO_3^-/NO_2^-} = 2; n_{NO_2^-/N_2} = 3$); rNO_3^-, rNO_2^-, and rN_2O are the nitrogen reduction rate in g N m_{NCC}^{-3} d^{-1}. For the energy consumption (Wh d^{-1}) (S5): E_{cell} is the cell potential (V); j is the observed current (A); and the result is multiplied by the 24 hours of operation in a single day. After this the energy was normalized by the amount of nitrate removed (kWh kg^{-1} NO_3^-) and the water treated (kWh m^{-3}). For cathodic

coulombic efficiency (%) (S6): *j* is the current (A) observed in reactors and jNO_3^- is the theoretical calculated current (A) for nitrate reduction.

Tables:

Table S1: Pathogen analysis of the effluent from the parent denitrifying bioelectrochemical reactor. The samples (n =3) were analysed externally (Cat-Gairín Laboratory, Girona).

T. coliforms	*E. coli*	*Enterococcus*
[ufc 100 mL^{-1}]	[ufc 100 mL^{-1}]	[ufc 100 mL^{-1}]
1.7 ± 2.4	0.0 ± 0.0	8.0 ± 9.3

Supplementary data: Chapter 4.4

Electrochemical water softening as pretreatment for nitrate electro-bioremediation

Alba Ceballos-Escalera, Narcís Pous, M. Dolors Balaguer, Sebastià Puig*

LEQUiA, Institute of the Environment, University of Girona, C/ Maria Aurèlia Capmany, 69, E-17003, Girona, Spain

Supplementary data, Tables.

Table 1: Groundwater characteristics from Navata, Girona (Spain), and characteristics after electrochemical softened and denitrifying bioelectrochemical treatment.

	Influent: Groundwater	Effluent from electrochemical softening	Effluent from electro-bioremediation	
pH	7.5 ± 0.2	6.5 ± 0.6	7.0 ± 0.2	
Electrical conductivity	0.7 ± 0.1	0.4 ± 0.0	0.4 ± 0.0	mS cm^{-1}
Hardness	325.3 ± 10.4	151.3 ± 3.2	140.5 ± 5.1	mg $CaCO_3$ L^{-1}
Sodium	17.3 ± 0.4	32.4 ± 0.3	38.0 ± 10.3	mg Na^+ L^{-1}
Potassium	2.4 ± 1.6	2.2± 0.9	3.0 ± 0.7	mg K^+ L^{-1}
Magnesium	11.2 ± 4.1	8.3 ± 1.9	5.1 ± 0.8	mg Mg^{2+} L^{-1}
Calcium	127.2 ± 20.6	53.6 ± 0.2	45. 9 ± 1.4	mg Ca^{2+} L^{-1}
Chloride	64.1 ± 5.4	68.0 ± 10.5	62.0 ± 12.9	mg Cl^- L^{-1}
Nitrate	25.1 ± 1.4	25.8 ± 0.4	3.3 ±1.6	mg N-NO_3^- L^{-1}
Nitrite	n.d.	n.d.	n.d.	mg N-NO_2^- L^{-1}
Nitrous oxide	-	-	n.d.	mg N-N_2O L^{-1}
Sulfate	9.6 ± 7.0	5.4 ± 0.8	5.8 ± 0.2	mg S-SO_4^{2-} L^{-1}
Phosphate	0.3 ± 0.4	0.5 ± 0.0	0.3 ± 0.2	mg P-PO_4^{2-} L^{-1}

† n.d.: not detected

† (-): not analyzed

APPENDIX
Supplementary data: Chapter 4.4

Supplementary data, Energy calculation.

The total energy consumption considered two key operating factors as the main energy consumers: (i) pumping system and (ii) external power supply. The pumping system assumed the feeding and recirculation in both reactors. The power consumption of a pump (P_{pump}, kW) is calculated according to Eq. S1 (Zou & He, 2018).

$$P_{pump} = \frac{Q_{pump}\, x\, (H_{hydraulic} + H_{dynamic})}{1000\, x\, \eta} = \frac{v\, \pi\, d^2 / 4\, x\, (\rho\, g\, h + \rho\, v^2 / 2)}{1000\, x\, \eta} \qquad \text{Eq. S1}$$

Where $H_{hydraulic}$ (Pa) and $H_{dynamic}$ (Pa) are the heads provide by pump. Each variable is attributed to:

- v (m s^{-1}) is the water velocity calculated from the flow rate divided into the section of the tube area.
- d (m) is the tube diameter. It was assumed to be 0.018 m for feeding and recirculation in both reactors.
- h (m) is the difference of water height before and after the pump. It is considered 0.5 m for the feeding and recirculation in both reactors.
- ρ (kg m^{-3}) is water density.
- η (%) is the pump efficiency. The efficiency varies in different types of pumps; it was considered 100% since peristaltic pumps in laboratory-scale have high efficiencies.

Supplementary data, Economic calculation.

The economic analysis was performed in a simplified way for electrochemical softening, ion exchange resins, and chemical precipitation. The following table shows the main assumptions for this calculation:

Water softening depth	170	ppm $CaCO_3$	
Energy cost	0.21	€ kWh^{-1}	(Eurostat, 2021)
Salt (NaCl)	0.32	€ Kg^{-1}	(Van der Bruggen et al., 2009)
Acid (HCl 20%)	1.16	€ L^{-1}	(HCl 20%, 25L, Valquimica)
Ti-MMO (or DSA) electrode	700	€ m^{-2}	(Zhi & Zhang, 2016)
Stainless steel	45	€ m^{-2}	(Zhang et al., 2010)
Cation exchange membrane	200	€ m^{-2}	(AMI-7001S/CMI-7000S, Price List - Membranes International Inc., 2021)
Granular graphite	2	€ kg^{-1}	(Mu et al., 2010)
Electrochemical water softening			
Power supply - electrochemical precipitation	0.68	kWh m^{-3}	Present study
Power supply - reverse polarity periods	2.59 x 10^{-3}	kWh m^{-3}	
Energy for pumping system	2.73 x 10^{-3}	kWh m^{-3}	
HCl 20% consumption	0.19	L m^{-3}	
Ion exchange softening			
Salt consumption	0.24	kg m^{-3} ppm^{-1} $CaCO_3$	(Van der Bruggen et al., 2009)
Energy consumption	0.09	kWh m^{-3}	
Chemical precipitation in a pellet reactor			
Reagents (NaOH)	3.18	€ m^{-3}	(Van der Bruggen et al., 2009)

References

Comprar Ácido Clorhídrico (25-1000 litros) | Varias Concentraciones. (n.d.). Retrieved August 27, 2021, from https://www.vadequimica.com/acido-clorhidrico-salfuman-25-litros.html

Eurostat. (n.d.). Electricity price statistics - Statistics Explained. Retrieved July 13, 2021, from https://ec.europa.eu/eurostat/statistics-explained/index.php?title=Electricity_price_statistics

Mu, Y., Radjenovic, J., Shen, J., Rozendal, R. A., Rabaey, K., & Keller, J. (2010). Dehalogenation of Iodinated X-ray Contrast Media in a Bioelectrochemical System. Environmental Science and Technology, 45(2), 782–788. https://doi.org/10.1021/ES1022812

Price List - Membranes International Inc. (n.d.). Retrieved August 27, 2021, from https://ionexchangemembranes.com/price-list/

Van der Bruggen, B., Goossens, H., Everard, P. A., Stemgée, K., & Rogge, W. (2009). Cost-benefit analysis of central softening for production of drinking water. Journal of Environmental Management, 91(2), 541–549. https://doi.org/10.1016/j.jenvman.2009.09.024

Zhang, F., Saito, T., Cheng, S., Hickner, M. A., & Logan, B. E. (2010). Microbial Fuel Cell Cathodes With Poly(dimethylsiloxane) Diffusion Layers Constructed around Stainless Steel Mesh Current Collectors. Environmental Science and Technology, 44(4), 1490–1495. https://doi.org/10.1021/ES903009D

Zhi, S. L., & Zhang, K. Q. (2016). Hardness removal by a novel electrochemical method. Desalination, 381, 8–14. https://doi.org/10.1016/J.DESAL.2015.12.002

Zou, S., & He, Z. (2018). Efficiently “pumping out” value-added resources from wastewater by bioelectrochemical systems: A review from energy perspectives. In Water Research. https://doi.org/10.1016/j.watres.2017.12.026

Supplementary data: Chapter 4.5

Advancing towards electro-bioremediation scaling-up: on-site pilot plant for successful nitrate-contaminated groundwater treatment

Alba Ceballos-Escalera[a], Narcís Pous[a], Lluis Bañeras[b], M. Dolors Balaguer[a], Sebastià Puig[a,*]

[a] LEQUiA, Institute of the Environment, University of Girona, C/ Maria Aurèlia Capmany, 69, E-17003, Girona, Spain

[b] Group of Environmental Microbial Ecology, Institute of Aquatic Ecology, University of Girona, C/ *Maria Aurèlia Capmany, 40,* E-17003, Girona, Spain.

* Corresponding author:

E-mail address: sebastia.puig@udg.edu (S. Puig)

Supplementary Equations: Equations for the calculation of reaction rates and coulombic efficiencies.

$$rNO_3^- = \frac{C_{NO_3^-\,influent} - C_{NO_3^-\,effluent}}{HRT_{cat}} \quad \text{(S1)}$$

$$rNO_2^- = rNO_3^- + \frac{C_{NO_2^-\,influent} - C_{NO_2^-\,effluent}}{HRT_{cat}} \quad \text{(S2)}$$

$$rN_2O = rNO_2^- + \frac{C_{N_2O\,influent} - C_{N_2O\,effluent}}{HRT_{cat}} \quad \text{(S3)}$$

rNO_3^-, rNO_2^-, and rN_2O are the nitrogen reduction rate in g N m_{NCC}^{-3} d^{-1}; $Cx_{influent}$ and $Cx_{effluent}$ represent nitrate, nitrite and nitrous oxide mass concentration in the effluent and influent (either in g N m^{-3}); and HRT_{cat} is the hydraulic retention time considering the net cathodic compartment in days. By the molar mass of nitrate (62 mg mol^{-1}) nitrate is converted to kg NO_3- m^{-3} d^{-1}.

$$j_{NO_3^-} = \frac{V_{NCC} \cdot F \cdot HRT_{cat} \cdot (n_{NO_3^-/NO_2^-} \cdot rNO_3^- + n_{NO_2^-/N_2} \cdot rNO_2^-)}{m_N \cdot t} \quad \text{(S4)}$$

$$Energy = j \cdot E_{cell} \cdot 24 \quad \text{(S5)}$$

$$CE_{cat} = \frac{j}{j_{NO_3^-}} \cdot 100 \quad \text{(S6)}$$

For the theoretical current for nitrate reduction (jNO_3^-, A): V_{NCC} is net cathode compartment volume in m^{-3}; F is the Faraday constant (96 485 C mol^{-1}); m_N is molar masses (14 g mol^{-1} for nitrogen); t is the time converting factor between day and seconds (86,400); HRT_{cat} is the hydraulic retention time considering the net cathodic compartment in days, respectively; n

represent the equivalent electrons required for each redox reaction ($n_{NO_3^-/NO_2^-} = 2; n_{NO_2^-/N_2} = 3$); rNO_3^-, rNO_2^-, and rN_2O are the nitrogen reduction rate in g N m_{NCC}^{-3} d^{-1}. For the energy consumption (Wh d^{-1}) (S5): E_{cell} is the cell potential (V); *j* is the observed current (A); and the result is multiplied by the 24 hours of operation in a single day. After this the energy was normalized by the amount of nitrate removed (kWh kg^{-1} NO_3^-) and the water treated (kWh m^{-3}). For cathodic coulombic efficiency (%) (S6): *j* is the current (A) observed in reactors and jNO_3^- is the theoretical calculated current (A) for nitrate reduction.

Supplementary Figures:

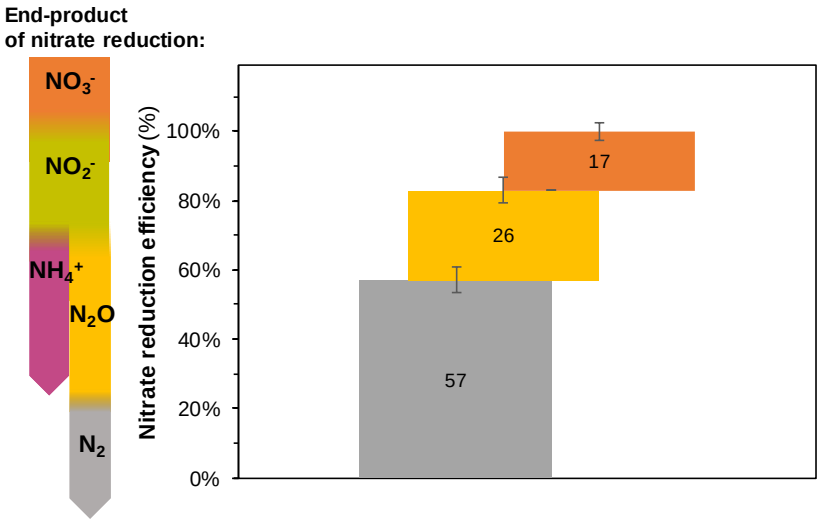

Figure S1: Percentage distribution of nitrogen species (nitrate-NO_3^-, nitrite-NO_2^-, nitrous oxide-N_2O, and ammonium-NH_4^+) after treatment at best condition (HRT_{cat} of 2.0 h and cathode potential of -0.75 V vs. Ag/AgCl). The influent contained only nitrate.

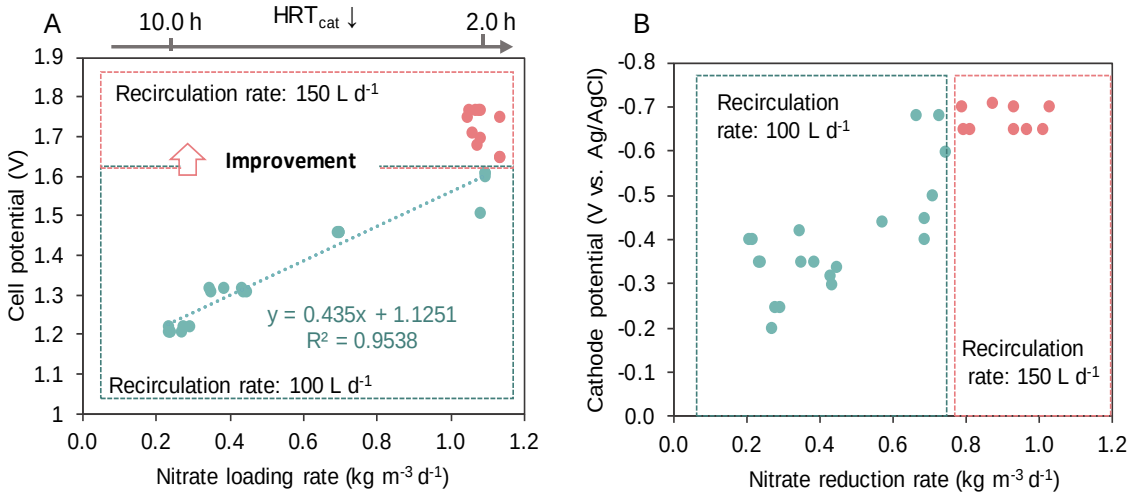

Figure S2: (A) Relationship between nitrate loading rate and fixed cell potential control. (B) Cathode potential and observed nitrate reduction rate.

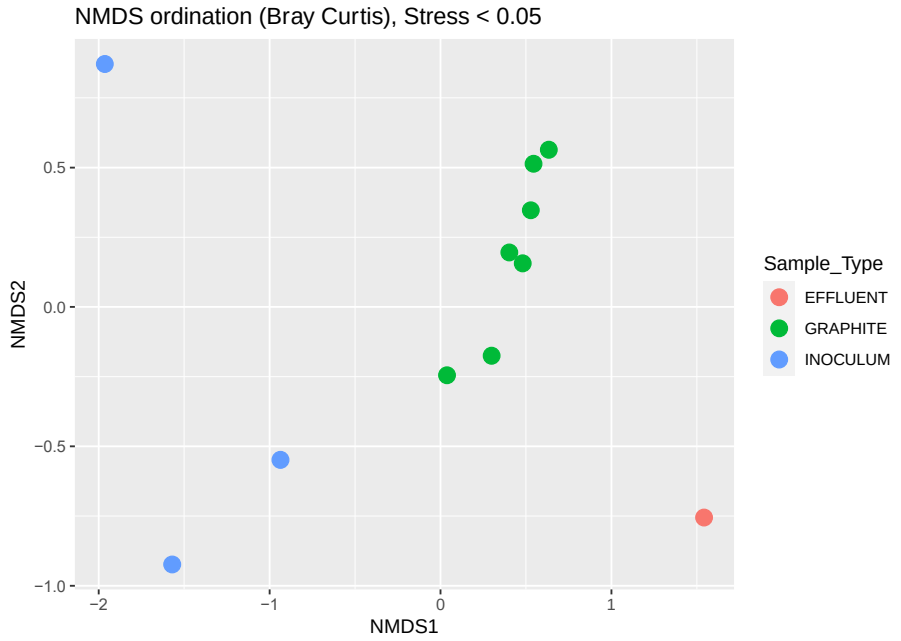

Figure S3. Non-Metric Multidimensional Scaling ordination of samples based on Bray-Curtis distant matrix calculated from the relative abundance of 1163 sequence signatures found in samples. Blue- Inoculum samples from previous Lab-operated BES reactors, Green- microbial communities determined in Graphite samples at the end of operation. Red- samples from the reactor effluent collected at the end of operation.

Figure S4: Image of the final inspection of the operational reactor, specifically focusing on the granular graphite within the cathode compartment.

Supplementary Tables:

Table S5: Summary of the values, assumptions, and references for the CAPEX and OPEX calculations.

CAPEX						
		Amount	Cost per reactor €	Adopted Life span year	Costs per year € year^{-1}	References and assumptions
1 module						
Body and ancillary material PVC		2.7 kg	50		2	
Anode	*Granular graphite*	1.4 kg	10		0	enViro-cell, Germany
	Ti-MMo rod	0.2 kg	490		16	Special metals and products, Spain
Cathode	*Granular graphite*	3 kg	13		0.4	enViro-cell, Germany
	Ti rod+ mesh	0.2 kg	411		14	Special metals and products, Spain
CEM membrane CMHPP		0.2 kg	356		12	Catex membranes Ralex®, MEGA, Czech Republic
Centrifugal pump (0.4 W, maximum flow 360 mL min^{-1})		1 unit	107		4	D200, RS Pro, Spain https://es.rs-online.com/web/p/bombas-de-agua/8170725
TOTAL 1 module			**1433**	**30**	**48**	
Facilities						
Control panel/power supply		1 unit	2500		83	TELWESA, Spain
Softening unit		1 unit	750		25	Concept, concept earth line 100, Spain
Air conditioner		1 unit	500		17	
Container		1 unit	3000		100	

OPEX				
Consumers		Consumption	Cost	References and assumptions
Electricity	Pumping recirculation [a)]	Power input of 0.4 W	0.20€ kWh^{-1} [b)]	a) D200, RS Pro, Spain https://es.rs-online.com/web/p/bombas-de-agua/8170725 b) Electricity prices for non-household consumers (Eurostat 2022) c) Assuming a constant consumption in the whole scenario
	Power supply	0.32 kWh m^{-3} [c)]	0.20 € kWh^{-1} [b)]	
Maintenance		3 % of the CAPEX		(Jourdin et al. 2020)

References:

Eurostat. 2022. "Electricity Price Statistics - Statistics Explained." Retrieved July 13, 2022 (https://ec.europa.eu/eurostat/statistics-explained/index.php?title=Electricity_price_statistics).

Jourdin, Ludovic, João Sousa, Niels van Stralen, and David P. B. T. B. Strik. 2020. "Techno-Economic Assessment of Microbial Electrosynthesis from CO2 and/or Organics: An Interdisciplinary Roadmap towards Future Research and Application." Applied Energy 279:115775. doi: 10.1016/J.APENERGY.2020.115775.